Synthesis and Characterization of Composite Coating for Wear Resistance Application

A THESIS

Submitted in partial fulfilment of the requirements for the award of the Degree

of

DOCTOR OF PHILOSOPHY

In

Mechanical Engineering

Submitted by

Kalpana Gupta

Roll No.: 2K18/PhD/ME/503

Under the Supervision of

Prof. Qasim Murtaza

(Professor)

Department of Mechanical Engineering

Delhi Technological University Delhi, India

Dr. N. Yuvraj

(Associate Professor)

Department of Mechanical Engineering

Delhi Technological University Delhi, India

Department of Mechanical Engineering,

Delhi Technological University (Formerly Delhi College of Engineering)

Main Bawana Road, Shahabad, Daulatpur, Delhi- 110042, India

August 2023

CERTIFICATE

This is to certify that the thesis entitled **"Synthesis and Characterization of Composite Coating for Wear Resistance Application"** being submitted by **Kalpana Gupta**, **Roll No.: 2K18/PhD/ME/503** to the Delhi Technological University, Delhi for the award of the degree of **Doctor of Philosophy** is a bonafide record of original research work carried out by her. She has worked under our guidance and supervision and has fulfilled the requirements for the submission of this thesis, which has reached the requisite standard.

The results contained in this thesis have not been submitted, in part or full, to any other University or Institute for the award of any degree.

Prof. Qasim Murtaza
(Professor)
Department of Mechanical Engineering
Delhi Technological University

Dr. N. Yuvraj
(Associate Professor)
Department of Mechanical Engineering
Delhi Technological University

ACKNOWLEDGEMENTS

Firstly, I wish to express my heartfelt gratitude to my supervisor Prof. Qasim Murtaza, Professor Department of Mechanical Engineering, DTU and co-supervisor Dr. N. Yuvraj, Associate Professor in Department of Mechanical Engineering, DTU for being very supportive, patient and continuously encouraging me to learn engineering by sharing his valuable knowledge. My sincere thanks to Dr. Anup Kumar, Associate Professor, Department of Metallurgical and Materials Engineering IIT Patna for his support and suggestions.

I would like to express my sincere and immense thanks to Dr. S. K Garg, Head, Department, of Mechanical Engineering, DTU Delhi for his vital discussions, encouragement, and insightful comments at various stages of my Ph.D. journey.

I am thankful to research scholars Mr. Satyajeet, Mr Abhinav, Mr Rakesh and Mr Alok from NIT for their support and guidance during my stay at NIT Patna. It is a pleasure thank to staff member, Mr. Krishna Kaushik, and Mr Ankit Kumar, DTU for carrying out XRD and FE-SEM characterization.

Finally, I would like to thank my beloved parents, my brother, my sister and my best friend for all their love and support throughout my research work.

Kalpana Gupta

Roll No.: 2K18/PhD/ME/503

Declaration

I certify that,

a) The work contained in this thesis is original and has been done by myself under the general supervision of my supervisors.
b) The work has not been submitted to any other Institute for degree or diploma.
c) I have followed the Institute norms and guidelines and abide by the regulation as given in the Ethical Code of Conduct of the Institute.
d) Whenever I have used materials (data, theory, and text) from other sources, I have given due credit to them by citing them in the text of the thesis and giving their details in the reference section.

Signature of the Student

Name: Kalpana Gupta

Roll No.: 2K18/PhD/ME/503

PREFACE

Chapter 1: Introduction

This chapter delves into the realm of Surface Engineering, Coating, and related concepts. It commences with an introductory framework, paving the way for subsequent discussions. Surface Engineering's significance is elaborated upon, emphasizing its role in enhancing material performance. The chapter extensively discusses various coating techniques, including nanostructured coatings and thermal spray methods like HVOF, Atmospheric Plasma Spray, Flame Spray, and Cold Spray. Tribology, wear behaviour, lubrication, corrosion, and Thermal Protection Systems are also explored, especially in the context of Hypersonic Vehicles, encapsulating the challenges they present.

Chapter 2: Literature Review

The second chapter embarks on an exhaustive Literature Review, focusing on ZrB2-SiC and Mo-NiCr composite coatings. It delves into research spanning decades, analysing properties, behaviours, application techniques, and adhesion, wear, and friction characteristics of these composites. High-temperature tribology and the influence of thermal shock on coatings are explored. Additionally, residual stress and microhardness behaviors are investigated, elucidating the impact of temperature. This chapter forms a robust foundation for understanding the intricate attributes of these coatings.

Chapter 3: Materials and Methods

This chapter presents coating materials, preparation techniques, substrate selection, and coating synthesis methods. Process parameters are detailed alongside characterization techniques, including XRD, SEM, FESEM with EDS, density, porosity, micro hardness, hot corrosion, and residual stress measurements.

Chapter 4 and 5: Results and Discussion

These two chapters unveils the outcomes of experiments. These chapters exhibit diverse composite coating systems crafted through HVOF and plasma spray methods. The results are visualized via tables, graphs, SEM, FESEM micrographs, and other characterizations. Wear behaviour, hot corrosion, micro hardness, and residual stress of developed coatings are extensively discussed. Each chapter begins with an introduction and concludes with drawn observations.

Chapter 6: Conclusions and Future Scope

This chapter is dedicated to presenting the conclusions and future Scope of the research study. In this chapter, the culmination of the research findings is articulated, outlining the key insights and discoveries derived from the experimental work. Moreover, the chapter offers a glimpse into the future Scope of research in the area. It identifies potential avenues for further exploration and development based on the gaps, challenges, and opportunities revealed by the current study.

References

Additionally, the seventh chapter lists the references used throughout the thesis, culminating the scholarly journey.

LIST OF CONTENTS

List of Figures

List of Tables

List of Symbols

A	Ampere
cm	Centimetre
cm^{-1}	Per Centimetre
mm	Micrometre
min	Minute
MPa	Mega Pascal
nm	Nanometre
rpm	Rotation Per Minute
s	Seconds
wt. %	Weight Percentage
%	Percentage
°C	Degree Celsius
kW	Kilowatt
θ	Theta
~	Approximately
°	Degree
Å	Angstrom
&	And
m^2	Meter Square
N	Newton
α	Co-Efficient Of Thermal Expansion
A	Ampere
P	Density
q̇	Heating
Vol.%	Volume Percentage
Vf	Volume Fraction
W/m^2	Watt Per Square Meter
$W.m^{-1}.\ °C^{-1}$	Watt Per Meter Celsius
$W.m^{-1}.\ K^{-1}$	Watt Per Meter Kelvin
wt.%	Weight Percentage
%	Percentage
g/min	Gram Per Minute

List of Abbreviations

APS	Atmospheric Plasma Spraying
TPS	Thermal Protection System
CVD	Chemical Vapour Deposition
TSCP	Thermal Spray Coating Process
TST	Thermal Spray techniques
PVD	Physical Vapour Deposition
ED	Electro Deposition
HVOF	High Velocity Oxy-Fuel
EDS	Energy Dispersive Spectroscopy
FE-SEM	Field Emission Scanning Electron Microscopy
Al_2O_3	Aluminium Oxide
HR-TEM	High-Resolution Transmission Electron Microscopy
XRD	X-Ray Diffraction
ASTM	American Society for Testing and Materials
SD	Spray Dried
SiO_2	Silicon Dioxide
T	Temperature
V	Velocity
Ar	Argon
H_2	Hydrogen
N_2	Nitrogen
W	Tungsten
C	Carbon
Re	Rhenium Zirconium Dioxide
ZrO_2	Zirconium Dioxide
HfO	Hafnium Oxide
C-C	Carbon-Carbon

SiC	Silicon Carbide
V_2O_5	Vanadium Pentoxide
$ZrSiO_4$	Zirconium Silicate
ThO_2	Thorium Dioxide
SC	Silicon Carbide
YAG	Yttrium Aluminium Garnet
V_2O_5	Vanadium Pentoxide
WC	Tungsten Carbide
ZrC	Zirconium Carbide
ZrN	Zirconium Nitride
ZrO_2	Zirconium Dioxide
MO	Molybdenum
Ni	Nickel
Cr	Chromium
WR	Wear Rates
NASA	National Aeronautics and Space Administration
LRO	Lunar Reconnaissance Orbiter
L/D	Lift/Drag
COF	Coefficient of Friction
CS	Cold Spray
BSG	Boro-Silicate Glass

Abstract

Degradation of the material because of wear and corrosion pose great challenges for the multiple industrial environments, forcing the researchers for the advance solution to enhance the life and applicability of the materials. To solve these problems, ultra-high temperature composite coatings have emerged as prominent solutions due to their property to mitigate the corrosion and wear of industrial materials.

In the current investigation of composite coating for wear resistance, friction, and corrosion applications at elevated temperature, two ultra-high temperatures composite coatings (ZrB_2-SiC & NiCr-Mo-WC) have been synthesised with Thermal Spray Techniques. The coatings have been developed with the constant process parameters of the machines.

A set of characterisation techniques with scanning electron microscope (SEM), X-ray diffraction (XRD), energy dispersive X-ray spectroscopy (EDS), is used to investigate the morphological attributes of the developed coatings, elemental distribution, and crystalline configuration. Mechanical and tribological properties have been studied with help of Vickers Micro-hardness tester, Pin-on-Disc Tribometer and Pulstec make residual stress analyser. Post hot corrosion test of the developed coating have also been analysed.

Investigation outcomes from the current study showed the exceptional wear and corrosion resistance efficiency of the developed ZrB_2-SiC and NiCr-Mo-SiC composite coatings system, surpassing the efficiencies of the traditional coatings.

The thickness of the ZrB_2-SiC coating was 300-400µm, Value of the (COF) coefficient of friction ranged from 0.57 to 0.7 and wear rate of the coating ($2.02 \times 10^{-3} mm^3/Nm$) was lower than the substrate material ($2.8 \times 10^{-3} mm^3/Nm$). ZrO_2 was formed as protective layer during the corrosion test against the molten sulphate/vanadate salt penetration. This coating has enormous potential to work as corrosion resistant for hypersonic applications. The hardness of the Mo-NiCr-Mo-W composite coating increased notably with the upsurge of temperature with the rise of temperature reaching at the value of 290.8V at 400^oC. Residual stress decreased with the increase of temperature with highest value of 354 MPa at 100^oC.The COF shows it maximum value at 400^oC and minimum at 100^oC while wear rate was maximum at 100^oC. SEM analysis shows that erosion, abrasion, worn surface and layer delamination as prominent wear mechanisms.

Keywords: Composite Coating, Wear Resistance, Corrosion Resistance, SEM, XRD, EDS, Synthesis

Chapter: 1

Introduction

This current chapter delves into a comprehensive exploration of Surface Engineering, Coating, and related aspects. The initial section introduces the Framework, setting the stage for understanding the subsequent discussions. Surface Engineering is then dissected, highlighting the significance of enhancing material surfaces for improved performance. Coating, as a fundamental technique, is discussed extensively, covering Coating Quality and the critical factors influencing it, such as Coating Process Parameters. The chapter explores an array of different coating techniques, ranging from nanostructured coatings and their role in enhancing wear resistance to thermal spray coating techniques like High-Velocity Oxy-Fuel (HVOF) Spray Process, Atmospheric Plasma Spray Process, Flame Spray Process, and Cold Spray Technique. Special attention is paid to Carbide Coatings and Oxide Coatings, with a focus on Thermal Barrier Coatings (TBCs) and Metallic Coatings, including Diamond Coatings.

The discussion then branches into Tribology, expounding on its benefits and properties in the context of friction, wear behaviours, and types of wear, covering various applications like the Piston-Cylinder System and Gas Turbines. The chapter further emphasizes Tailoring Coating Properties to enhance wear resistance and provides insights into Recent Trends in Metal Wear. Lubrication and Corrosion emerge as crucial considerations, with a comprehensive analysis of various Types of Corrosion. The final stretch of the chapter delves into the domain of Thermal Protection Systems (TPS), especially in the context of Hypersonic Vehicles, addressing the unique Challenges faced during hypersonic flight. Overall, the first chapter offers a multifaceted exploration of Surface Engineering, Coating Techniques, Tribology, Lubrication, Corrosion, and their implications in the realm of cutting-edge technologies like Hypersonic Vehicles.

1.1 Background

Friction and wear are consistently recognised as problem creators in moving device assemblies and components operating at a very high temperature. Aerospace, metalworking industries, and power generation units are some examples. It has been seen that wear and friction are responsible for carrying maximum manufacturing costs in the manufacturing industries. This cost is generated due to friction and wear, which consists of energy cost that includes the cost of spending on energy to save the component from friction or overcome the friction.

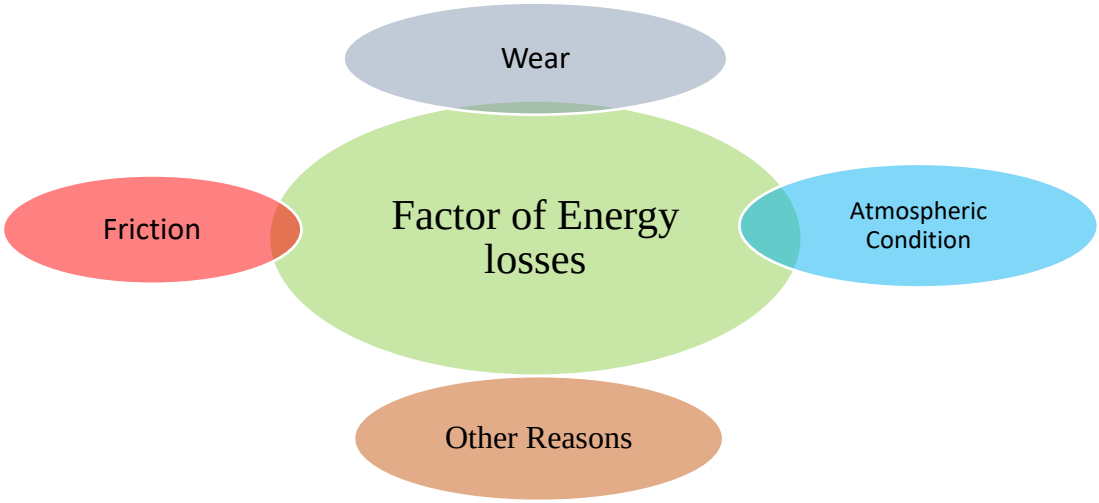

Figure 1.1: Factor of Energy losses

This energy is required to produce, replace, and spare worn-out parts and maintenance linked with this cost. The result of wear on an economic coat of industries is more critical than friction as it could be responsible for the calamitous stoppage and breakdown of machines, part components, etc., which results in high overall costs. According to one study, new spraying methods, new materials, excellent lubrication properties, several surface modification techniques, and many more can reduce friction and wear among the moving parts and save up to 40 % of energy and cost. If this energy is saved, it would be 1.4 % annual GDP of the entire world. The saved energy can be used to protect the environment by reducing carbon emissions by up to 3140 metric carbon dioxide[1].That's why it is essential to control friction and wear to improve product quality, cost, and productivity.

Wear is explained as losing material from the contacting exterior surface when they come near each other. In other words, the material is not entirely lost; it only moves from one surface to another. Wear will be responsible for the performance dropping or complete failure in maximum cases. A system cannot bear high temperatures when it’s lubricated system not able to bear high temperature. Usually, at 300^0C, lubricate starts quickly decompose [2]. At high temperatures, thermal fatigue, increased oxidation, chemical reactions (Tribo) and mechanical vagaries in

material properties occur compared to low temperatures. It has been observed from the literature surface engineering is the best answer to these challenges. Surface engineering is well-defined as properties changing process of materials to get the desired properties that cannot be achieved from the bulk material alone[3]. ST and Coatings with varying thickness, adhesive strength, cost and spalling nature are the important parameters which are needed to consider while developing the coatings. These coatings are used for protecting the surface of components against wear, tear, friction, corrosion and many more. Now a days ceramics coatings are developing due its capability to stand at high temperature for several applications. This means the material can be modified by utilizing surface treatments and surface coatings to get the desired properties. The strengthen and strong coatings can be developed by using bulk materials which protects the components and provide excellent wear resistance and corrosion resistance properties. That's why the bulk materials can be the choice of engineers to producing coatings with low cost[3]. Researchers are rigorously developing coatings that withstand high temperatures and wear resistance worldwide.

Many studies have been done to investigate the wear behaviour at ambient temperature, nonetheless less investigations have been performed on high temperatures which can stand beyond 2000^0C with hard metal coatings. For instance, in hypersonic vehicles, the temperature of these leading edges is passed through 2000^0C at hypersonic flight, which is far above the temperature of the material we know. Usually, Hypersonic is the symbol of speed where the speed is more than Mach 5, or in other words, speed is five times the speed of sound, for instance, ~1, 235 km/h[4], [5] It has been seen that when a hypersonic vehicle travels with a hypersonic speed, its whole body parts are re-exposed to high-temperature heat because of drag at the time of re-entry, and leading edges also suffer from the same as shown in figure 1.2

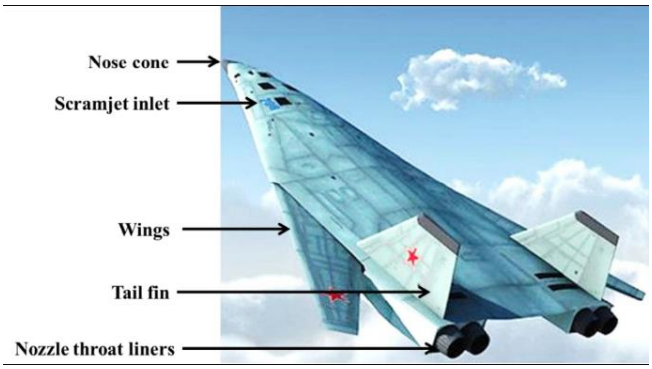

Figure1.2: Displays the leading-edge components of hypersonic vehicle[6].

These parts include the plane nose, wings, scramjets, and tail fins and are subjected to high temperatures and severe thermal exposure[7]. That's why researchers are still working on technology for developing a more efficient coating for airplanes, especially for hypersonic vehicles. These hypersonic vehicles also require a hard metal composite coating that could provide excellent hardness, high wear resistance, hot corrosion resistance, molten salt blend resistance and significant toughness. Molybdenum, tungsten, nickel-chromium carbide, chromium carbide, chromium, etc., are the composite materials that could be used as a hard coat material for applying hypersonic vehicles. These materials can provide corrosion resistance, toughness, and hardness to the substrate materials[8]–[10].In the same concern, Mo particles are employed for improving the melting point, thermal expansion, durability, COF, and strength[11]. In the early days, silicon carbide material was used by NASA (National Aeronautics and Space Administration) for designing space vehicles such as the space shuttle orbiter and LRO (Lunar Reconnaissance Orbiter) by adding large and blunt leading radius edges(figure 1.3)[12], [13].

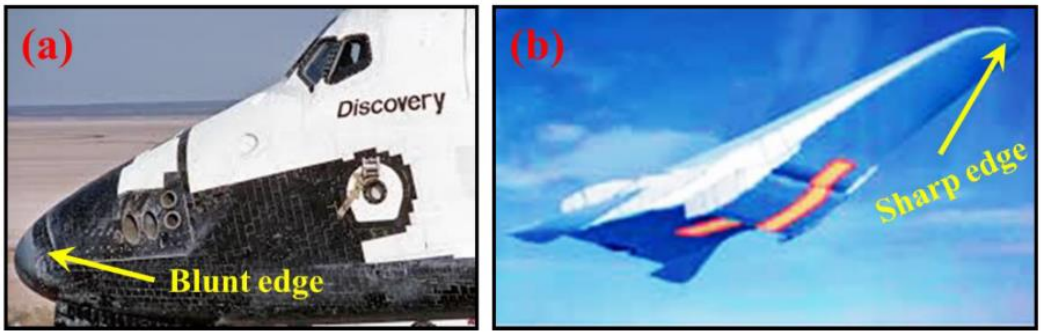

Figure 1.3 (a) Represent the digital image of a space shuttle orbiter with blunt edge[13] (b) Indicate sharp leading edge of hypersonic Vehicle [14].

NASA considers this design to reduce the aerodynamic heating of hypersonic vehicle body parts at 1500^0C throughout the vehicle during re-entry. But, these large body parts of hypersonic vehicles imposed too many drawbacks during the vehicle trajectory, are follows below[15].

- Reduce the L/D ratio (Lift/Drag); this dramatically reduces the vehicle's manoeuvrability.
- It also reduces the ross range of the vehicle at the time of descent from the orbit.
- It enhances the chances of ditching the vehicle ocean and provides less time for aborting the launch.

Thus, Kolodziej et al. used lean aerodynamic shapes and sharp leading edges application [16]. However, the space vehicle temperature rises to 2000^0C if the radius of leading edges is reduced. This is per the empirical relation shown in equation 1.1[17].

$$\dot{q} \cong 1.83 \times 10^{-4} V^3 \sqrt{\frac{\rho}{r_{nose}}}$$ Equation 1.1

Where $\dot{q}$ denotes heating rate of vehicle's (W/m^2), V represents the velocity (vehicle) (m/s), ρ: Air density (kg/m^3)

r_{nose} : vehicle's nose radius (m).

From the above-said relation, it is clear that the temperature of the leading edges grows at a high rate reducing the radius of leading edge structures such as nose cones, tails fins, and wings, as the heating ($\dot{q}$) contrariwise proportional to the square root of leading-edge radius (nose)[17].

Figure 1.4 a shows the severe bow shock waves at sharp leading edges, nose cones, wings, tail fins, and scramjet at hypersonic speed. Figure 1.4 b shows the interaction between the bow shock waves and a hypersonic vehicle's leading edges (sharp). The shock off-land distance is between the bow shock and the location on the leading edge, facing directly into the airflow (stagnation point). The atmospheric air or gas molecules such as N_2 and O_2 started to flow in the compressed state with static enthalpy, high density, temperature, and high pressure. It has been seen that when compressed gases with high enthalpy impose on the surface of sharp leading edges, a boundary layer forms along the surface, as shown in Fig 1.4b. The N_2 and O_2 molecules separate from each other and become highly reactive N and O atoms on the surface leading edges. All these occurrences coincide during hypersonic flow; the old SiC-based material is more prone to failure from thermal shocks, high temperatures, melting, and oxidation. Wuchina et al., reported that using conventional SiC-based material as sharp leading edges results in active oxidation and direct formation of the SiO gaseous phase at 1350 °C instead of having a protective SiO_2 layer [5].

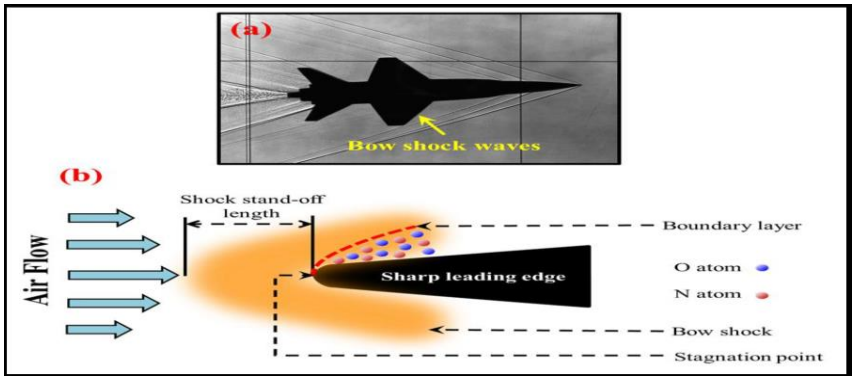

Figure 1.4 (a) Represent the formation of bow shock waves along the sharp leading edges of the hypersonic Vehicle [46] and (b) is the schematic illustration of hypersonic bow features [47].

Further, they also stated about the decomposition of already formed SiO_2 layer into SiO gas at extremely high-temperature environments, i.e., beyond 2000 °C. Hence, it is evident that new materials are required for sharp leading edges of hypersonic vehicles to withstand extreme temperatures and thermal shocks.

Seeing the literature, the researcher can decide on the materials required to identify a significant potential for structural application in hypersonic vehicles. The required properties of materials are shown as follows [15], [18], [19]:

- The melting temperature of the material should be more than 2000 °C.
- The material should have high strength at temperatures more than 2000 °C.
- The material should higher conductivity, i.e.,>14.5 $W.m^{-1}. K^{-1}$.
- Oxidation resistance should be <80 gm^{-2} above 2 Hour at 1400 °C.

Figure 1.5, bar shows the melting temperature of various high-temperature materials, including oxides, borides, and nitrides elements [20].

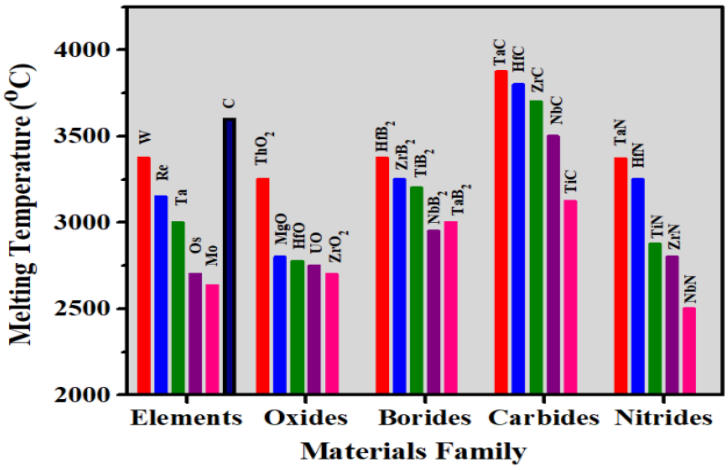

Figure 1.5: Depicts the melting temperature of various materials family [5].

Several non-oxide materials, such as tungsten (W), carbon (C), and rhenium (Re), carry a melting point of more than 3000°C. These materials were observed as active material which goes oxidation and forms solid, liquid, or gaseous reaction products that would provide safety to space vehicles. Further, the metal oxides like hafnium oxide (HfO), zirconium dioxide (ZrO_2), and thorium dioxide (ThO_2) were not considered because of their low thermal conductivity values (1.9 – 3.6 $W.m^{-1}. K^{-1}$), which leads to poor dissipation of heat under extreme temperature (> 2000 °C) [5]. Ceramic materials with mechanical solid, thermal, and chemical strength can be used at extremely high temperatures. The materials in these applications are subjected to high temperatures and a flowing environment and are highly reactive (e.g., O, O_2) [5], [6]. Chemically, thermally, and mechanically stable candidates for the material are also required. The

relevance and high demand for UHTC applications have increased research and development efforts to produce UHTCs. A functionally sound/stable UHTC requires temperatures between 1000 and 2000 °C[21][22]. The ZrB_2-SiC-based coating system is now receiving a lot of interest among other coating systems. ZrB_2 is the widely explored UHTCs material due to its higher value of thermal conductivity, i.e. (58.2 W m^{-1} K^{-1}), high melting point (3519 K), advanced electrical conductivity, relatively less density (6.09 g/cm^3), low thermal expansion's coefficient (5.8 x 10^{-6} °C^{-1}), strong thermal shock resistance, and high hardness [23][17]. Because of these properties, these coatings (ZrB_2-based) are used as TBCs in the thermal protection system (TPS). Thermal Barrier Coating (TBCs) results grounded on ZrB_2 are frequently used. Furthermore, ZrB_2-based coatings protect C-C (carbon-carbon) composites from oxidation at elevated temperatures by work through abstraction -resilient coatings. Therefore, Carbon/Carbon composite is the best choice for structural and thermal components.

Although ZrB_2 is oxidized at high temperatures, its applicability has been severely limited. Several investigations have been conducted on ZrB_2 oxidation behavior, and several strategies have been devised to increase ZrB_2 oxidation resistance. The amalgamation of ZrB_2 and SiC growths the oxidation resistance at 1000–1800 °C with building of low impulsive Boro-Silicate Glass (BSG) with decreased oxygen permeability[24]. Researchers employed in high- rise temperature conditions to tolerate oxidation, corrosion, and wear. ZrB_2-SiC ceramics modernly react with air at 800–1200°C, yielding ZrO_2 and B_2O_3. A protective scale of molten B_2O_3 can be applied to boost oxidation resistance. As the temperature rises, the SiO_2 layer is developed on the surface due to the oxidation of SiC, which can further restrict oxygen entrance into the matrix [15], [25]. Simultaneously, $ZrSiO_4$ may be produced by reacting ZrO_2 and SiO_2, which enhances the resistance to oxidation for the coating system. Incorporating a Silicon Carbide ceramic into ZrB_2-dependent ceramics can noticeably upgrade oxidation performance within the moderate elevated-temperature kind, with the ideal quantity of Silicon Carbide ranging from vol% of 15% to 20%.

The oxidation performance of ZrB_2-based ceramic coatings is studied, at high temperatures. In maximum studies, the impact of ZrB_2 density has been calculated, but no studies performed on the hot corrosion behaviour of ZrB_2-SiC composite coatings against the corrosive salt environment of V_2O_5 and Na_2SO_4 at temperatures more than 900 ^{0}C[20]. The result is to prevent this hindrance, i.e., in the molten salt flow of ZrB_2-SiC. The present research aims to develop the ZrB_2-Silicon carbide (SC) plasma spray coatings on an Inconel-718 substrate for protecting hypersonic vehicles from hot corrosion.

A work showed by[22] Shrirshendu et al., found that the wear resistance of ZrB_2-TiB_2 had shown excellent wear-resisting behaviour due to fracture toughness and hardness. Jitendra et al., investigated the effect of COF while increasing the formation of tribo-chemical films and found the value of COF decreased[26]. Some studies also settle on study of the wear and oxidation behaviour of APS(Atmospheric Plasma Spray)ZrB_2 grounded coatings.

Researchers are working towards developing a composite coating that can offer excellent hardness, wear resistance at high temperatures, hot corrosion resistance, hard composite coating for wear resistance, and hot corrosion resistance applications.

The surface engineering techniques help retain substrate mechanical properties while providing hardness or corrosion-resistant layers at the surface. Traditional surface modification methods such as nitriding, boriding, or carburizing suffer from 3 disadvantages: long treatment time, uneven treatment depths, higher costs, and damage environment by releasing a large amount of CO_2. Thermal spraying practices. Chemical Vapour Deposition (CVD), Physical Vapour Deposition (PVD), and are cast-off widely for different wear and corrosion applications. But in comparison, thermal spray coatings have better properties, higher coating thickness, and lower application costs and are less damaging to the environment than other processes [27].

Among different coating methods, thermal spraying techniques can spray the most comprehensive materials with an extensive range of coating thickness and coating properties. Due to these advantages, Thermal Spray Techniques continuously used in many applications such as automobile, mining, aviation, thermal power plant, printing, orthopaedic and dental implants, etc.

However, less research has been done on studying high temperature and hot corrosion tribology-related applications such as Hypersonic Vehicles, the performance of HVOF, and thermal spray technique, respectively. The compositions of materials for surface coating on hypersonic vehicles must be developed, and their uses at high temperatures must be studied further. The aim of the current research is to recognize composite coating compositions and tribological behaviour of synthesize coating at high temperatures and in the environment of hot corrosion, thus do develop the knowledge and gaining noble knowledge. HVOF-sprayed Mo-NiCr-W-WC and thermally sprayed **ZrB_2–SiC** are applied to the substrate material and tested against high temperature, oxidation resistance, and hot corrosion.

Mo-NiCr-W-WC is the self-fluxing alloy. Kashani et al.[28], investigated hard coatings, which are Ni-based, provide excellent wear resistance to forging dies when mixed with cobalt. This happens to die to the formation of compact oxide when it is exposed to high temperatures at sliding conditions[29].

It has been seen that when the researchers require the amalgamation of corrosion and wear, these two are taken together (NiCrBSi) and showed a most attractive option in the case of Ni hard-facing alloys [30][31]. Thus, good metallurgical interface bonding is achieved due to their lower melting point and good mixing characteristics that make them the best [5]. Because of this, NiCrBSi alloys provide various applications in surface coatings, repair, and manufacturing [32]. Kaiming et al.[33] added 10 percent Mo and carbides in Ni-based hard coatings and found improved microstructure and better wear resistance capability of outcome composite that has produced for NiCrMo steel plate.

Hou et al.[34] also mixed NiCrBSi with Mo and found good wear-resisting properties with uniform microstructure at room temperature. But unfortunately, their work falls short in the worn surface characterization and testing mechanism of the wear mechanism. Additionally, the addition of Mo in the fabricated coatings has shown the introduction of the oxide layer (thin) and forms MoO_2 at the time of rubbing. Mo enhanced the hardness, decreased COF, and acted as a solid lubricate[35], [36].

In this respect, the current study is conducted on HVOF spray, a deposited composite mixture of MO and NiCr-W-WC powders) to enhance the wear resistance associated with creating molybdenum oxide, which is present on a layer of worn surface [34] .

Grigorescu et al.[37] also found that adding chromium to the complex phase alloy powders can enhance corrosion and wear resistance.

Zikin et al.[38]also investigated the repeated impact nature of abrasive wear of NiCrBSi hard-facing powders when reinforced with plasma-sprayed TiC-NiMo and Cr_3C_2-Ni at cladding temperatures of 550, 350, 700 and 20°C. In the obtained result, it has been found that at a room temperature of 650°C, the wear rate of TiC-NiMo increased, while hard coatings of Cr_3C_2-Ni illustrated the uniform behaviour from 350 °C to 650 °C.

Garcia et al.[39] and Ahn et al.[40] described WC, NbC, Cr_3C_2, TiC, SiC, VC, and WC-Ni hard reinforcement particulates to NiCrSiFeBC matrix. Outcome showed enhance wear execution. Tungsten Carbide generally present rigid coating is always cast-off for wear resistance usage because of their promising possessions like high hardness, high M.P, and low thermal expansion COF Gupta et al.[41], Kaushal et al.[25].

Currently, industries are adopting several coating spray technologies, such as HVOF, atmospheric spray, etc. The wear resistance affects the coating microstructure and properties such as sprayed coating, hardness, porosity, oxidation, particle degradation, and decomposition of the hard phase. The HVOF spray technology increased in popularity because of its machinery portability and could be applied in industry. It has been observed that the coating quality received

from HVOF spray technology provides the best properties (such as the highly fine, densely packed structure of particles of molten splat) compared to other coating techniques. According to [42], HVOF-coated coatings possess a low content of oxides that is less than 1% because of low in-flight oxidation. On the other hand, atmosphere plasma spray technology is also used by industries to reduce wear among the components. Parthasarathi et al.[43] used APS technology for spraying NiCrBSi coatings onto the different substrate material.

1.2 Surface Engineering

Surface engineering techniques consist of various surface treatments/ coatings applied to change the component surface's mechanical, chemical, and physical properties without changing the bulk properties. Many mechanisms causing failure, namely abrasion, adhesion, plastic deformation, etc., occur at the tool-work-piece interface's intersection. Surface engineering via surface treatment or coating provides desired wear resistance/ corrosion resistance at the surface according to the application requirement, while the bulk material provides mechanical strength/ toughness. The assortment of a specific surface modification technique depends upon the application's requirements. The main approach to decreasing wear and improving components' life is to protect the surface from the dominant wear mode. Surface engineering processes include thermal treatments (flame hardening, induction hardening, and laser hardening). In these techniques, the surface of steels is heat-treated by heating them above austenitizing temperature and then cooling them quickly to form hard, wear-resistant surfaces. Thermally assisted diffusion processes are very popular in the surface treatment of die steels. These techniques include carburizing, nitriding, boriding, etc. Thin Surface coatings (thickness up to 500 μm), hard carbides, and nitrides are applied on the surface by employing numerous techniques such as PVD CVD, chemical processes (such as phosphating, anodizing, etc.), electroplating. Thick coatings are developed generally by welding or thermal spraying processes[44].

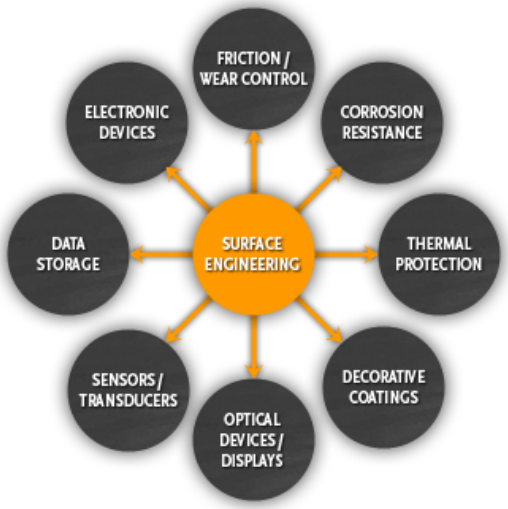

Figure 1.6: Application of Surface Engineering

De Masi-Marcin and Gupta (1994) reported that the CVD technique requires adequate masking and special tooling, which makes this technique quite expensive [45]. Illavsky et al. (2000) stated that the coating prepared by thermal spray results in better properties at lower costs and fewer environmental issues compared with CVD, PVD, and hard chromium plating[46]. The lamellar splats typically formed in a thermal spray process are parallel to the surface and provide better resistance to applied mechanical load than PVD deposits that are columnar and perpendicular to 24 the surface (Chattopadhyay, 2001). Moreover, Nicholls and Stephenson (1995) reported that overlay techniques such as thermal spray improved results in high-temperature applications[47].

1.3 Coating

Coating techniques are processes used to apply a layer of material onto a substrate surface for various purposes, such as protection, decoration, functionalization, or enhancement of specific properties. Air Spray method uses compressed air to atomize the coating material into small droplets, which are then sprayed onto the substrate. HVLP (High Volume Low Pressure) Spray: Similar to air spray, but it uses lower pressure to reduce overspray and increase transfer efficiency. In Electrostatic Spray the coating material is charged, and the substrate is grounded, causing the charged particles to be attracted to the substrate for uniform coverage[48]. In Airless Spray a high-pressure pump forces the coating material through a small orifice, breaking it into fine droplets that are sprayed over the base materials. In Dip Coating the base material (Substrate) is immersed into a container of the coating material, and as it is withdrawn, the excess material drips off, leaving a uniform coating on the substrate. Spin Coating the substrate is placed on a spinning platform, and a small amount of liquid coating material is dispensed at the centre.

Centrifugal force spreads the liquid across the substrate, creating a thin, uniform coating[49]. Roll Coating the substrate passes between two rollers, one of which is partially submerged in the coating material. The material is transferred from the roller to the substrate[50]. In Physical Vapour Deposition (PVD) evaporation or sputtering is used to deposit material in a vacuum chamber onto the substrate. Common methods include evaporation, magnetron sputtering, and ion plating. In Chemical Vapour Deposition (CVD) gases containing the desired coating material are introduced into a chamber, where they react and deposit a solid coating onto the substrate[51]. Electroplating is a process where metal ions in a solution are reduced and deposited onto a conductive substrate under the influence of an electric current. Anodizing is an electrochemical process that enhances the thickness and density of the naturally occurring oxide layer over the metal surface like aluminium, creating a protective and decorative coating. In Powder Coating finely ground particles of coating material are electrostatically charged and sprayed onto a grounded substrate. The coated substrate is then heated, causing the powder to melt and form a continuous film. In Sol-Gel Coating a solution containing precursors of the desired material is applied to the substrate, and through controlled chemical reactions, a solid coating is formed as the solvent evaporates. In Plasma Coating plasma is used to create high-energy, reactive species that interact with coating materials, leading to enhanced adhesion, improved properties, or the formation of thin films[52]. In Laser Cladding a laser beam is used to melt and fuse coating material onto a substrate, creating a metallurgical bonded coating layer. Physical Masking techniques such as stencilling, masking tape, or photoresist are used to selectively shield parts of the substrate from the coating process, creating patterned or masked coatings[53]. These coating techniques are just a subset of the many methods available for applying coatings to different types of substrates in various industries, including manufacturing, electronics, automotive, aerospace, and more. The choice of coating technique depends on factors such as the substrate material, desired properties, cost-effectiveness, and application requirements.

1.4 Coating Quality:

Quality parameters for the composite coatings can vary on the basis of application and utilization of the coating. However, here are some common quality parameters that are often assessed when we evaluate the quality of composite coatings[54].

Figure 1.7: Quality parameters

i. **Adhesion Strength:** The strength of the bond amid the coating and the base material. A strong adhesion ensures durability and prevents delamination.

ii. **Thickness Uniformity:** The evenness of the coating's thickness across the base material. Inconsistent thickness can lead to variations in performance and properties.

iii. **Microstructure:** The internal structure of the composite coating, including the distribution of reinforcement materials. A uniform microstructure contributes to consistent mechanical and thermal properties.

iv. **Porosity:** The presence of voids or pores within the coating. Excessive porosity can weaken the coating and reduce its protective capabilities.

v. **Corrosion Resistance:** The ability of the coating to protect the substrate material from corrosion and environmental degradation.

vi. **Wear Resistance:** The coating's ability to withstand abrasion and wear, which is crucial for applications in high friction environments.

vii. **Hardness:** The resistance of the coating to indentation or scratching, indicative of its overall durability.

viii. **Coefficient of Thermal Expansion:** The change in size of the coating due to temperature fluctuations, which should match that of the substrate to prevent cracking.

ix. **Thermal Conductivity:** The ability of the coating to transfer heat, which is important in applications where thermal management is critical.

x. **Electrical Conductivity:** Relevant for coatings used in electronic or electromagnetic applications, where specific electrical properties are required.

xi. **Surface Finish:** The texture and smoothness of the coated surface, which can impact

aesthetics, functionality, and ease of cleaning.

xii. **Chemical Resistance:** The coating's ability to resist chemical interactions, crucial in environments where exposure to corrosive substances is likely.

1.5 Composite Coating[55]

Composite coatings involve the application of a layer or film containing a combination of different materials to a substrate surface. These coatings are designed to take advantage of the unique properties of each constituent material, resulting in enhanced overall performance.

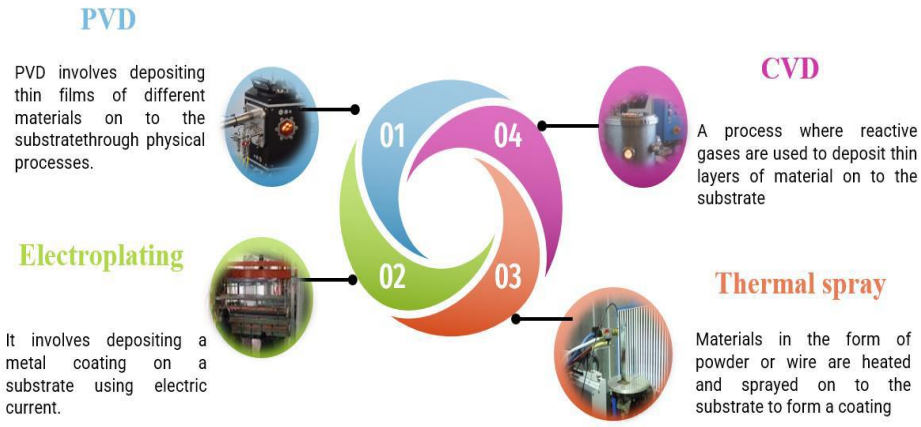

Figure 1.8 Composite Coating Fabrication Techniques

Composite coatings find applications in various industries, ranging from aerospace and biomedical fields. It's important to note that designing and applying composite coatings can be complex due to the interactions between the different materials and their processing methods. The choice of materials, preparation techniques, and deposition methods play a significant role in achieving the desired properties and performance of the composite coating [56].

1.5.1. Advantages of Composite Coatings:

Composite coatings can consist of different materials, including polymers, metals, ceramics, nanoparticles, and more. The selection of materials based on the required properties and the specific application. Some common types of composite coatings include [57]. Composite coatings offer several advantages over single-material coatings. Despite significant attempts to create novel coating system, only a few, largely "simple-structured" films were successful and are still in demand. The majority of saleable PVD and CVD coatings are made up with the help of a mono layer that frequently only contains one (or two) single phases. It required high cost for tool cost and storage dumping [58].

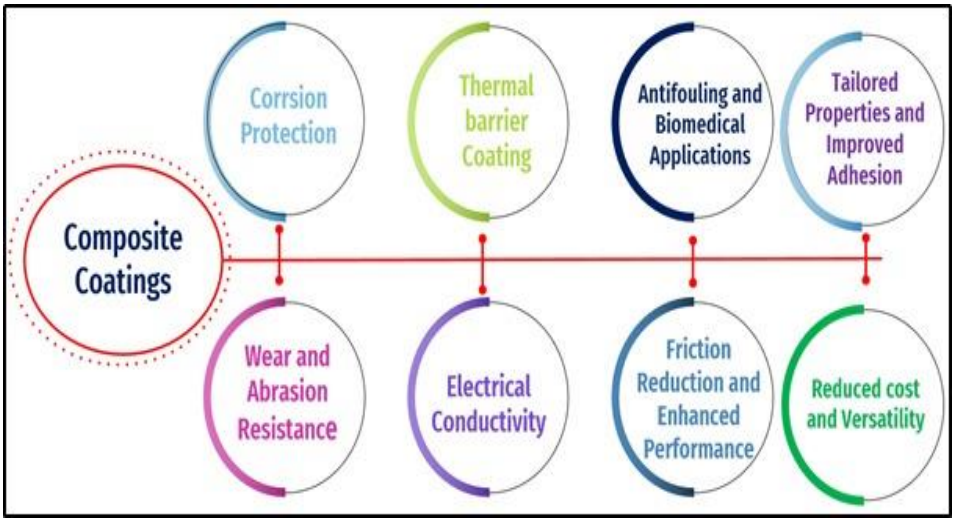

Figure 1.9 Advantage of Composite Coating

1.5.2 Application of Composite Coatings:

Composite coatings consists a broad range of applications, including[59].

I. **Wear and Abrasion Resistance:** In industries like manufacturing, mining, and aerospace, composite coatings can provide enhanced wear resistance and prolong the lifespan of components.

II. **Corrosion Protection:** Composite coatings can protect substrates from corrosion in harsh environments.

III. **Electrical Conductivity:** Composite coatings with conductive materials are used in electronic and electrochemical applications.

IV. **Biomedical Applications:** Composite coatings can provide biocompatibility and controlled drug release for medical implants.

V. **Thermal Barrier Coatings:** These coatings are used to protect components from high temperatures in aerospace and gas turbine engines.

VI. **Aerospace and Aviation**: Composite coatings are utilised in aerospace applications to improve the performance and longevity of aircraft components. They offer resistance to wear, corrosion, and high temperatures, making them ideal for engine components, landing gear, and structural sections.

VII. **Automotive Industry:** Composite coatings are employed to improve the wear resistance and frictional properties of engine components, such as pistons, cylinders, and crankshafts. These coatings contribute to improved fuel efficiency and extended engine life.

VIII. **Oil and Gas Industry:** Oil and gas industry used part components are frequently exposed to adverse and corrosive environments. Composite coatings provide corrosion resistance and anti-wear qualities for components such as valves, pumps, and pipelines, extending their life and lowering maintenance costs.

IX. **Industrial Machinery:** Composite coatings are used on industrial equipment such as pumps, bearings, and rollers to increase durability, reduce friction, and save downtime. This increases the productivity and efficiency of production processes.

Figure 1.10 Applications of Composite Coatings

1.6 Different Coating Techniques[42]

Coating techniques can be classified based on various criteria, including the method of application, the nature of the different coating material and the intended purpose of the coating. Remember, these classifications are not exhaustive, and coatings can often fall into multiple categories. The choice of coating technique and material depends on factors such as the intended application, performance requirements, environmental considerations, and cost-effectiveness.

1.6.1 Thermal spray Coating Process

The term thermal spray defines coating processes that utilize an energy source to heat and propel coating material on the substrate to form relatively thick coatings. The sprayed material is initially in powder, wire, and rod. The sprayed particulates are in a half-molten or fully molten state in these methods, and they form mechanical bonds upon impact with the substrate. These processes are very flexible and are used to spray different metallic-based and non-metallic-based materials for protection against wear, erosion, corrosion, and fatigue. Any material can be thermally sprayed if it doesn't putrefy, evaporate, transfer, or disconnect on heating. These

methods could coat materials with very low melting points without excessive heating or grain structure distortion of the substrate. When the coatings are damaged after prolonged exposure to working conditions, thermal spray coatings can be stripped off and re-applied without changing substrate properties or dimensions.

These processes are classified according to the heat source into 3 important classes, i.e., Flame spray, electric arc spray, and plasma arc spray. From a wide variety of Thermal Spray techniques accessible, choosing a specific technique be contingent upon the necessities of components, the flexibility of materials required for specific applications, and the cost of coating, which the industry can pay [42], [60].

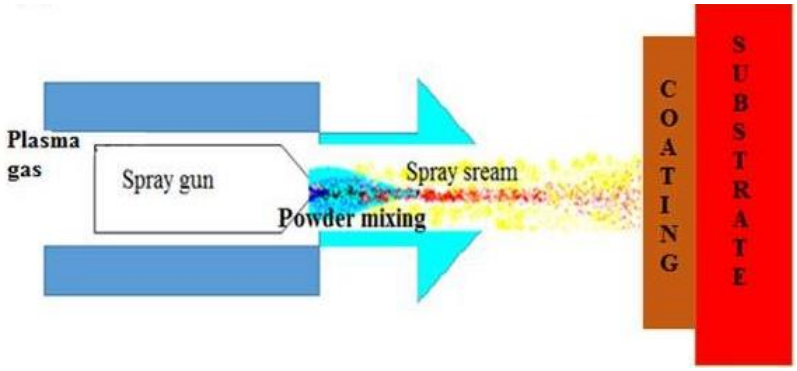

Figure 1.11: Systematic diagram of thermalspray process [61]

Very high particle temperatures and high particle speeds (50 to >1000 m/s) produce coatings with a characteristic lamellar structure consisting of layers of compressed splats formed after each pass of the spray torch. The coated particles cool very quickly to form uniform, fine-grained and hard coatings. Some porosity (between 0-10%) and oxide inclusions are inherent to these processes, which post-treatment can reduce.

1.6.2 Classification of Thermal spray Coating Process

Advanced coating methods called thermal spray techniques are utilized to apply a variety of materials on a variety of surfaces. These methods entail melting or softening the coating substance before projecting it onto the substrate, where it hardens to create a layer that is either protective or useful. Different thermal spraying methods have unique characteristics and are appropriate for varied applications. The selection of method hinge on aspects like the substrate material, application environment, economic concerns, coating material and desired qualities. Thermal spray processes listed below each have strengths and drawbacks. Here are some common thermal spray techniques and their roles.

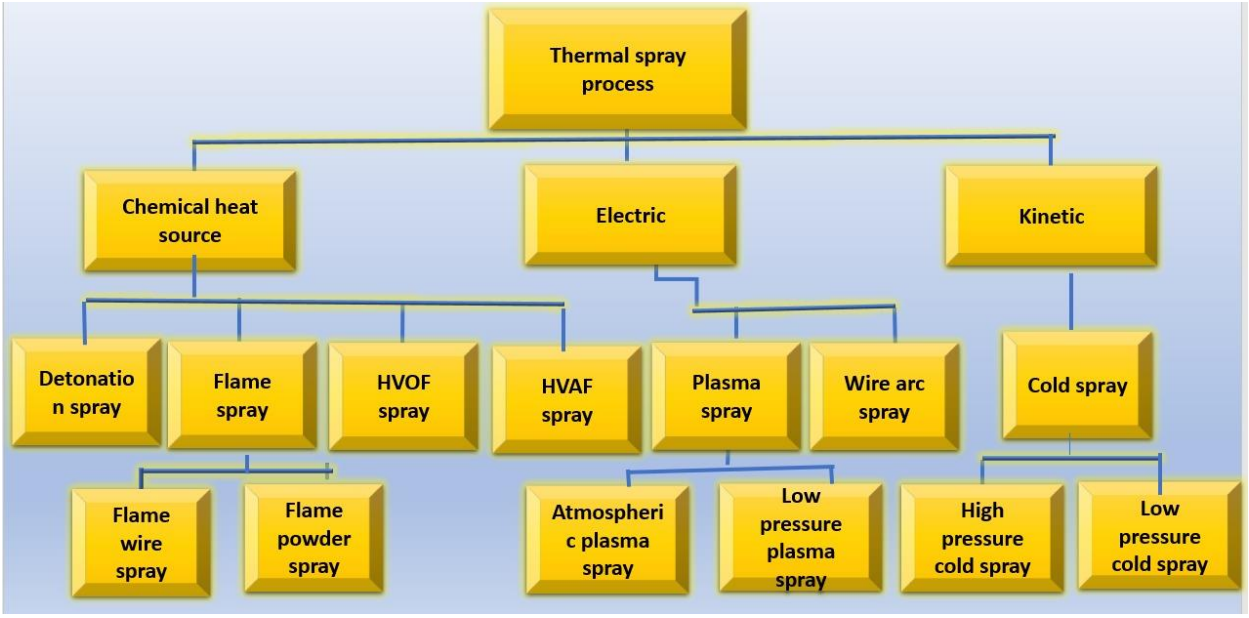

Fig 1.12 Classification of various thermal spray coating processes

1.6.2.1 High-Velocity Oxy-Fuel (HVOF) Spray Process

HVOF spray is utmost popular thermal spray technique due to the more properties of as-sprayed coatings produced by it. This process supplies much fuel gas and air into a combustion chamber. These gases expand and exit through a long nozzle (8 to 30 cm long) upon combustion. The convergent and divergent design of the nozzle results in supersonic gas speeds (1500-1800 m/s)[8], [48]. Hydrogen, propylene, propane, acetylene, and kerosene are mostly used fuel gases. Air is also supplied for combustion. Air or water cooling is employed for cooling the combustion chambers and barrel of HVOF guns. A carrier gas such as helium, nitrogen or argon feeds the coating powders into a barrel. The powder particles are heated up to 3300°C and reach speeds up to 1000 m/s [8]. These particles impinge on the substrate with huge forces and produce very dense coatings with very low porosity, excellent adhesive and cohesive strength, and low oxide content. The in-flight particle temperature and oxidation are quite low compared with other thermal spray processes, this aspect makes HVOF particularly suitable for applying hard cermet coatings such as WC/Co or Cr_2C_3/NiCr. The minimal decomposition of WC into W_2C occurs in this process, which helps the cermet coating retain its hardness. Low particle temperature also ensures that the coating leaves a low thermal imprint on the substrates and consequently they do require any stress-relieving. When the spray parameters and conditions are optimized HVOF coatings produce bond strength more than 80 MPa and porosity of less than 1%. High impact forces also produce high compressive residual stresses in the coatings which are beneficial in most of the coating applications. HVOF has helped in spreading the spectrum of thermal spray to new applications by spraying powders of particles which couldn't be sprayed by any other

thermal spray technique. The gases leaving the nozzle have such high speeds that “shock” diamond patterns are visible which are generally exhibited by supersonic jet aircraft. These high speeds are accompanied by very high noise levels up to 135 decibel.

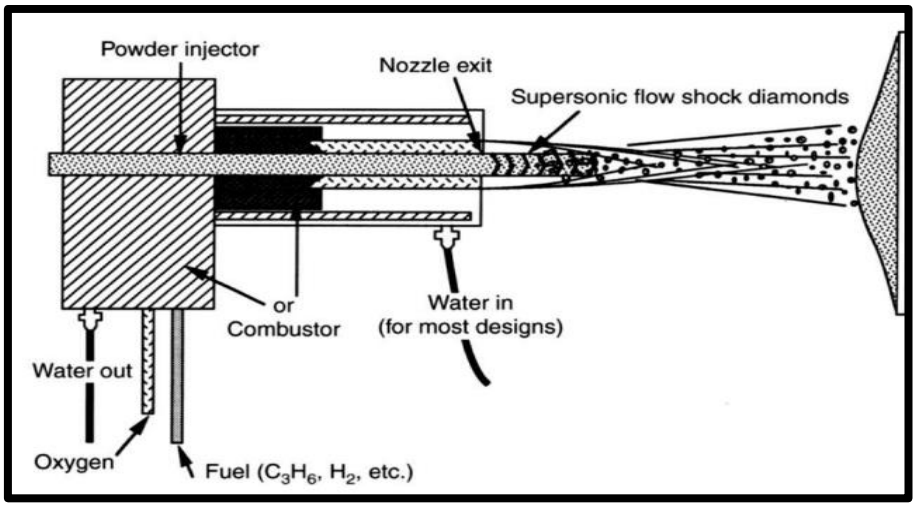

Figure 1.13: Representation of the HVOF spray process [48]

HIPOJET-2700M GUN: Powder is sprayed with supersonic velocity using a spray gun. When employing fuel gases like LPG (liquefied petroleum gas), propylene, propane or natural gas, the typical gun can be set to spray HVOF-grade powders. The HIPOJET-2700M Gun from MEC is used as a powder sprayer in our current study [26]. Figure 2.9 displays the schematic for the HIPOJET-2700M Gun of the HVOF thermal spray system. The gun's internal axial-feed powder injection is one of its design elements. With the aid of specially designed water-cooled gas mixing and combustion chambers, high thermal efficiency,

Figure 1.14: HVOF Spray Gun

maximum particle heating, and unrestricted gas and powder movement are all made possible. Because of the dense, low oxide coatings that are produced by high particle velocities, operating costs are reduced. The overall design is compact and streamlined because every hose connection enters the gun axially. Simple maintenance methods are made possible by the gun's flexible body design.

Grid Blaster: Utilising dry compressed air, an additive layer is applied to substrate materials using a pressure blaster of the MEC PR-9182 model. High-velocity abrasive particles are released from the blast nozzle and utilised to remove or prepare substrate materials. Pressure blasting cabinets are used to collect the dust created during the blasting process as well as to ventilate the blasting chamber of dust and fumes while reducing noise levels. In this, dust is collected using a high-efficiency fabric dust. The figure displays the HVOF thermal spray system's pressure blaster's systematic diagram.

Figure 1.15: Systematic diagram of grid blaster of HVOF system

DUST COLLECTOR: It is a form of mechanical separator that uses centrifugal force as its operating mechanism to separate metals or dust particles from the air steam of the spraying zone. Additionally, it offers large separation velocities. The figure depicts the HVOF thermal spray system's spray chamber in systematic way.

Figure 1.16: Systematic diagram of HVOF dust collector

Control Panel: The MEC makes the control panel model, which connects the gun to the gas supply and serves as the system's brain, one of the most crucial components of the HIPOJET-2700M HVOF powder spray system. It is a priceless piece of equipment utilised to gauge and control the flow of oxygen, air and fuel gas to the HVOF powder flame spray cannon. It is one of the most trustworthy gas flow indicators and helps with the best coating. It is a tough gadget designed to control and securely monitor the oxygen, fuel gas, and air flow to the HIPOJET-2700 Spray Gun. Due to its connection to both the gas supply and the gun, it serves as a reliable gas flow indication and aids in providing the best coating quality.

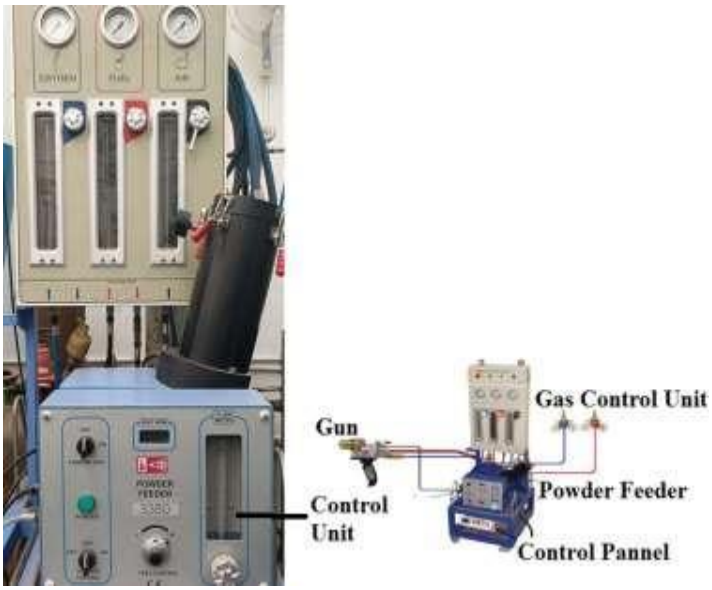

Figure 1.17: HVOF powder spray system

One pressure gauge each for oxygen (0–21 kg/cm^2), fuel gas (LPG or propane) (0–10 kg/cm^2), and air (0–10 kg/cm^2) are present on this console. The pressure can be changed thanks to the installation of gas regulators and air regulators on gas cylinders and air control units, respectively. The control panel also has three flow metre (one for oxygen, one for fuel gas and one for air) to measure the flow of these gases in SLPM. The graphic displays the control panel's schematic diagram for the HVOF thermal spray system.

Powder feeder: In thermal spray applications, the MEC PF-700/PF-3350 powder feeder is employed as an exact powder feeder system. The powder feeder system consists of a pressurized powder container filled with powder that feeds into a slot in a powder wheel. The powder feed hose receives the powder from the powder wheel, and the carrier gas then transports the powder to the spray gun [26]. The powder wheel at the base of the canister has slots that are filled with powder. The rotating powder wheel pushes the powder into the exit holes. An inert carrier gas transports the powder from the exit ports through the powder hose and onto the thermal spray gun. The technology is built to withstand the spray environment. The blanket heater has a programmable temperature control with adjustable increment. The figure displays the HVOF thermal spray system's powder feeder in a systematic diagram.

Figure 1.18: Systematic diagram of powder feeder of HVOF system

1.6.2.1.1 Advantages of the HVOF System

HVOF process provides coatings with excellent mechanical properties mainly due to very high spray particle velocity. Following are the main advantages of HVOF technique over other methods [8], [60]

- Effective heating of sprayed particles caused by high turbulence in the combustion zone.
- High particle speeds result in very low exposure time, leading to low particle oxidation compared to other thermal spray methods.
- The mixing of air with sprayed particles is almost eliminated.
- Particle temperatures achieved in HVOF spray are much lower (around 3000^{o}C) than other techniques like plasma spray, flame spray, and arc spray.

The desired flame temperature in an HVOF system can be achieved by using suitable fuel and altering the fuel-air ratio. The particulate temperature depends on the powder injector location, angle, carrier gas, and powder flow rates. Improvement in the design of HVOF guns has led to improved coating quality over time. The first and second-generation HVOF guns, such as Top Gun, Jet-Kote, etc., could work at 3-5 bar combustion pressure, and typical coatings like WC-Co could be accelerated to about 450 m/s. But the third-generation spray guns like Diamond Jet Hybrid 2600 and 2700, JP-5000, etc., can withstand 6-10 bar combustion pressure safely, resulting in improved spray rates and particle speeds ([8], [62]). The HVOF system used in the current work consisted of HVOF spraying gun, powder feeding system, hoses for supplying carrier and fuel gas, gas regulators, and air-cooling circuit.

1.6.2.2 Atmospheric Plasma Spray Process (APS)

In the plasma spray process, a very high DC voltage ionizes gases like argon, helium, nitrogen, etc. These ions recombine with free electrons and release a large amount of heat energy resulting in a plasma jet temperature of 10,000 K[63]. Heat and expansion cause gas acceleration within the torch. To achieve desired plasma jet and particle velocities the nozzle exit is designed accordingly. A convergent/ divergent nozzle is used to achieve supersonic jet velocities. But in many designs, subsonic velocities are desired to achieve higher dwell time. The plasma electrodes are generally made of tungsten doped with inert elements. Coating powders enters the 28 jets either radially or axially. The powder particles get heated (and melted in most cases) and impact on the substrate with high velocities. The molten splats cool and solidify to form coatings. Due to high particle temperature, a higher degree of melting, and comparatively higher particle speeds in the plasma spray process, the coatings produced have higher density and bond strength than electric arc and flame spray coatings. When spray parameters are optimized for a particular coating, low porosity values (less than 1%) comparable with detonation gun and HVOF spray could be achieved. The high kinetic energy imparted to powder particles leads to effective particle deformation on impact, and increased heating/melting promotes particle flow and deformation. Due to the high temperatures achieved in the plasma jet, almost any liquid phase

material can be melted and sprayed using this technique with minimum distortion of the base material. This makes plasma spray the most versatile spray technique in terms of materials that can be coated.

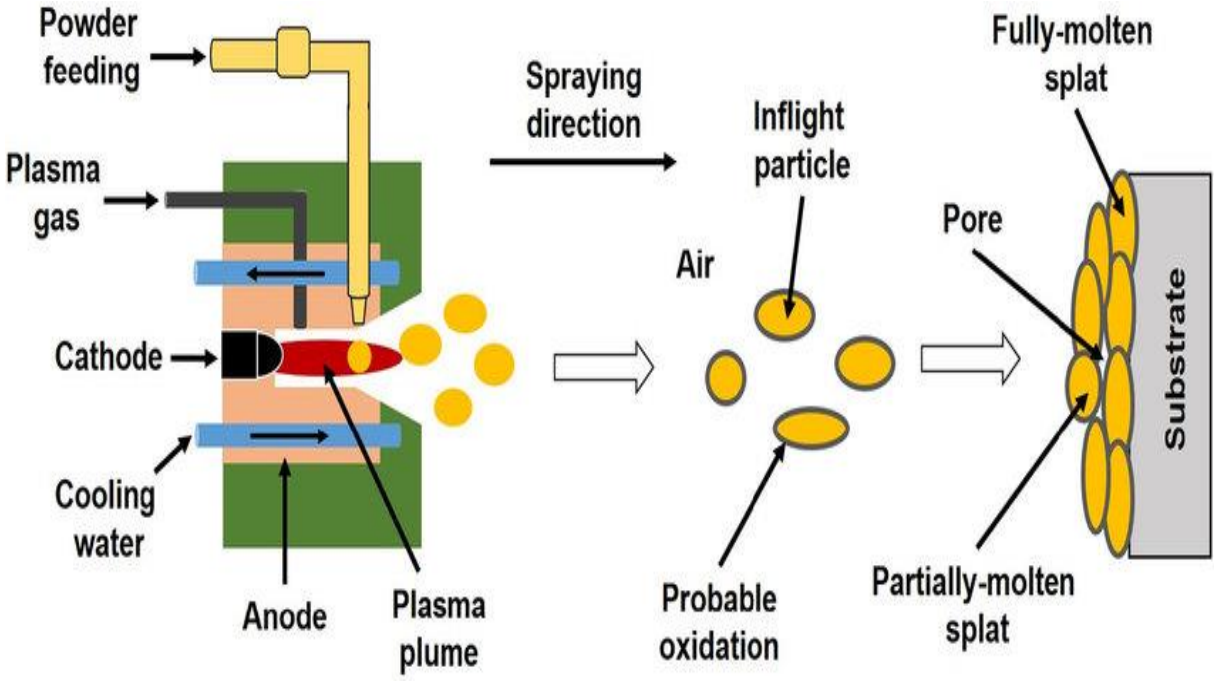

Figure 1.19: Atmospheric Plasma Spray Process[64].

The extensive variety of materials comprises carbides, metals, alloys, ceramics, and refractory oxides. The bond strength achieved in a typical plasma spray operation range from 34 MPa to 69 MPa when tested according to ASTM C-633 standards. Due to the use of inert gases in the plasma jet, less in-flight oxidation is observed in this process than in other thermal spray techniques. However, due to high particle temperature and interaction with the atmosphere, some in-flight particle oxidation occurs, and some oxide inclusions are entrapped in splats. This effect could lead to a lowering of some of the coating properties. For minimizing oxide inclusions, spray parameter optimization of mainly spraying distance, particle velocity, and particle temperature should be done. But due inherent nature of the process, some amount of oxidation always happens during plasma spraying [63]. The diagram of the APS process is shown in figure. 1.15 The plasma spray system, consists of a Gas regulator, Gas hoses, Gas flowmeters, Plasma arc spray gun and Gas supply and water-cooling circuit.

Plasma Torch: The plasma torch is the heart of the APS system. A plasma torch capable of operating at supersonic speeds with axial injection of feedstock. The principal axis of the plasma torch is perpendicular to the feedstock injection direction, which is aligned with the plasma jet emerging from the torch. The plasma torch has a slightly ascending current voltage characteristic and a fixed arc length. In comparison with conventional linear plasma spray torches, APS, HVOF, and VPS exhibit intermediate electrical, thermal, and kinetic characteristics.

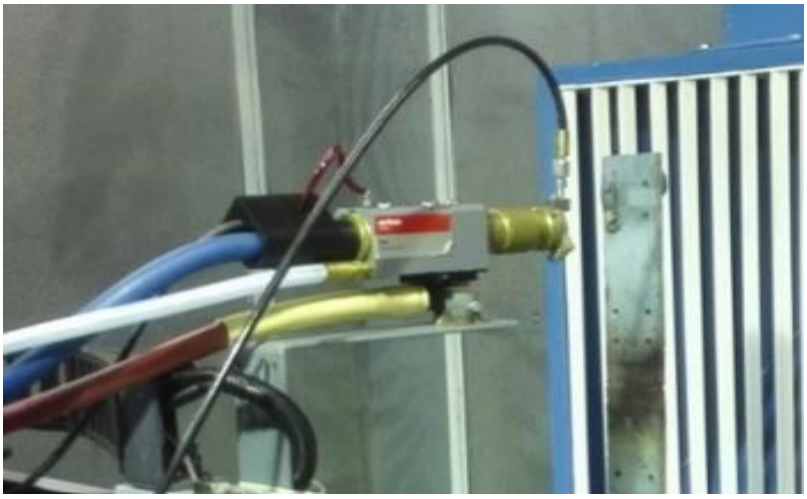

Figure 1.20: Systematic diagram of APS plasma torch

The plasma torch developed in this study has a high arc voltage (370 V) and a low arc current (100 A. A gas (often argon or nitrogen) is passed through an electric arc to produce a high-temperature plasma jet. Temperatures of 10,000 to 15,000 degrees Celsius are reached by the plasma. A cathode, anode, and nozzle are among the parts of the plasma torch, which also includes other parts.

Powder Feed System: Usually, the coating material takes the shape of a fine powder. Using a powder feed mechanism, this powder is injected into the plasma jet. A carrier gas (often another inert gas like argon) can transport the powder to the plasma torch nozzle after it has been fed through a powder hopper. Powder feed systems are used in plasma spray apparatus to carry powdered materials such as metals, ceramics, inter-metallics to the plasma flame or stream. The powdered material is carried through the feed tube and toward the plasma flame by a pressurized gas. A powder feed system with a re-circulator is provided for a plasma spray apparatus so that spraying operations may be started and stopped abruptly. The subject system utilizes a pressurized gas to direct a powdered material from a powder feed hopper to the plasma spray applicator. A diverter valve is located intermediate the powder feed hopper and the plasma spray applicator and near the plasma spray applicator for selectively diverting the powdered material

toward or away from the plasma spray applicator. Powdered material diverted away from the plasma spray applicator is directed to a powder accumulator for subsequent reuse.

Figure 1.21: Systematic diagram of powder feeder

Gas Supply: Inert gases like argon or nitrogen are used to create and stabilize the plasma jet. These gases are supplied from gas cylinders or a gas distribution system. The gas supply can be divided into two categories: primary gas and secondary gas. The primary gas is the main gas that forms the plasma, and it can be argon, hydrogen, nitrogen, or helium, or a mixture of these gases. The secondary gas is the gas that is used to inject the material particles into the plasma jet, and it can be argon, nitrogen, or helium. The secondary gas can also be used to modify the plasma properties by changing its composition or flow rate. The choice of the gas supply depends on the type of material to be sprayed, the desired coating properties, and the cost and availability of the gases.

Figure 1.22: Systematic diagram of gas cylinder

For example, argon is a completely inert and easily ionized gas that can be used as both primary and secondary gas. Hydrogen is a highly energetic gas that can increase the temperature and velocity of the plasma jet, but it can also react with some materials and substrates. Nitrogen is a cheaper alternative to argon, but it can also form nitrides with some materials. Helium is a lighter and more diffusive gas that can produce a wider and more uniform plasma jet, but it is also more expensive and less ionizable than argon.

Control unit: The entire APS process is typically controlled by a computerized control system. This system regulates various parameters such as plasma gas flow, powder feed rate, torch movement, and substrate positioning to achieve the desired coating thickness and quality. The control unit in atmospheric plasma spray is a device that regulates the operating parameters of the plasma spray process, such as the power supply, the gas supply, the arc starter, the material feeder, and the process control and diagnostics. The control unit can affect the quality and performance of the coatings by adjusting the arc current and voltage, the plasma gas flow rates, the material feed rate, the torch movement, the substrate temperature, and other variables. The control unit can also monitor and measure the plasma parameters and the coating properties to ensure a stable and optimal process.

Figure 1.23: Systematic diagram of APS control unit

Dust collector: It is a type of mechanical separators which works on the principle of centrifugal force and used to remove metallic or dust particles from air steam of spraying zone. It is also used toprovide high separation velocity.

Figure 1.24: Systematic diagram of APS dust collector

Grid blaster: Pressure blaster is used to deposit additive layer on the substrate materials with the help of dry compressed air. Abrasive particles come out from theblast nozzle with high velocity and used for removal/ preparation of substrate materials. The dust produced during blasting process is collected using pressure blasting cabinet, which is used to reduce noise levels produce during blasting process and used to ventilate dust andfumes from the chamber. Grit blasting parameters, such as grit size, pressure, distance, angle, and time, can affect the surface roughness, grit residue, and residual stress of the substrate. These factors can influence the coating quality and performance. For example, larger grit size can increase the roughness and the depth of the plastic zone under the substrate, but also increase the grit residue and the compressive residual stress.

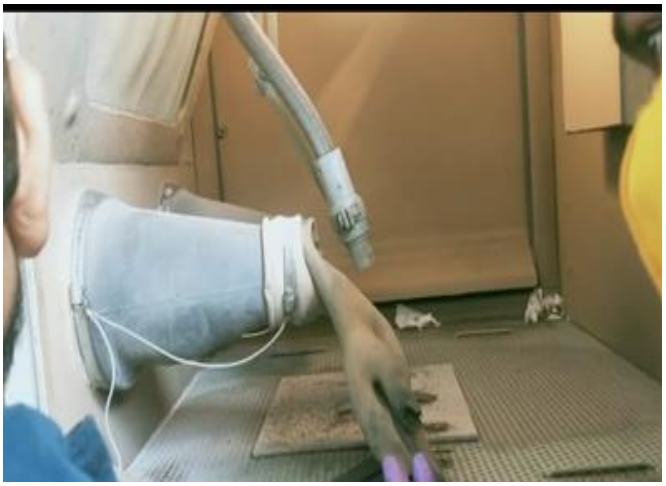

Figure 1.25: Systematic diagram Grid Blaster

1.7 Tribology

Tribology is a Greek word derived from tribo, which means "to rub." Jost created the term in 1966, and the study of tribology is related to mate surfaces in motion. Tribology is made up of three basic components: friction, wear, and lubrication. The primary goal of tribology is to increase product performance and life while cutting costs and saving energy. Tribology is important in the context of the thermal spray technique, which involves depositing a coating onto a substrate by melting or softening the coating material and then pushing it onto the substrate surface. Here we study about interacting surfaces' friction, wear, and lubrication, and it has several major implications in the subject of thermal spray.

1.7.1 Tribological properties:

Here we research on friction, wear, and lubrication of interacting amid surfaces in comparative motion. It encompasses, science and technology of surfaces in contact and the effects of friction, wear and lubrication on the performance and longevity of mechanical systems. Tribology is crucial in various industries, including manufacturing, automotive, aerospace, energy, and more, as it helps optimize the design and operation of components and systems. Tribology involves several key concepts and types. Nanostructured coatings can modify the surface's tribological behavior, enhancing its ability to withstand sliding, rolling, and impact forces. Applications of nanostructured coatings for wear resistance span various industries, including automotive, aerospace, manufacturing, and medical devices. For example, these coatings can be applied to engine components, cutting tools, bearings, implants, and electronics to extend their service life and maintain performance under demanding conditions[65]–[67].

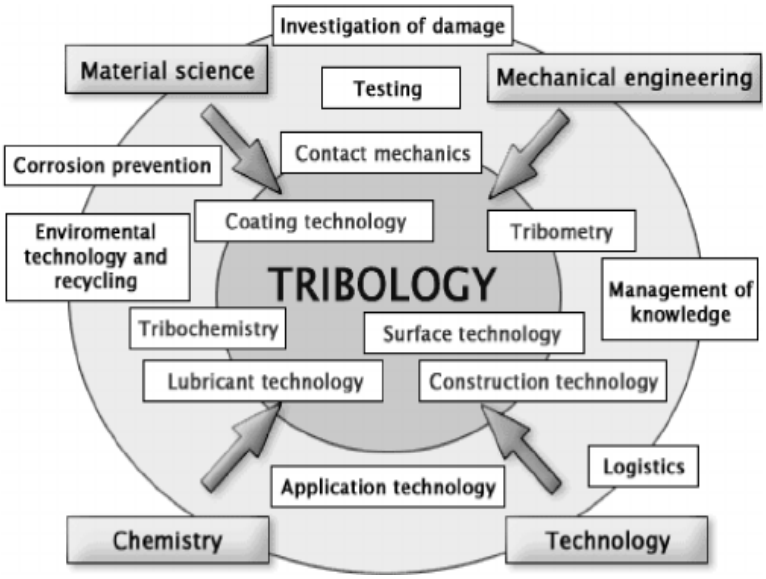

Figure 1.26: Tribology properties[68]

As research and technology continue to advance, nanostructured coatings hold immense potential for addressing wear-related challenges and revolutionizing the durability of composite coating materials in a large variety of applications. In summary, tribology plays a multifaceted role in thermal spray applications. From selecting appropriate coating materials to ensuring adhesion and uniformity, tribological considerations are integral to achieving the desired functional and performance characteristics of thermal spray coatings [80].

1.7.1.1 Friction[69]

This is the force which gives opposition to the relative motion amid surfaces. COF is represented as, and it is a dimensionless item. The ratio of frictional force to normal force applies force to both bodies at the same time.

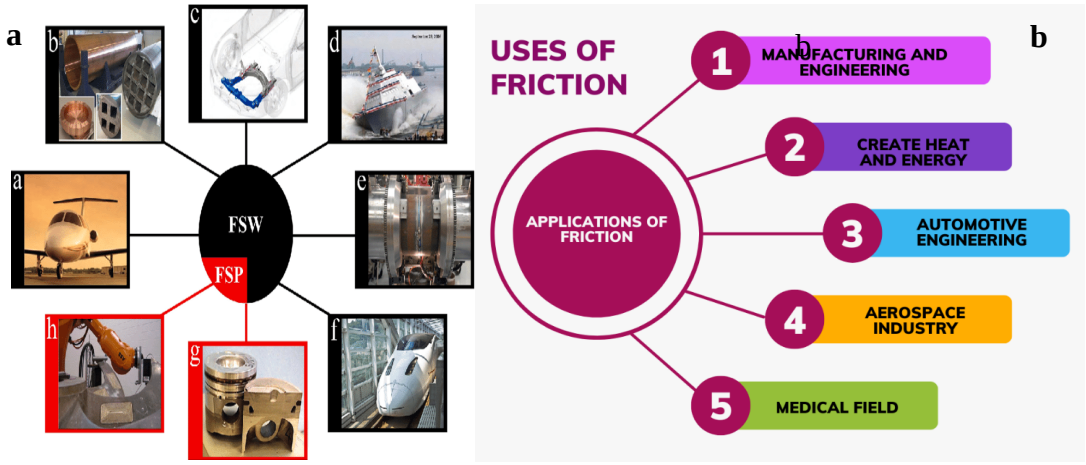

Figure 1.27: (a) Different types of friction (b) Application of friction

Friction is divided into 4 parts: static friction, rolling friction, fluid friction, and static friction. Amonton laws state that the frictional force between two surfaces is independent of the apparent contact area and proportional to the applied load. Based on Amonton laws, Coulomb developed an approximate model to measure friction written as

$$F \leq \mu N \qquad \text{Equation 1.2}$$

Here, F indicates the frictional force which acts parallel to opposite of surface to the force applied, μ indicates the COF and N shows the value of normal load acting perpendicular to the surface. For surfaces at rest $\mu = \mu_s$,

μ_s: is the COF).

for two surfaces between relative motion $\mu = \mu_k$

Where μ_k = coefficient of kinetic friction

1.7.1.2 Wear

Wear mechanism occurs when the material is starting to remove from the mating surface. This material is removed as debris from either one or both surfaces; it can be transferred of material from a soft mating surface to a hard surface. It can be defined as mass loss per unit distance travelled. Wear behaviour plays a critical role in both piston-cylinder systems and gas turbines, affecting the efficiency, reliability, and overall performance of these mechanical components.

1.7.1.2.1 Wear Behaviour in Piston-Cylinder System [70]–[72]:

In internal combustion engines, such as those found in automobiles, the piston-cylinder system is a fundamental component where wear behaviour is of utmost importance.

i. **Impact on Performance**: Wear in the piston-cylinder system can lead to increased friction between the piston rings and cylinder walls. This friction consumes energy and reduces engine efficiency. Excessive wear can also result in decreased compression, leading to lower power output and increased fuel consumption.

ii. **Ring and Cylinder Wear**: The piston rings, which seal the combustion gases and maintain compression, experience significant sliding against the cylinder walls. Over time, wear between the rings and cylinder walls can lead to reduced sealing efficiency and enhanced oil consumption.

iii. **Lubrication and Cooling**: Proper lubrication is crucial to minimize wear in the piston-cylinder system. Lubricants not only reduce friction but also help dissipate heat generated during operation. Wear can be exacerbated by inadequate lubrication, resulting in increased friction, overheating, and accelerated wear.

iv. **Material Selection and Coatings**: Choosing suitable materials and applying wear-resistant coatings to cylinder walls and piston rings can extend the lifespan of these components and mitigate wear-related issues.

1.7.1.2.2 Wear Behaviour in Gas Turbines[73]:

Gas turbines are used in various applications, including aviation and power generation. Wear behaviour is significant in gas turbines due to the high temperatures, speeds, and stresses involved.

i. **Blade and Rotor Wear**: Gas turbine blades and rotors operate at high rotational speeds and are exposed to extreme pressures and temperatures. Wear on these components can result from erosion caused by abrasive particles in the air or from thermal fatigue due to rapid temperature changes.

ii. **Abrasive Particles**: Inlet air for gas turbines can contain solid particles that act as abrasives, causing erosion of the turbine blades and other components. Controlling and filtering the intake air to minimize the presence of these particles is crucial for reducing wear.

iii. **Thermal and Creep Effects**: Gas turbine components are subjected to cyclic temperature changes and thermal stresses during operation. This can lead to thermal fatigue and creep, resulting in wear and deformation over time.

iv. **Ceramic Coatings**: In some cases, ceramic coatings can be developed on gas turbine components to improve wear resistance and thermal protection. These coatings can reduce the impact of erosive particles and thermal stresses.

v. **Balancing Efficiency and Wear**: Designing gas turbines involves balancing the need for high efficiency with wear considerations. Components optimized for efficiency might experience higher wear rates, so engineering decisions must carefully consider this trade-off.

Both in piston-cylinder systems and gas turbines, understanding and managing wear behaviour are critical for ensuring operational reliability, minimizing maintenance costs, and extending the service life of these complex mechanical systems. Archard formed a quantitative model to quantify wear using pin-on-ring tester. According to him: wear occurs due to plastic deformation and fracture due to localized pressure at contact. Archard said that wear is proportional to the load applied and contact area. The arched equation is said below:

$$W = K\,P/\,pms \quad \text{Equation 1.3}$$

Here,

W indicates the worn material wear,

K = wear constant, Applied pressure = yield strength of soft material, and

S = Total sliding distance.

K compares the tribological behaviour of materials tested under similar conditions.

$$K = W\,sP \quad \text{Equation 1.4}$$

Where K, in [mm^3 /Nm] is equal to the wear constant, W [mm^3] is the worn volume, s[m] is equal to the total sliding distance and P [N] is the applied normal load. The mechanisms that are relevant to wear are briefly explained below:

1.7.1.2.3 Tailoring Coating Properties for Enhanced Wear Resistance[74]–[76]

Tailoring coating properties for enhanced wear resistance involves the deliberate selection and optimization of various coating parameters to improve the ability of a material to withstand friction, abrasion, and other wear-related stresses. This process is crucial in an extensive range of industries, with aerospace, and machinery, automotive, where components and surfaces are subjected to harsh operating conditions. Successful tailoring of coating properties for enhanced wear resistance requires a multidisciplinary approach, involving materials science, engineering, and careful consideration of the specific application and operating conditions. Collaboration between researchers, materials engineers, and industry experts is crucial to develop effective solutions that extend the lifespan and performance of components subjected to wear. Here are some key factors and strategies to consider when tailoring coating properties for enhanced wear resistance.

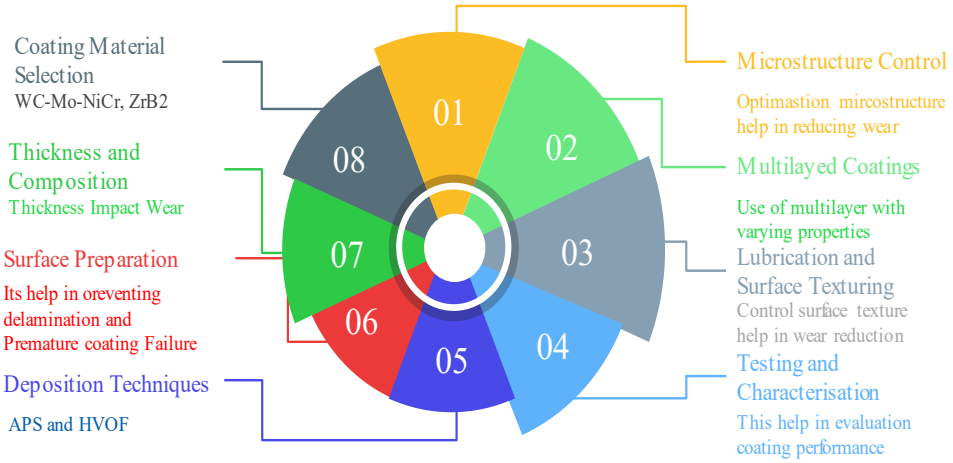

Figure1.28: Tailoring coating properties for enhanced wear resistance

1.8 Lubrication[77]

Lubrication aims to reduce both friction and wear. Additionally, lubricants also provide cooling, lower vibrations, and inhibit corrosion. There are two main mechanisms by which lubricants lower friction. One is in which a stable lubricant layer is formed between the surfaces. This causes complete surfaces separations, and friction takes place because of lubricating shear resistance. In other cases, the lubricant film is unstable but still lowers friction coefficients and temperatures. Wear is also lowered extensively due to lower flash temperature and removal of any worn particles by a lubricant.

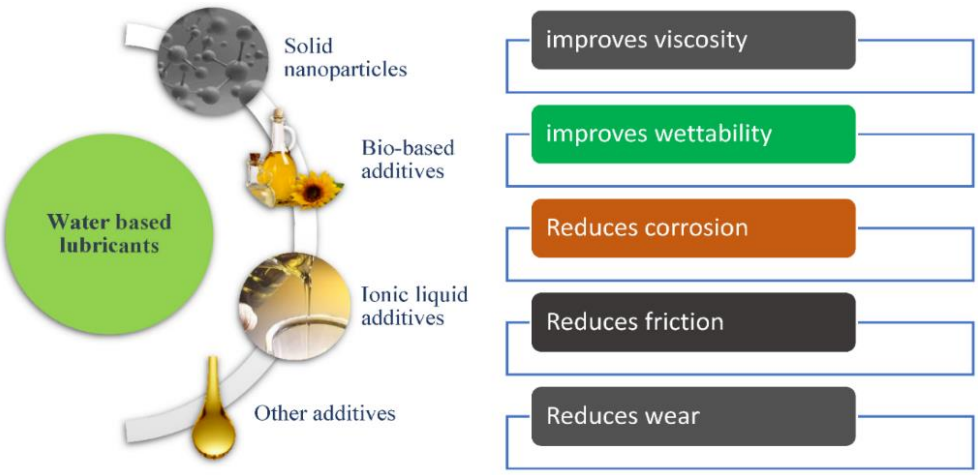

Figure 1.29: Application of lubrication

A suitable fluid or solid lubricant could be selected according to the working parameters, i.e., load, working temperature, and surrounding environment. Metals, oxides, sulphides, graphite, etc., could act as lubricants, and they need not be necessarily oil or grease. In certain cases, the lubricant residues could be problematic. The disposal of these residues may be harmful to health and the environment.

1.9 Corrosion

Corrosion is the term for the slow deterioration or breakdown of materials, typically metals, brought on by chemical interactions with their surroundings. This process is a natural consequence of the interaction between a material and substances like water, air, or chemicals. Corrosion can lead to structural damage, reduced functionality, and even failure of the affected material or object. A refined metal is converted naturally by corrosion in stable state, like oxides. It is a slowly decay the materials (mainly metals) that result of chemical interactions with their environment. Metals reacting with elements in their environment cause corrosion, which is essentially an electrochemical process[78].

Figure 1.30: Example of corrosion[79]

This refers due to reaction of electrochemically metal oxidations reaction with oxidants, like oxygen. Electrochemical corrosion is recognized for producing iron oxides, called as rusting. Oxides and salts are produced from original in this sort of damage, resulting in a unique orange colour. The term corrosion can be used to describe materials other than metals, such as ceramics, although decline is linked with these materials. Materials and buildings become less effective when they are corroded because corrosion reduces its strength, look, and porousness to liquids and gases. Some structural alloys rusted just from interaction with dampness in the air, but some compounds can have a substantial effect on the progression. Result of this techniques such as passivation and chromate conversion that decrease the commotion of the opened surface may enhance a material's resistance to corrosion. Another side, certain corrosion mechanisms are less noticeable & less expectable.

Figure 1.31: Corrosion types

1.9.1 Corrosion prevention Process[80], [81]

To increase the durability and structural integrity of materials and structures, corrosion avoidance is crucial. Corrosion prevention and mitigation techniques come in a variety of forms. Here are some typical techniques for preventing corrosion:

i. **Protective Coatings and Paints**: A material's surface can be painted or coated to form a barrier between it and its corrosive surroundings. These coatings can be made to withstand corrosive chemicals, dampness, and other elements.

ii. **Galvanization**: Galvanization entails applying a layer of zinc to metals like iron or steel. Zinc serves as a sacrifice for protection because it corrodes more slowly than steel. It is frequently utilized in construction projects including bridges, pipelines, and fences.

iii. **Anodizing**: Anodizing is a procedure mostly utilized for aluminium. It increases the metal's corrosion resistance by forming a shielding oxide layer on its surface.

iv. **Cathodic Protection**: In this technique, the metal structure acts as the cathode by receiving a direct electric current, which stops corrosion. There are two: impressed current cathodic protection and sacrificial anode cathodic protection.

v. **Alloying**: By combining metals to form alloys, corrosion resistance can be increased. For instance, chromium, which creates a shielding oxide layer, is present in stainless steel.

vi. **Coating Systems**: Coating systems with several layers, like epoxy coatings, polyurethane coatings, and fusion-bonded epoxy coatings, can offer long-lasting defence against corrosion.

vii. **Polymer and Composite Materials**: Materials made of polymers and composites provide corrosion resistance in addition to other desirable qualities. They are employed in sectors including maritime engineering and aircraft.

1.10 Thermal Protection System (TPS) for Hypersonic Vehicles[82]–[85]

A frequent and essential method for defending and improving the performance of components in hypersonic vehicles is thermal spray coating. These vehicles (fig 1.21) are made to move at speeds that are often five times the speed of sound or higher. They consequently endure tremendous aerodynamic forces, intense heat, and harsh climatic conditions while in flight, which can cause material degradation and failure. When it comes to overcoming the difficulties faced by hypersonic vehicles, thermal spray coatings offer a number of benefits. Remember that the components of the hypersonic vehicle's specific needs, the operating environment, and the intended performance characteristics will determine the assortment of thermal spray coating

materials & application techniques. These coating methods are frequently being improved by new materials and continuous research.

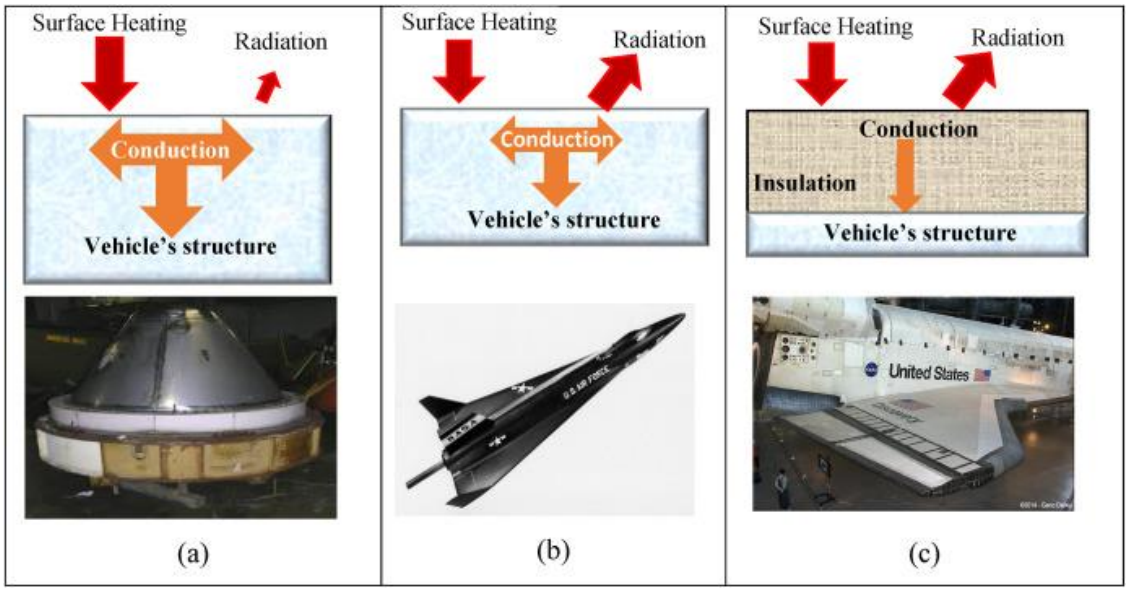

Figure 1.32: Hypersonic Vehicle Structure[82]

i. **Thermal Protection:** Controlling the intense heat produced during flight is one of the main issues for hypersonic vehicles. By minimizing heat transfer to the underlying components and insulating them from the high temperatures experienced during hypersonic flight, thermal spray coatings can effectively insulate a surface.

ii. **Oxidation and Corrosion Resistance:** Hypersonic aircraft travel at great heights, where the atmosphere includes corrosive substances like oxygen. Thermal spray coatings can fortify surfaces against oxidation and corrosion, preventing component wear and extending their lifespan.

iii. **Abrasion and Erosion Resistance:** As hypersonic vehicles travel at high speeds, powerful aerodynamic forces are applied to their surfaces, which can lead to wear and erosion. Thermal spray coatings can provide a robust barrier that withstands abrasion and erosion, protecting the structural integrity.

iv. **Thermal Spray Coating Types:** There are several different kinds of thermal spray coatings used in applications for hypersonic vehicles. Plasma spray coatings, high-velocity oxy-fuel (HVOF) coatings, and cold spray coatings are examples of typical types. Each variety has distinct characteristics, and the one picked depends on the particular needs of the application.

v. **Material Compatibility:** Coating can be developed on metals, ceramics, and composite materials with thermal spray technology. This adaptability enables engineers to decide which coating material is best for a given component based on its operating environment and performance requirements.

vi. **Weight Considerations** To reach the required speeds and manoeuvrability, hypersonic vehicles need lightweight solutions. Thermal spray coatings several different kinds of thermal spray coatings are a good option for weight-sensitive components because they are often lightweight in comparison to other forms of protection.

vii. **Reparability:** Thermal spray coatings may occasionally be able to be repaired or reapplied, increasing the lifespan of the coated components and lowering maintenance costs.

1.10.1 Challenges of hypersonic vehicles during hypersonic Flight[86]

Hypersonic flight refers to travel at incredibly high speeds, typically exceeding five times the speed of sound (Mach 5) or even greater. Vehicles designed for hypersonic flight operate in extreme conditions, experiencing intense aerodynamic forces and extreme temperatures due to friction with the atmosphere. These challenges necessitate advanced materials and technologies to ensure the safety, performance, and longevity of hypersonic vehicles. Thermal spray coating plays a vital role in the successful operation of hypersonic vehicles by addressing several critical challenges they face during flight:

i. **Thermal Protection:** Hypersonic flight generates enormous amounts of heat due to air compression and friction. Thermal spray coatings can serve as effective thermal barriers, protecting the underlying components from excessive temperatures. They reduce heat transfer and help manage thermal loads, preventing overheating and potential material failure.

ii. **Aerodynamic Heating Resistance:** As hypersonic vehicles travel at such high speeds, they experience severe aerodynamic heating. Thermal spray coatings are designed to endure these extreme conditions, resisting the intense heat and preventing structural damage.

iii. **Oxidation and Corrosion Resistance:** Hypersonic vehicles operate at high altitudes where the atmosphere contains oxygen and other corrosive agents. Thermal spray coatings can act as a protective layer, preventing oxidation and corrosion of critical components and increasing their lifespan.

iv. **Abrasion and Erosion Resistance:** High-speed flight exposes the vehicle's surfaces to intense aerodynamic forces, which can cause abrasion and erosion. Thermal spray coatings provide a durable shield against these forces, preserving the structural integrity of the components and ensuring their longevity.

v. **Structural Integrity Enhancement:** By providing an extra layer of material, thermal spray coatings can enhance the overall structural integrity of components, making them more resilient to mechanical stresses during flight.

vi. **Weight Optimization:** Hypersonic vehicles must be lightweight to achieve the necessary speeds and manoeuvrability. Thermal spray coatings offer a lightweight solution for protective measures compared to other bulkier alternatives.

vii. **Reparability and Maintenance:** In some cases, thermal spray coatings can be repaired or reapplied, reducing maintenance costs and extending the operational life of components.

In conclusion, thermal spray coatings performs an important act in enabling successful operation of hypersonic vehicles. They provide thermal protection, resist aerodynamic heating, prevent oxidation and corrosion, and enhance the structural integrity of critical components. As research and technology advance, thermal spray coatings continue to be essential for improving the safety, performance, and reliability of hypersonic flight.

Chapter: 02

Literature Review

In the recent years, lots of researchers have shown their interest in the development and characterisation of advanced composite coating for various industrial applications as well as for the high temperature applications. Composite coatings offer improved mechanical, thermal and chemical properties compared to the traditional coatings making them suitable for industries applications as per requirements. This literature review aims to provide an overview of the research and developments in two specific types of composite coatings: ZrB_2-SiC composite coating and Mo-WC-NiCr composite coatings.

2.1 ZrB_2-SiC composite coating

The successful re-entry of the space vehicle hinges on the effective thermal protection system. To enhance the working efficiency and consistency of upcoming re-entry vehicles, a shift towards utilising single-body hot structure, which are self-sustaining and structurally sound parts, have been proposed. This is different as of current practices of employing tile covered surfaces[87].

Additionally, there are focus on adopting sharp aerodynamics profile instead of blunt edges in the current phase. We are expecting drag reduction and manoeuvrability with these profiles. To meet these objectives the researchers are exploring novel material and manufacturing process. These innovations aim to achieve the optimised performance with reduced cost and complexity.

In the view of this application, two materials have been under research by different researcher: Carbon fibre composites specifically those with Silicon Carbide matrix and UHTC (ultra-high temperature ceramics) as ZrB_2, SiC and Mo-WC-NiCr etc. The carbon fibre composites show remarkable thermomechanical properties along with very low density however they necessitate effective protection against oxidation. Other side Ultrahigh thermal ceramics gives exceptional oxidation resistance at elevated temperatures but the density of these ceramics are high[5], [88].

Within the family of Ultra high temperature ceramics, ZrB_2 emerged as an exceptionally intriguing candidates for the application in the thermal shielding. This is because of ZrB_2 remarkable attributes, including its exceedingly melting point, impressive hardness, and robust mechanical integrity even at elevated temperatures. Although the ZrB_2 was first time used in the year 1960s and 1970s but recent advances in manufacturing techniques have rekindled interest in exploring properties[89], [90].

The oxidation process of ZrB_2 initiates relatively at modest temperatures leading to the formation of oxides of Zr and B. As the B_2O_3 layers over the surface becomes adequately liquid, it effectively gives protections to substrates from the external environments, exhibiting exceptional performance like a dispersion obstacle against the O_2 (oxygen) ingress. Though, its point to consider that the partial pressure of B_2O_3 remains significant at the higher temperatures, ultimately resulting in its volatilisation. Researchers have explored and exploring various methods for enhancing the oxidations resistance of ZrB_2. The addition of SiC in the ZrB_2 have shown tremendous results in bolstering the oxidation resistance[91]–[93].

Zirconium diboride and SiC are refractory ceramics known for their high melting points (>3000^0C), excellent thermal conductivity (65-135$Wm^{-1}K^{-1}$), high hardness (22GPa), good oxidation resistance, ablation resistance and remarkable mechanical properties. ZrB_2 are among the best materials known for the oxidation resistance. These ceramics are called as UHTC as discussed above. The combinations of these two materials in the composite coating is new type of oxidation resistance coating and garnered significant attention due their capability to improve the performance of protective coatings in the high temperature and corrosive environment[94].

While ZrB_2 ceramics boasts numerous advantages, but its inherent brittleness poses challenges, especially in term of thermal shock resistance, restricting its widespread utilisation specifically in the extreme environments[95]. Addressing this limitation, the addition of precise amount of SiC and graphite flakes merges as viable strategy to augment the overall enactment of ZrB_2 grounded composites. Silicon Carbide serves as the bolster of mechanical properties but also enhances ZrB_2 oxidation resistance. This is because SiC facilitates in the formation of silicon-based glasses, which effectively hinder the oxidation within the temperature range of 800 to 1000^0C. The addition of graphite flakes into the ZrB_2-SiC composites contributes to heightened fracture toughness and better thermal shock resistance, distinguishing it from ZrB_2-SiC composites[96]–[101]

Several studies have been conducted and investigated the corrosion response of ZrB_2 and ZrB_2 grounded composite across varying erosion environments at room temperature. Lee et al. reported in their research that the corrosion propensities of ZrB_2 powders at wet processing were the unaltered and corroded powder surfaces were primarily coated with ZrOH, along with a discernible presence of Zr-B bonding[95].

Huang et al., in his work delved into the corrosion behaviours of ZrB_2 when immersed in water, concluding that a thin layer of ZrO_2, with thickness 4.67nm, developed on the ZrB_2 surface following a 1-hour dip in the water[102].

Monticelli et al., did extensive research into the electrochemical corrosion characteristic of ZrB_2 within the aqueous acidic solutions featuring a variety of aggressive anions, including perchlorates, chlorides, sulphates, and oxalates. They found that ZrB_2 underwent a conversion process, yielding both insoluble products as ZrO_2 and soluble products such as boric acid along with some intricate products formed between diverse anions and Zr (IV)[103].

Levrenko et al., investigated the electrochemical oxidation tendencies of ZrB_2 and $MoSi_2$ refractory compounds along with ceramics of the same upon exposure to a 3% NaCl solutions. They reported that composite containing the relatively modest quantity of $MoSi_2$ (5-10 wt. %) exhibited the highest degree of corrosion resistance. This enhanced resistance was because of the stable passivation exhibited by these composite at comparatively low anodic potential[104].

Lin et al., did investigation of oxidation behaviour of ZrB_2-SiC composite coating doped with Y_2O_3 at temperature of 1773K for 100 minutes duration. They prepared the samples of ZrB_2-SiC with varying composition of Y_2O_3 by plasma spray techniques. They find that oxidation properties of the developed coating have been enhanced by the addition of Y_2O_3. The result may be accredited due to some points (i) the formation of Zr-Si-Y-O glass barrier film that effectively impeded oxygen dispersal and enabled the curative of cracks.(ii) reduction in m-ZrO_2 traces , which mitigated volume expansion of coating and minimised the likelihood of spallation and (iii) the incorporation of $Y_2Si_2O_7$ as a restraining stage there by inducing modifications in the steadiness of fluid SiO_2 at high temperature[105].

Xie et al., examined the consequence of Lu_2O_3 on the oxidation nature of the Zrb_2-SiC composite coating at elevated temperature (1500^0C) in the static air environment. The incorporation of Lu_2O_3 into the SiC-ZrB_2 composite coating resulted in the excellent protective effect on C/C composites, effectively mitigating oxidation for an impressive duration of 836 hours at elevated temperature, with minimal mass gain of merely 0.62mg/cm^2. This may be because of the potential diffusion tendency of Zr and Lu atoms into SiO_2 network. This diffusion phenomenon notably contributed to the reinforcement of $SioO_2$ structure stability. Consequently, thus structural enhancement significantly bolstered the overall oxidation resistance of Lu_2O_3-SiC-ZrB_2 fused coating, providing the excellent performance in the extreme conditions of high temperatures[106].

Liu et al., investigated the continuous gradient coating prepared by the high-speed cladding technology using ZrB_2-SiC powder on the 304 stainless steels. The continuous gradient structure significantly contributed to the coatings excellent interfacial binding properties and remarkable surface mechanical properties, particularly in form of hardness and wear opposition. At the room temperature, the harness was quite high $1810HV_{0.5}$ and this hardness level remained impressive high, more than $1000HV_{0.5}$ even at the temperature of 800^0C. Further the study revealed the reduction of coefficient of friction with the increase of temperature from 0.58 to 0.27. This shows that ZrB_2-SiC composite coating are quite good at wide range of temperatures even at high temperatures[107].

Mor et al. deliberated the tribological behaviour of (UHTCMCs), Ultra High temperature ceramic matrix composites. The samples were prepared using ZrB_2-10Vol%SiC reinforced with randomly oriented carbon fibre. To analyse the tribological behaviour, a custom designed dynamometer was employed where the UHTCMC pads were coupled with the carbon fibre reinforced carbon-silicon-silicon carbide disks. Two loads were considered for the investigation (1 and 3MPa). This investigation revealed that C/C-SIC disk showing constant breaking performance and were even at high mechanical stresses. Significantly high value of coefficient of friction (0.5-0.7) that remained same throughout the testing. The observed valued of coefficient of friction found to be acceptable collectively position these materials as potential candidates for the automotive brakes system also[108].

Nickolai et al, did high speed continuous sliding experiments on the ZrB_2-20Vol%SiC ultra-high temperature ceramic to investigate the intricate details of tribo-oxidation occurring under the condition of subsurface deformation and friction induced heating. They find that the formation of subsurface layer structure with the distinct phase composition, providing evidence of highly active mass transfer processes. Substantially born depleted layer and mechanically mixed layer were also generated having silicate glass, iron, and high temperature phase of zirconia and carbides of silicon. This MML (mechanically mixed layer) acted as protective layer for the underlying ZrB_2 grains. Along with this also led the creation two transition layers of borosilicate glass, zirconia, and iron oxyborides. The MML also plays key roles in the oxidation process of silicon carbide grains[109].

Chen et al., investigated the tribological properties of ZrB_2-20%VolSiC composite. The sample was produced by hot pressing of ZrB_2 and SiC powders, and performance has been investigated on different temperature and frictions conditions taking WC and Al_2O_3 as counter parts. Finding shows that the coefficient of friction of the composited remained same with both

counter bodies across the temperature in the ranges of 0.5-0.6. The wear rate was $10^{-4}mm^3N^{-1}m^{-1}$. With the WC counter bodies the tribo-layers was discontinued and with Al_2O_3 the layer was continuous without any significant effect on the lubrication properties[110].

Gupta et al., examined properties such as the wear and friction of ZrB_2-SIC composite with varying content of SiC (10, 20 & 30 Vol. %) developed by plasma spray process. For the wear investigation they considered different counter bodies SiC (thermal conductivities 100W/m-K, Hardness 15GPa), Al_2O_3 (Thermal Conductivity 30W/m-K, Hardness 28GPa), ZiO_2 (thermal Conductivity 25W-m-K, Hardness 12.5GPa). The range of coefficient of friction was 0.49 to 0.69 and wear was in the range 0.006 to0.152mm^3. The variations were because of content of SiC and different counter bodies. They found that with the upsurge of SiC content the COF and wear cuts because of increase of fracture toughness and hardness of the established composite coatings. They also investigated that the thermal conductivity of counter bodies plays a great role in the wear and friction of developed composites. The wear mechanism of composite basically includes fracture, pull out, deformation and re-oxidation[111].

Malik et al., inspected the result of ZrB_2-20%Vol SiC composites against the sliding speed & loads with counter body of diamond. They found the wear was significant at low sliding speed and higher loads condition. With the investigation of wear debris, they found that grain pull-out, micro-cutting and oxidation as major wear mechanism of the coatings[112].

Medved et al. explored the wear behaviour of ZrB_2-SiC, B_4C & ZrC composites on the different loads and sliding speeds. They found micro-cracking and tribo-film formation during the tribological investigation[113].

Chakraborty et al. investigated the scratch resistance of ZrB_2-TiB_2 with the counter body of diamond. They found that ZrB_2-30wt%TiB_2 have grander wear resistance because of its fracture toughness & hardness. The wear resistance were constant under varying conditions of temperature making it most suited for the tribological applications[114].

Wei-Ming et al., synthesised the powder through boro/carbothermal reduction route under vacuum condition at temperature of 1750^0C with the help of ZrO_2, B_4C and carbon precursor. They find that the addition of ZrC with varying % within the temperature range of 30-1400^0C increased the activation energy of the oxidation leading to the increase of oxidation resistance.

Zhu et al., investigated the properties of ZrB_2-SiC composite with the induction of boron carbide and carbon as a sintering additive. These additive shows reactions with the impurities.

This shows sufficient increase of the properties by incorporating 10wt. % nano-sized carbon black that's leads to the activation of crack, deflection, and bridging at temperature of 1850^0C[115].

Shahidi et al., developed ZrB_2-ZrC based composite using ZrB_2, ZrO_2, and graphite as initials reactants. They investigated tremendous increase in the indentation hardness by addition of 6wt% nano graphite flakes into the composites. They also investigate that the toughening properties of the ZrB_2-ZrC based composite have been also increased by the addition of graphene into the composite powders[116].

ZrB_2-SiC have got great attention from the researcher worldwide because of its properties to increase the thermal shock resistance of SiC by ZrB_2 but the processing of these composites are the major challenges for the researchers in the efficient and cost-effective manner. This is bases of the different thermodynamics profile and different sintering temperature of the constituent. Various techniques can be used for the dispensation of ZrB_2-SiC composites as Spark-Plasma Sintering, encompassing hot pressing, sensitive melt infiltration, pack cementation, chemical vapour deposition, electron beam melting, binder jet additive manufacturing and plasma spray techniques. These methods offer control on the microstructure and properties, enabling tailoring of the coating for the specific applications.

After details and comprehensive review of the ZrB_2-SiC composite coating we released, that these composite shows improved wear resistance, oxidation resistance and thermal stability over the single-phase coatings. The synchronised effects ZrB_2 and SiC contributed to enhancement of the mechanical and thermal properties making them most suitable contenders for the (TBC) thermal barrier and protective coatings for extreme environments.

2.2 Mo-NiCr based Composite Coatings

In the context of linkage of the deposited coating with the substrate, the predominant mechanism involves chemical interactions, geometric contacts, and mechanical anchorage at the interfering surface of the coating and substrate. While talking about the adhesion of the deposited coatings to the metal substrate researchers are working extensively since last several decades. They claimed that most dominant mechanism for the adhesion is chemical bonding or mechanical anchorage. Empirical and numerical investigations done by the researchers proved that prominent mechanism for the adhesion is chemical binding and mechanical anchorage. It's the

main reason for the successful formation of metallurgical bond and chemical bond during the deposition of Mo, NiCr and W particles on the substrates[117], [118].

In the recent decades the researchers are extensively exploring material for the application of marine engineering equipment's. Carbon and low alloy steels have been majorly cast-off in the sea structure and grease pipeline applications because of its availability, cost effectiveness and suitable mechanical properties. But to ensure the sustainable operational performance and safety issues related with this material because of tribo-corrosion is very challenging. For addressing this type of problem in the marine engineering component a most suitable and cost-effective techniques with robust protective capability ad inherent self-lubricating properties surface coating technologies came into the light. The addition of alloying elements and meticulous microstructural optimisation is one of the viable means to substantially augment corrosion and wear resistance[119].

The researchers have explored the utilisation of nickel like an alloying constituent to supress corrosion resistance of enduring steel. This also help in the mitigating brittleness and formation of compact oxide passivation film. The increase of Ni% shoes the potential to foster a more robust amalgamation of molybdenum and chromium atoms in the matrix of steel[120].

Banerjee at al., have studies the influence of chromium on the constancy of breakable well-ordered intermetallic phases. They found that addition of minimum 11 wt. % of Cr led to the formation of support own-healing alternative layers on the steel external surface. Thoughtful utilisation of Ni-Cr based alloy coatings has demonstrated significant contributions to enhancing in both corrosion and mechanical properties of steel. Addition of the Mo along with the Cr has been shown to mitigate the occurrence of pores and cracks in the corrosion product layers. The internal film if the resulting passive film exhibits robust barricade properties in contradiction of the chloride ions. Molybdenum for self-lubricating oxides (MoO_3) during the wear test which contributes to the reduction of wear and frictions. Additionally, the Mo facilitates the promotion of amorphous forming ability, improving corrosion and steel wear properties. The application of NiCrMo alloy coating have significant impact on the materials as mild steel showing exceptional results against opposing, fracture and stress corrosion[120]–[127].

Wang et al. & Li et al also did similar experiment and produced the NiCrMo composite with the help of laser cladding and investigated their hardness, and tribological properties in the corrosive environments and find the fantastic corrosion preventions in the steel components[125], [128].

Guilemany et al.[60] Used Scanning White Light Interferometry (SWLI) and SEM analysis to comprehend the friction and wear behaviour of plasma-sprayed NiCrBSi and other thermal sprayed coatings. The tribological testing was conducted using a ball-on-disc apparatus. Plasma sprayed coating, the counter face material was a steel ball (with an HVN100 = 585). The author's revealed adhesion was the dominant wear mechanism in plasma sprayed NiCrBSi coating. Material removed from the developed coating and moved to steel sphere produced a deep groove on the surface, seen clearly in the SWLI analysis. The main reason for adhesive wear was low hardness and affinity between elements of metallic surfaces.

Parthasarathi and Duraiselvam [43] tested the high-temperature wear of plasma-sprayed NiCrBSiCFe coatings. The tests experimented on a high-temperature pin on disc Tribometer at ambient temperature, 150, 250 & 350°C, 20N load, and 2000m sliding distance. The substrate was AISI 316 stainless steel, and the counter face material was EN-8. The authors reported that the coated steels indicated developed high wear resistance than the non-coated specimen at every testing temperatures. At ambient temperature, primary wear mode was delamination. At 250°C, ploughing was reported as the dominant wear mode. The authors reported a lower wear rate at 350◦C and attributed it to the formation of protective oxides. These oxides provided a lubricating effect and reduced wear rates. The primary wear mechanism at 350°C was reported to be mild abrasion. In another study (Parthasarathi et al., 2012), the authors studied the load consequence load& spraying distance on the high-temperature wear behaviour of thermal spray coatings. The authors reported that coating with greater spaying distance showed higher micro-hardness due to optimum powder melting, powder flow, and lesser voids. These coatings consequently show higher wear resistance. The authors also reported an increase in wear rates when the practically applied load was enhanced from 20 N to 40 N.

Kesavan and Kamaraj [129] deposited Ni-based alloy Colmonoy-5 on 316 L (N) on the stainless steel substrate using a plasma-transferred arc welding process. Developed coating high-temperature friction and wear behaviour studied by means of the pin-on-disc apparatus at room temperature, 573 Kelvin, and 823 Kelvin. Microstructural analysis revealed the presence of hard boride and carbide precipitate phases in the Ni matrix. Coted sample hardness was measured at 430 VHN. Obtained wear results, the authors reported that the COF and WR (wear rates) of the coating reduced with an up surging in temperature. The primary wear mechanism during test was abrasion and delamination at room temperature examinations. Three-body abrasion resulted from ploughing produced by hard particles in wear debris. An increase in temperature caused oxidation and compaction of debris and coating surface on the wear track. This led to the

development of an oxide layer that is stable. These layers withstand the abrading action of debris, reduce metal-to-metal contact, and lead to a lowering of COF and wear rates. The primary wear mechanism at higher temperatures was reported to be tribo-oxidation.

Sari and Yilmaz [130] studied abrasive wear resistance of AISI 1050 steel subjected to different heat treatments (induction hardening), surface treatments boronizing, gas nitriding, salt bath nitriding, and plasma nitriding) and flame sprayed NiCrBSi and NiCrBSi –tungsten carbide coatings, 35% WC + 65% (Cr-Ni-B-Si) with HVOF sprayed. The testing was done in a specially designed apparatus made to simulate wear experienced by mining and earthmoving equipment. The abrasive particles were flintstones. The thermal sprayed coated specimen showed better wear resistance than other surface treatments. The nitride and boride specimens were worn out by the micro-cracking mechanism produced by the impact of abrasives.

Winkelmann et al.[131] developed the NiCrBSi-60%WC (and three other materials) through plasma sprayed and studied the plasma -transferred abrasive wear behaviour. The substrate material was mild steel. High Temperature-Continuous Impact Abrasion Test (HT-CIAT) was used for abrasive wear testing at testing temperatures of room temperature, 500, 600, 650, 700, and 750°C. Hot hardness was also measured employing a high-temperature Vickers hardness test rig. Worn morphology was studied using OM and SEM. The hot hardness of the NiCrBSi-60%WC developed coating reduced continuously as temperature increased, and at 800°C, the hot hardness was 400 HV. This value was higher than other materials tested: stainless steel, high-speed tool steel, and Fe-Cr-C-Nb-Mo-W-B alloy. The authors reported the highest wear resistance for NiCrBSi-60%WC coatings among the tested materials at all temperatures. An increase in wear rate was observed at temperatures above 600°C mainly because of oxidation and fracture of tungsten carbide.

Guo et al.[132] paralleled the high-temperature tribological behaviour of laser-clad NiCrBSi coating and NiCrBSi/WC-Ni composite coating. Stainless steel was used as a substrate. Wear tests were steered through a ball-on-disc apparatus at 500°C and 5N load. Si_3N_4 balls were used as counter bodies. Wear mechanisms were analysed using SEM and three-dimensional surface mapping. XRD of as-sprayed NiCrBSi coatings revealed the presence of a dendritic Ni matrix along with precipitates of $FeNi_3$, $Cr_{23}C_6$, Fe_2Si, CrB, and Ni_3B. The NiCrBSi/WC-Ni coatings had phases like WC, W_2C and Ni_2W_4C formed by the decomposed WC and Ni reaction. The hardness of NiCrBSi coating was reported to be 5 times more than substrate steel, mainly because of the formation of hard precipitates. The NiCrBSi/WC-Ni coatings reported hardness even higher than NiCrBSi coatings because of the hard WC/W_2C phase. The NiCrBSi/WC-Ni

coatings demonstrated higher wear resistance than NiCrBSi coatings, mainly owing to hard WC reinforcements. The wear mechanism for uncoated substrate was severe abrasion, adhesion, and plastic deformation. In contrast, the coated pins showed only mild abrasion and fatigue. The coated pin surface showed no signs of severe adhesion and fatigue.

Zikin et al. [38] premeditated the high-temperature abrasive and erosive wear of NiCrBSi coatings reinforced by WC, TiC-NiMo, and Cr_3C_2-Ni and mass-produced by plasma-transferred arc that is called cladding. Abrasive wear testing was carried out using a high-temperature recurring influence scratch tester (HT-CIAT) at ambient temperature, 300, 550 & 700°C. The authors reported that the WC-reinforced coating shows excellent wear behaviour up to 550°C. But at 700°C, wear rates increased due to high oxidation and fracture of WC along with a decrease in the hardness of the matrix with temperature.

Torgerson et al. [133] studied the high-temperature wear behaviour of cold-sprayed Ni and Ni-WC coatings deposited on the substrates of mild steel. The wear experimentation was taking place by using a pin-on-disc tribo-meter. According to the authors, the Ni-WC coating showed better wear resistance than Ni coatings, mainly due to higher hardness and wear resistance from load-bearing WC particles. The testing temperatures were room temperature, 200°C, and 400°C. WC-Co balls were used as counter bodies. The author reported that the wear rate and COF improved when the temperature was elevated to 200°C. This was because the Ni matrix's softening led to adhesion, plastic deformation, and pull out of WC due to the weakening of bonding between matrix and WC which caused three-body abrasion. Also, stable oxide films did not appear at 200°C. At 400°C, COF & wear rates again decreased mainly owing to stable, NiO-rich oxide layers (MML) forming on the coating surface. The main wear modes at room temperature were adhesion, abrasion, and plastic deformation. Abrasion caused by pulled-out WC was the dominant wear mechanism at 200°C. At 400°C wear mechanism was stated to be oxidation. It is commonly thought that by increasing hard particles, overall rigidity and hence wear resistance of the coating is improved. But literature revealed that very high WC content has negligible or no effect on wear resistance. Because of the higher costs of WC, the percentage of WC in the matrix should be optimized for the best combination of wear resistance and cost.

Weng et al.[134] conducted room and high-temperature wear testing of laser-clad Ni & Ni-WC coatings sprayed on a stainless steel substrate. The testing was done at room temperature, 600°C, and 700°C on a ring-on-block wear tester with WC percentages of 10, 20, 40, and 60%. The authors reported that the wear resistance of coating increased with an increase in WC. Wear rates increased at 600°C due to matrix softening, high plastic deformation, and thin and unstable

oxide layers. But wear rates decreased at 700°C chiefly because the formation of steady oxide layers, which limited wear loss. The main wear mode at room temperature for the pure Ni coating was plastic deformation and adhesive wear. For the Ni-WC coatings, abrasive wear was leading. Adhesion and oxidation wear were dominant, at higher temperature

Chen et al.,[135] studied the ZrB_2 behaviour at temperature 800C and found that it starts to oxides at this temperature and produces B_2O_3 and zirconium oxide. B_2O_3 gave a protective layer above 450^0C to the surface and restricted the oxygen diffusion. Whereas at the temperature above 1200^0C, evaporation started of B_2O_3 and could not protect the surface. That is why research has been done on a combination of ZrB_2 with SiC and found that it upsurges the oxidation resistance at 1000-1800^0C through generating fewer instable borosilicate glass with low absorptivity [136]. Its results researchers developed ZrB_2-SiC coating to fight against oxidation, wear, and corrosion. Usually, the combination of these materials protects the substrate surface from high temperatures [136],[137]. The oxidation behaviour of SiC ceramic can tend to improve ZrB_2 oxidation behaviour[21].

Shirshendu et al. investigated the composite scratch resistance on ZrB_2-TiB_2 and found that the developed composite coating possesses good wear resistance due to high fracture toughness and hardness[22].

Jitendra et al. also studied the tribological behaviour of the same composite coating and found decrement in coefficient of friction(COF), improved hardness, and enhanced the formation of tribo-chemical films [138]

Tobar et al., investigated several samples of own-fluxing NiCrBSi alloy powders combined with nickel clad WC powder. This composite powder was subjected to laser cladding onto austenitic stainless-steel substrate of AISI304 grade. The goal of the investigation was to study the impact of bulk fraction of WC particle on the development and recital of the composite layer. They found the if the volume fraction of WC particles is more than 50% then pores were there in the sample. Contrary to this if the volume fraction is less than 50% then resulting clad layer shows excellent characteristic including homogeneity, density, and absence of cracks. The micro-hardness was also excellent in the range of 600-1000HV depending upon the WC contents levels[139].

Katsich et al., reported in his detail's investigation of effect of carbide degradation within a Ni-based hard facing reinforced with WC/W_2C under the condition of impact and abrasion. The samples were prepared by plasma transferred arc welding technique. The loss of carbide

contents increases the wear rate, and the mechanism was prominently three body mechanism. They reported that with the loss of carbide content directly impact the wear rate of the specimen[140].

Gua et al., investigated on the laser cladding developed NiCrBSi Coating along with NiCrBSi-WC-Ni composite coating on the stainless-steel substrate. The researched were majorly focused on the wear and friction behaviours of the coatings under the counter body of Si_3N_4 ball at temperature of 500^0C. Result showed that micro-hardness and wear resistance was higher than that of laser cladded coating. Furthermore, the composite coating NiCrBSi-WC-Ni shows enhance enhanced high temperature that that of NiCrBSi coatings. This may be because of the robust WC phase formed in the developed composite coating[141].

An alloys Mo, WC, and NiCr for are well searched by the researcher for their well-known properties like strength, wear resistance and corrosion resistance. Adding these materials into a composite coating has potential to increase the surface properties of the components used by the different industries ultimately increasing the life spans of the component in the corrosive and abrasive environment. As per the review there are several methods for the synthesis of these composites like thermal spray, laser cladding, plasma sparing and electrodeposition. These developed coatings show excellent wear resistance, hardness, and chemical stability into the different severe conditions.

The success of the developed composite coatings be contingent on the even distribution of WC particle and best bonding between the phases and decreasing the risk of delamination.

Both the composite coatings ZrB_2-SiC and Mo-NiCr-W-WC represent the promising opportunities for the advancing of protective coating technologies. These composite coating offers enhanced mechanical, tribological, thermal and chemical properties. Because of these properties they attractive for the various industrial applications.

2.3 Research Gap

Composite coating involves the deposition of combination of materials on the substrate, have achieved significant attention in the recent years from the researchers worldwide due to their potential of enhancing the properties of the substrate as per the requirement of various industries. While a substantial body of research exists on the composite coating still there are several notable gaps that merit further research on the composite coatings.

i. Lack of comprehensive studies of the composite coating for high temperature applications
ii. Composite coatings for hypersonic vehicle application
iii. Lack of corrosion studies on Composite Coatings

In conclusion, while the literature on the composite coating for the higher temperature applications has made significant strides, there are evident gaps that require further investigation. There is limited literature available on composite coatings for higher temperature application, wear behavior and corrosion behavior of composite coatings. Also, very limited work has been done applications of composite coatings for hypersonic. Addressing these research gaps could lead to the development of composite coatings with optimized properties and functionalities, paving the way for their widespread application across the industries for high temperature applications.

2.4 Research Objectives

Based on the exhaustive literature review and with the consultation of different expert in the field of tribology and composite coating along with our mentors we have locked the following research objective for the current research:

a. To develop composite coating for the wear resistance applications
b. To Characterize and analyze the Mechanical properties of the developed composite coating.
c. To study the high temperature wear behavior of the developed composite coatings

Chapter 03

Experimental Procedure and Research Methodology

In the present work, the experimental procedure to develop the composite coating along with the detailed process parameter have been discussed. The characterisation techniques utilised for the investigational study have also been discussed in this chapter.

3.1 Introduction

This chapter provides an in-depth overview of the comprehensive experimental methodologies implementing and executing the experiments at several phases, the materials employed in the study, and the specialized equipment utilized to evaluate the performance of the newly developed materials through experimentation. Each piece of equipment utilized for the purpose of characterizing the materials is meticulously detailed, including its distinct role within the investigation, as well as its specifications and particulars.

Furthermore, the chapter encompasses the range of materials and chemicals essential for fabricating the composite-coated specimens, along with the electrolytic solution utilized for the deposition process. A systematic progression of steps, beginning from substrate preparation and extending to the deposition procedure, is extensively expounded upon.

3.2 Material and Methods

3.2.1 Coating Material & its Groundwork

Table 3.1 presents the Coating materials employed in this present research work, along with details such as the manufacturer's name and the level of purification achieved. It's noteworthy that all chemicals used in this study are of analytical grade and have been utilized without the need for additional purification.

Table: 3.1 List of Coating and substrate material along with specifications

S. No	Coating Material	Manufacturer and Specifications	Substrate Material
1	Mo, NiCr, WC, W	Trixo-Tech Advanced Material Pvt Ltd (Average particle size of 40 to 65 ±5 μm, with a purity of 99.99%)	Mild Steel (Dimensions: 80 × 80 × 2.5 mm)
2	ZrB_2 80 vol. %-SiC 20 vol. %)	Trixo-Tech Advanced Material Pvt Ltd (Average particle size of 40 to 65 ±5 μm, with a purity of 99.99%)	Inconel 718 (Dimensions: 80 × 80 × 2.5 mm)

Planetary ball milling finds widespread application in grinding, mechanical activation, and surface coating of powder particles. In the realm of mechanical alloying, critical elements include the raw material in powder usage and the practice variables [142]. Key process variables encompass milling speed, temperature, duration, and the ratio of balls to powder. These variables hold a significant impact on the ultimate composition of elemental powders, thereby influencing the end outcome.

First of all, the elemental powders (Mo, NiCr, and WC, W) are composed using an experimental laboratory ball mill for 2 h. After confirming the even mixing, the mixture is then heated at 100 C for 1 h to eliminate the moisture beforehand loading into the feeder. Here and now the coating powder is available for HVOF Thermal spray method for coating deposition.

On the Other hand, the coating powder compositions of ZrB_2 80vol. %-SiC 20vol. % were got by mingling ZrB_2 & SiC. To mix the mixture, a spray drying technique was used. Spray drying procedures enhance the smoothness of powder flow in the plasma spraying feeder nose[143] . Spray drying is performed to get nano, sub-micron-sized particles from the liquid and slurry to fabricate the solid agglomerates particles[144] . In the spray-dried technique, the slurry is sprayed hooked on the dry chamber by use of a spray nozzle. In this drying chamber, the warm air is transferred inside the drying cavity, and the liquid evaporates by leavening dried agglomerates powders resultant sphere-shaped grain particle powder with average particle size in amid 40-60 μm, appropriate in atmospheric plasma sprayed thermal spray deposition. This agglomerated powder is simultaneously stored in the chambers where powders are collected that are presented in the downside of the drying chamber revealed in Figure 3.1.

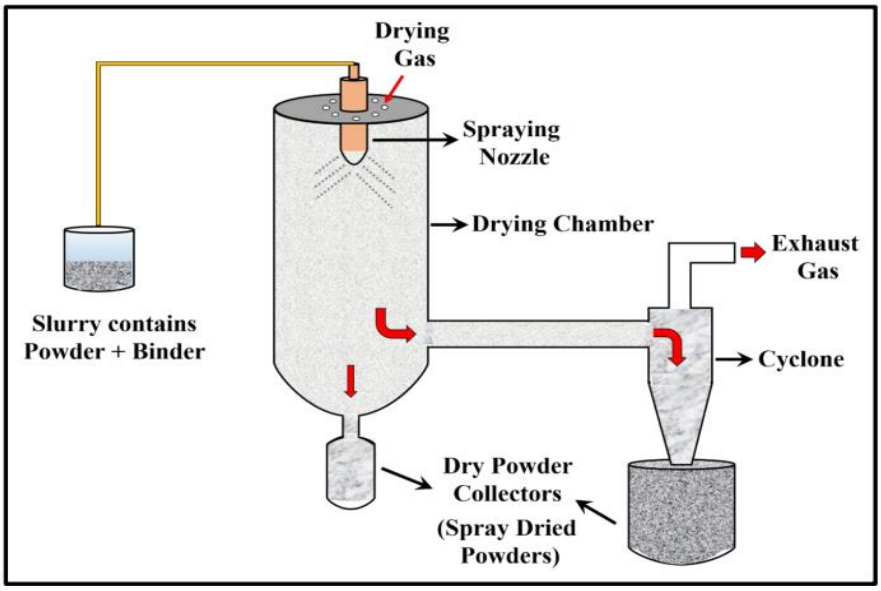

Figure 3.1: Schematic diagram showing the spray drying process used in the study

3.2.2 Substrate Selection & its Preparation

The Substrate serves as the foundation upon which the coating is deposited and significantly influences the overall performance and durability of the coated system. The choice of substrate for plasma-sprayed and HVOF coatings directly impacts the coating's performance, adhesion, mechanical integrity, thermal behaviour, and overall suitability for the intended application[145] . Careful consideration of substrate characteristics and compatibility is essential to achieve a successful and reliable coated system. Therefore, Surface finishing, microstructure, and substrate topography are important in coating formation. Impurities such as oily and grease over the surfaces might reduce the adhesion of the coatings. That is why it is very important to prepare the substrate with proper attention.

In the current work, we have used two different substrates with the same dimensions. The substrate materials selected in the current study were mild steel and Inconel-718. The selected dimension of the steel substrate is, and Inconel -718 substrate is taken as 80 × 80 × 2.5 mm. Before synthesizing the composite coating through HVOF and plasma sprayed thermal process, the substrates went to the cleaning. The samples are cleaned in the ultrasonicator under the acetone in a water bath. After the cleaning, the substrate is passed through grit blasting (MECPL equipment, India) with 20 µm grit size alumina. Figure 3.2 (a, b & c) shows the grit blasted mild steel substrate. The grit blasting aims to enhance the roughness of the substrate materials so that the coating can adhere nicely to the substrate[146]. Grit blast offers an excellent surface for interlocking places between the coating and substrate[147]. After grit blasting, the substrate was cleaned minutely with the acetone using the ultra-sonification bath to remove the grit residues left over in the substrate as much as possible. Any grit particle adhered to the metal substrate will cause a flaw, that is exaggerated by its subjection to a temperature disparity in maximum cases because of the thermal discrepancy between substrate metal and grit materials, which directly gives birth to an expansion mismatch between them.

To perform the various experimental tests, the substrate and the coated specimen were cut into regular pieces as per requirements. To avoid the heat impacts on the substrate, the cutting is performed by using a high-speed diamond saw using a water jet to save the substrate from heat shown in Figure 3.3. This cut rectangular specimens are well polished using the grinder and polisher instrument with various types of emery paper like grid size 400, 600, 800, 1500, 2000, 3000 and then the final polishing of 0.04 µm silica suspensions.

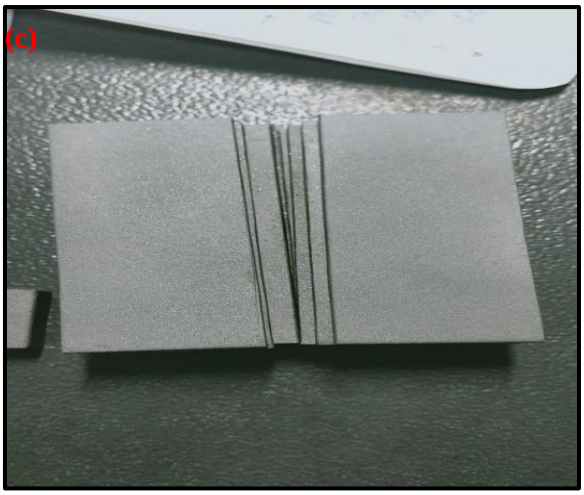

Figure: 3.2 (a, b) Front & Side view - Grit blaster equipment used in the study

(c) Mild steel substrates after grit blasting

Figure 3.3: High speed Diamond saw (ATM Brilliant 220) used for cutting the samples.

3.2.3 Coating Synthesis Methods and Process Parameters

HVOF and Plasma spray thermal processes are widely used due to their impressive coating deposition onto the substrate materials.

HVOF coatings are known for their high quality, low porosity, high hardness, and excellent wear and corrosion resistance[148] . Plasma spray coating proves invaluable for components subjected to extreme heat stress. Deposited protective layer against the surface of these parts, enhancing their ability to withstand high temperatures and thermal fluctuations. In this process, a plasma torch is employed to heat a powdered coating material to its molten state. The melted unit particles are then pushed against the substrate's surface, wherever they quickly coagulate, forming a dense & resilient coating[149], [150].

3.2.3.1 Coating Synthesis via HVOF Thermal Spray Method

The Mo-NiCr-WC-W composite coatings were applied using the HIPOJET HVOF thermal spray system, manufactured by MEC and accessible at DTU. The HVOF thermal spray equipment [Refer figure 3.4 (a)] consisted of a HIPOJET-2700 spray gun, a control panel, an X-Y manipulator, and a powder feeder. This system operated with argon, oxygen, and LPG cylinders. The substrate, composed of grit-blasted mild steel measuring 80 x 80 x 2.5 mm, was coated using the MEC PR-9182 model pressure blaster. This equipment was engaged to create and bonded an additional layer on the substrate. The dust generated during the blasting process was collected by a dust collector. This supplementary layer was utilized to improve the closed strength amid the substrate & coating.

In the HVOF thermal spray procedure, the HIPOJET-2700M MEC HVOF system was utilized to spray composite powder containing hard ceramics at supersonic speeds. To facilitate the growth of subsequent layers, a continuous supply of nitrogen (N_2) gas was provided to both the steel plate and the powder spray system.

3.2.3.2 Coating Synthesis via Plasma Spray Method

Plasma spray techniques are used due to their impressive coating deposition onto the substrate materials. In the present study, ZrB_2 80 vol. %-SiC 20 vol. % were used for spraying on the surface of the Inconel-718 with the dimension of 80 x 80 x 2.5 mm by using 9 MB plasma spray gun (Oerlikon Metco, USA). The amalgamate powders were carefully cast-off to deposit coating by means of the shrouded APS technique to prevent from oxidation. The primary plasma and powder carrier gas are argon, and hydrogen is engaged as the secondary gas. An inert

atmospheric shroud is used and placed at the forward-facing of the 9 MB plasma gun as shown in Figure. 3.5. Various test experiments were performed by considering method parameters for coating samples are firm and embodied in tabular form in further section.

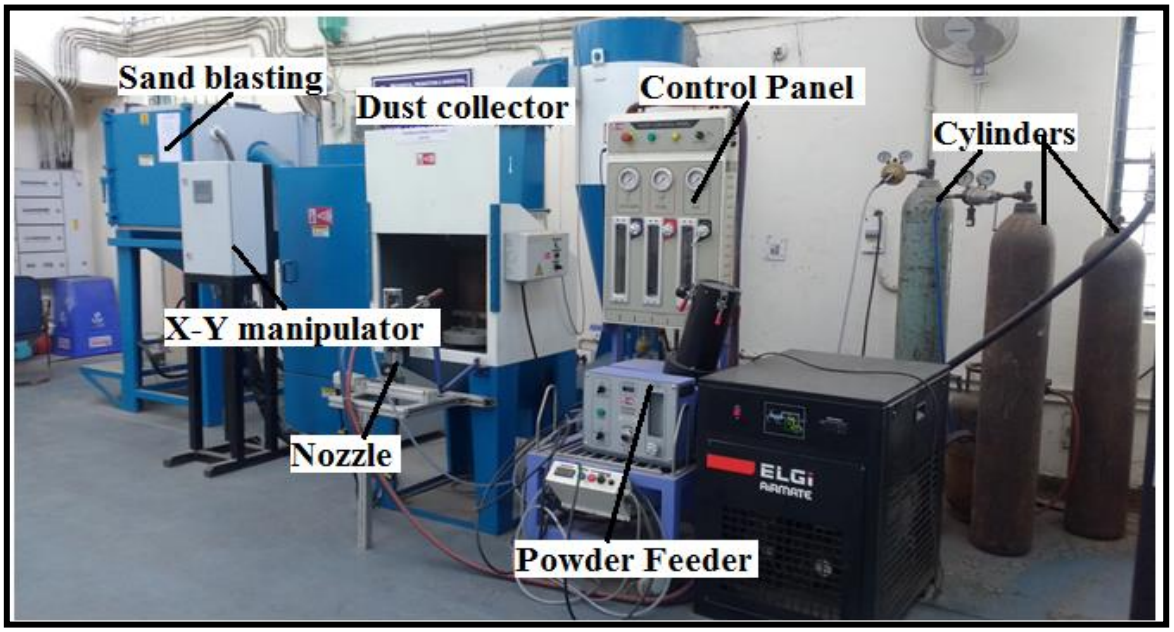

(a)

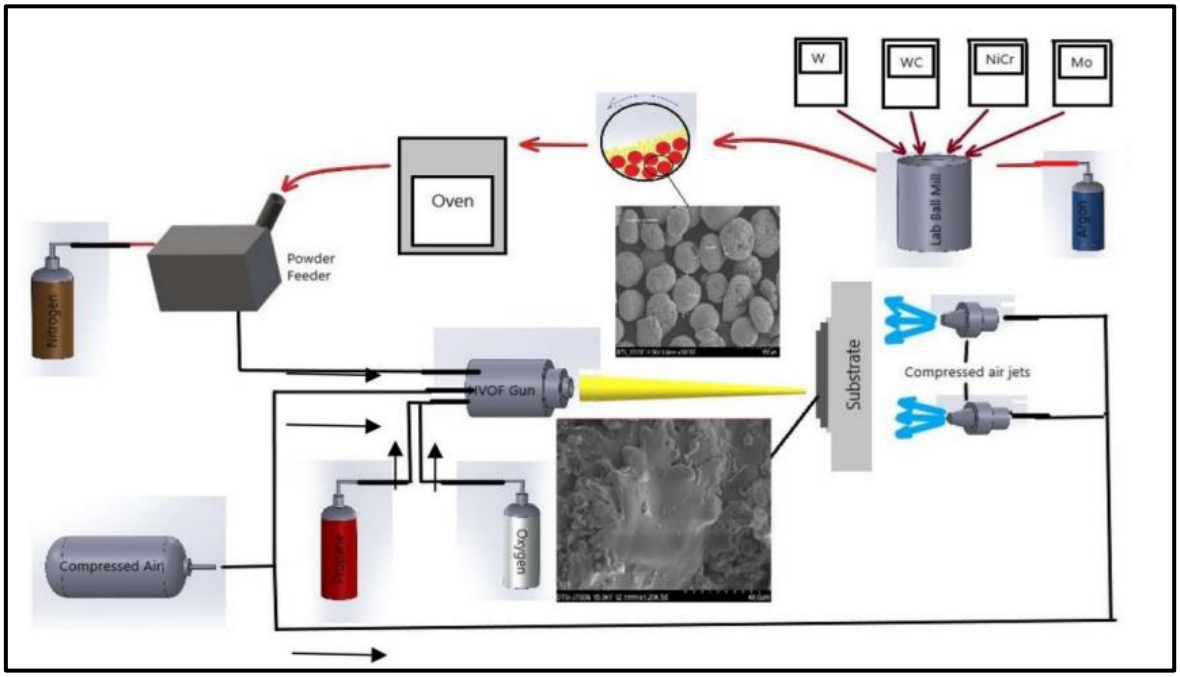

(b)

Figure 3.4 (a) Displays the HVOF thermal spray coating equipment and (b) Coating process setup

3.2.3.3 Process parameter

The optimal process parameters for HVOF and plasma spray coating are contingent upon several factors, encompassing the material under coating, the desired coating attributes, and the intended application. Among these considerations, there are various key parameters that are frequently fine-tuned to achieve effective plasma spray coating. These includes Stand-off distance, gas flow rate, Powder feed rate Plasma Torch Power, Substrate Preheating Temperature, Rotation and Traverse Speeds, Powder Particle Size, Gas Mixing Ratios, Spray Pattern, Cooling Rate and Substrate Temperature, Multiple Passes and Overlapping[151], [152]. Some of the highlighted process parameters are mentioned in the separate table

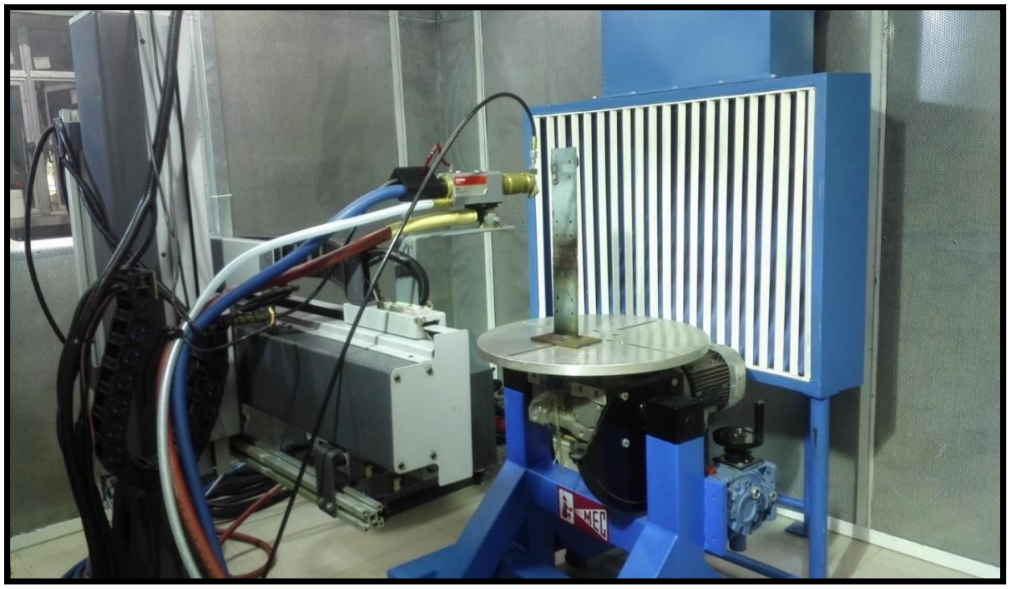

Figure. 3.5 Shroud attached Plasma Spray set-up

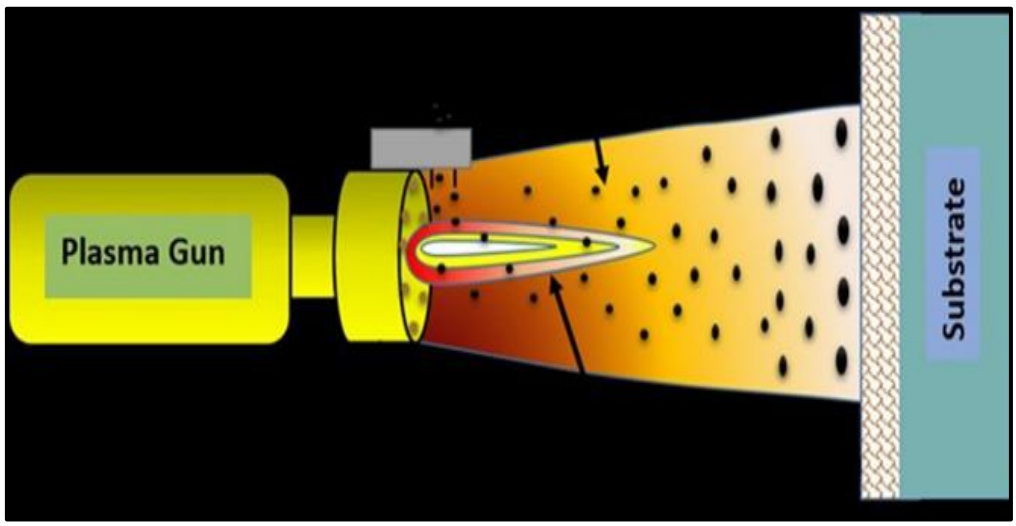

Figure 3.6: Simplified Schematic of Plasma Spray Process Typical Illustrating Powder Particle Deposition on the Substrate

3.2.3.4 Process parameter of HVOF and Plasma Sprayed Composite Coating

Various test experiments were performed by considering process parameters for coating samples using HVOF Thermal spray method. Table 3.2 presents the process parameters used in the present study for deposition of Mo-NiCr-WC-W composite coatings.

Table: 3.2 Process parameter of HVOF coating for the deposition

S. No.	Parameters	Values
1	Air flow (SLPM)	100
2	Carrier gases pressure (N_2) kg/cm^2	5
3	Air pressure kg/cm^2	05
4	Oxygen pressure kg/cm^2	08
5	Oxygen flow (SLPM)	250
6	Carrier gas flow (SLPM)	15
7	Fuel (LPG) pressure kg/cm^2	06
8	Fuel flow (SLPM)	

Table: 3.3 Optimized Process Parameters used to Fabricate Atmospheric Plasma Sprayed ZrB_2-SiC Coatings

Plasma Spray Parameters	Current (A)	Voltage (V)	Standoff distance (mm)	Primary flow, Argon (slpm)	Feed Rate (g/min)	Secondary flow, Hydrogen (slpm)	Shroud Gas Pressure (psi)
Value	506	60	110	54	12	5.1	40

3.3 Powder and Coating Characterisation

3.3.1 X-Ray Diffraction (XRD) study

X-Ray Diffraction techniques are used for characterizing a crystallographic phase's identification of the samples. This method is grounded on the dispersed intensity of an X – ray beam that has knockout (Scatter) a sample where it is function of angle of incidence and angle of scatter. The XRD principle is expressed using the Bragg's Law (Equation 2.1), $n\lambda = 2d \sin \theta$ (2.1) Where, λ is the wavelength of the fall X- ray radiation, d = the spacing between the planes in the atomic lattice, θ is the angle between the incident X ray and the scattering planes and n is an integer determined by the order given. Cu-kα1 radiation with a wavelength of 1.5418 Å is commonly used in XRD[153]. An incident beam hits the sample with an angle of θ, for which diffraction takes place in very likely location of 2θ. The bent beam is observed by means of a mobile sensor that is linked to a computer. In usual use, the scan is used over a range of 2θ values at constant angular velocity. The crystallographic phase identification of all the HVOF and plasma sprayed coatings was performed at room temperature using the X-ray diffractometer (XRD) (Rigaku, Model: TTRAX III, Japan), which is shown in the Figure 3.7. XRD was carried out in 2θ range between 20° and 80 ° at a Scan rate of 2°/min with the Step size of 0.02° and it is operated in the 25kV and 15 mA current. In the present thesis, the obtained XRD patterns were compared with the ICDD database to confirm the phase purity of the powders, pellets as well as plasma sprayed coatings. Quantification of phases in the obtained XRD pattern was accomplished using X′Pert high score plus software.

Figure: 3.7 X-ray diffractometer (Rigaku, Japan (Model: TTRAX III) used in the study

3.3.2 SEM and FESEM with EDS Characterization

The initial powder and developed powders detailed microstructure were carried out by using FESEM (field emission scanning electron microscopy (Hitachi, Model: S-4800, Japan) shown in Figure 3.8 (a, b). Further the same FESEM machine was used to study the hot corrosion test. All the analysis was performed under the vacuum chamber by using voltage of 10-20 kV. Energy Dispersive X-ray Spectroscopy (EDS) mapping is an analytical technique used in materials science to visualize the distribution of elements within a sample[154]. The elemental composition of the considered samples was identified by EDX (Energy dispersive X-ray spectroscopy) that is connected to FE-SEM. The study provides valuable insights into the spatial arrangement of different elements, helping researchers understand the composition and elemental interactions within a material. EDS mapping relies on the principle that when a sample is shelled with an electron beam in an SEM, it emits characteristic X-rays as a result of interactions between the electron beam and the atoms in the sample[155]. EDS mapping is often combined with scanning electron microscopy (SEM) to get high-resolution pictures along with elemental information. This EDX detector detects the characteristics of X-ray energy and the corresponding intensity generated from the sample. Each element emits X-rays with unique energies, which are detected and analysed to determine the presence and distribution of elements in the sample.

The chemistry of elements present and intensity count in the samples can be studied by using X-ray. Hence, the coting used over the samples are ceramics and non-ceramics so for ceramics the chances of charge accumulation is more at the surface which could be responsible for blur image ,so for avoiding this ,the samples were coated by ultrathin gold layer to make it conductive using ion sputtering unit (Hitachi, Model: E-1010, Japan) shown in Figure 3.8 (b).

3.4 Study of Mechanical Properties

Mechanical properties studies on Thermal spray coating (APS or HVOF) are of paramount importance due to its profound implications for the performance, durability, and reliability of coated components. Mechanical properties assessment provides critical insights into how the coating will respond under various loading conditions, impacting its ability to withstand mechanical stresses, thermal cycling, and wear. By comprehensively understanding the mechanical behaviour of coatings, we can make informed decisions regarding material selection, process optimization, and component design, leading to enhanced overall performance and longevity in various applications.

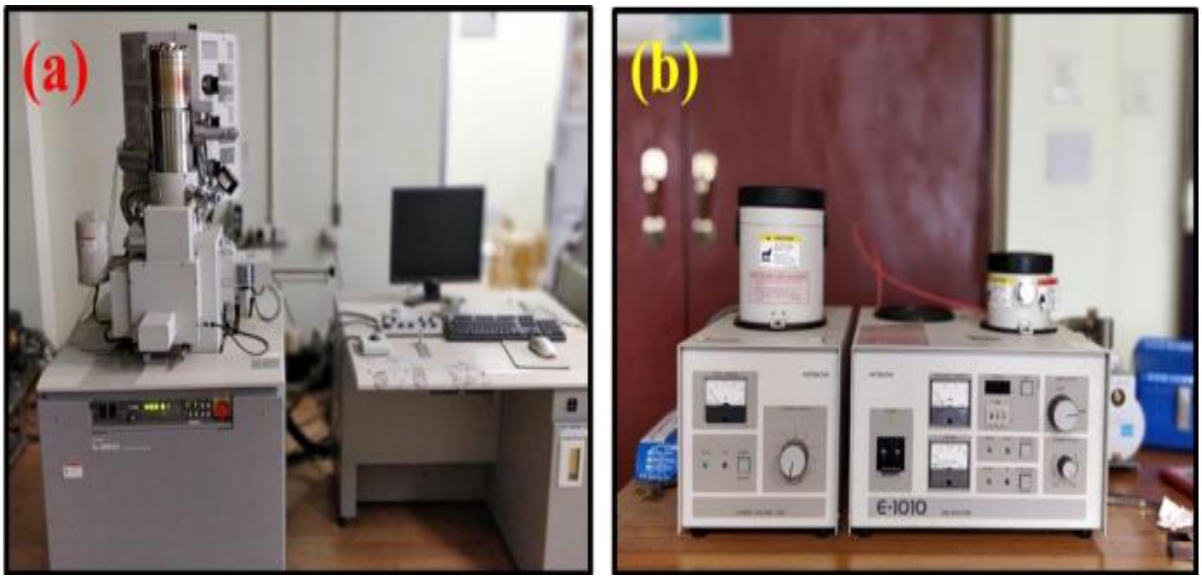

Figure:3.8 (a) the digital image of field emission scanning electron microscope (FE-SEM) supplied by Hitachi, Japan (Model: S-4800) and (b) is the digital image of ion sputtering unit (Hitachi, Model: E-1010, Japan) used to coat the samples before FE-SEM.

3.4.1 Density and Porosity Measurement

HGP (Helium Gas Pycnometer) Ultrapyc, Model 1200e, and Quanta chrome instrument made by the USA was considered to measuring the density of delaminated coating. The helium gas was used at an outlet gas pressure; 0.34 bar in 0.25cm^{-3} of the sample cell. In current thesis work, mixture rule was employed to calculating the relative densities of Mo-NiCr-WC-W and ZrB_2 +SiC by following formula. Figure 3.9 (a) depicts the image of Pycnometer.

$$Bulkdensity = \frac{DryWeight}{Volume} \quad \cdots\cdots\cdots\cdots \text{Equation: 3.1}$$

$$\text{Relative Density= Bulk density} \div \text{Theoretical density} \cdots\cdots \text{Equation: 3.2}$$

$$\text{Porosity} = 1 - \frac{\text{Real Density}}{\text{Theoretical Density}} \times 100 \quad \cdots\cdots\cdots \text{Equation: 3.3}$$

The bulk densities of all plasma sprayed coatings were determined using the Archimedes water immersion technique. This arrangement involves suspending a pan by a string within a glass

beaker filled with water, as illustrated in Figure 3.9 (b). In this thesis, the assessment of density adhered to the ASTM C20-00 (2015) standard. According to this guideline, a small section of self-supporting coatings was positioned within a container, and its weight was measured under dry, suspended, and soaked conditions using a precision digital balance (Citizen, Model: CY 220C, India). To determine the volume, the weight of the plasma sprayed coatings when immersed in a soaking state was subtracted from the weight while suspended. Subsequently, the bulk density of the coating was derived by dividing its dry weight by the calculated volume, as demonstrated in Equation 3.1. Furthermore, the RD, relative density of the coating was determined by dividing the bulk density/theoretical density, as expressed in the following equation. Porosity in the plasma sprayed coatings were measured by the empirical equation 3.3

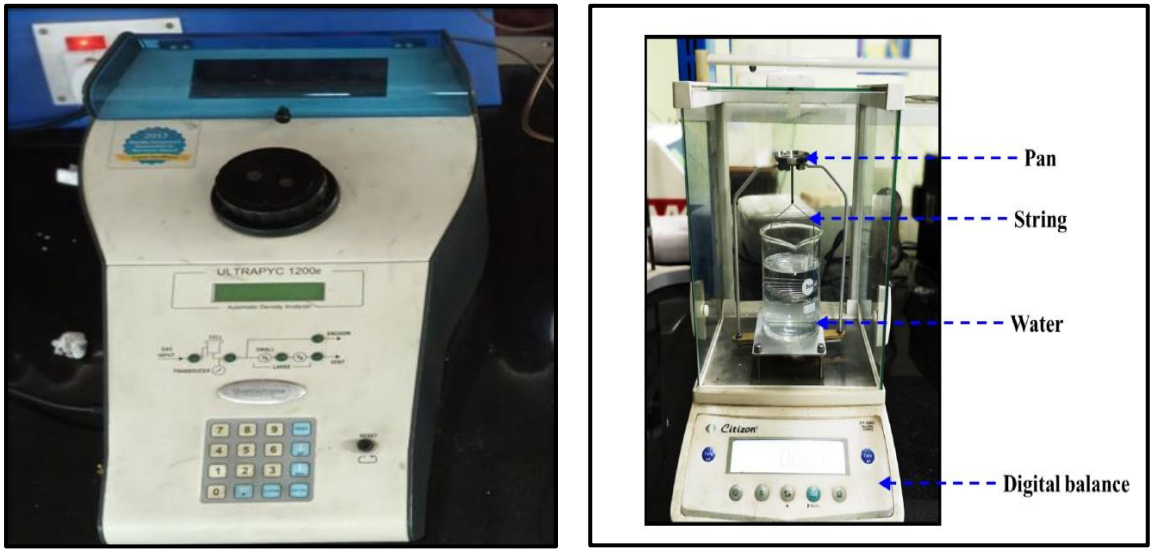

(a) (b)

Figure: 3.9 (a) Pycnometer used to calculate density of delaminated coating, (b) Suspended pan-string setup for the measurement of bulk densities using Archimedes water immersion technique

3.4.2 Micro Hardness Study

Micro-hardness values were measured by using Ficher micro hardness tester, which was present in Delhi Technological University, New Delhi. The principle of Micro-indentation hardness testing Vickers hardness test, but in this test less loads were produced more microscopic indentations i.e., almost 10–200 µm. This testing also called as micro-hardness testing which was commonly employed to measuring the hardness in local field/area. For example distinguish microstructural stages or surface layers[156]. Whereas, in Vickers hardness test, diamond shaped pendant was taken to put the impression over the specimen exterior surface with application of

force for 10-15 seconds. The range of force are one to thousand gf. The size of impression is calculated by considering microscope with indenter angle of 136° (Face Angle). The value of hardness are calculated by considering below formula:

The micro-hardness of NiCr-W-WC-Mo composite coating was obtained 240.75, 240.8, 284.29, 290.8 HV.

Vickers micro-hardness (HV) = $\frac{2F \sin(\frac{\alpha}{2})}{D^2}$ ---------- Equation: 3.4

Where:

F = load in Kgf

α = diamond indenter (136^o), Face Angle

D= [D= (d_1+d_2) / 2]

Where D; mean diagonal indentation in mm

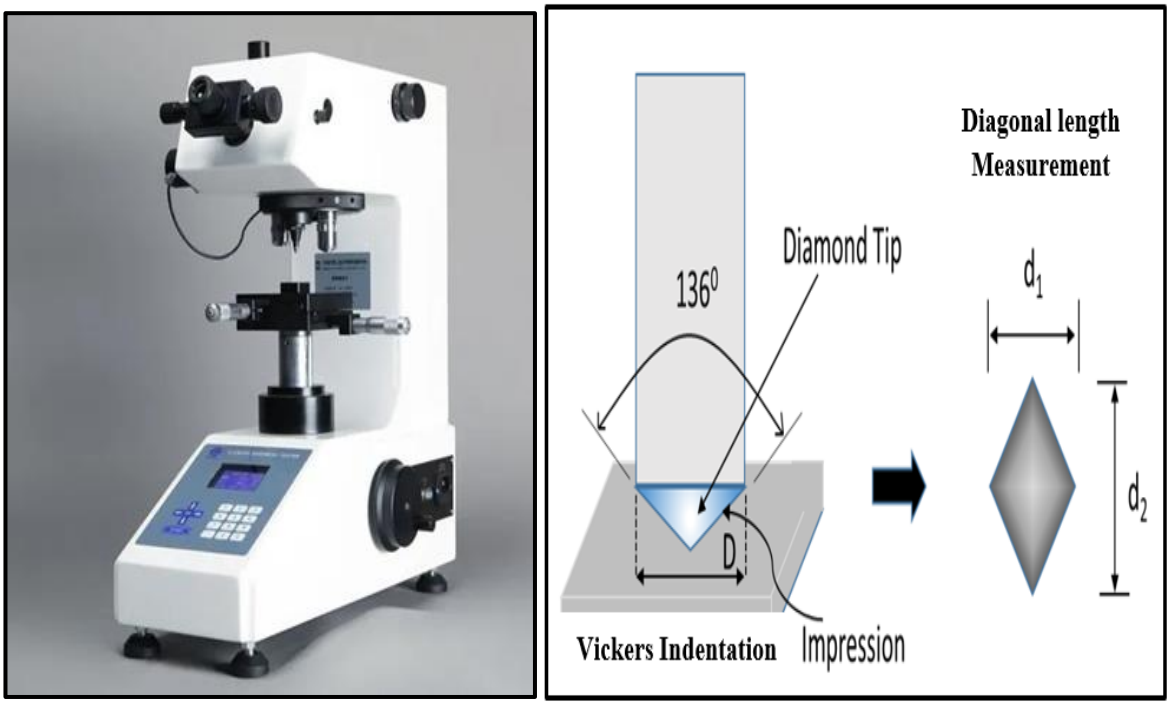

(a) (b)

Figure 3.10: (a) Vicker hardness tester and (b) Its mechanism used for measuring micro-hardness of composite coating

3.4.3 Hot Corrosion Study

As a critical evaluation method for Plasma spray coatings, the hot corrosion test simulates the actual corrosive conditions (typically salts) in a controlled environment. Thermally coated samples are exposed to high temperatures to test corrosion resistance and degradation behaviour. Typically, the arrangement consists of a high temperature furnace or testing enclosure that can achieve the targeted temperatures, along with a system for introducing the corrosive substances. The coated samples undergo meticulous preparation and mounting procedures to ensure precision and uniformity in the outcomes. During the test, the coated samples will be subjected to $Na_2SO_4 + V_2O_5$ salts for thirty hour at a 1600^0C and then detached for characterization later cooling to room temperature The proposed coating combination ought to display an indispensable part in melted salt diffusion extenuation through working as a external barrier. The said coatings interact thermally and chemically with the molten salts, altogether preventing liquefied salt penetration and make strong root.

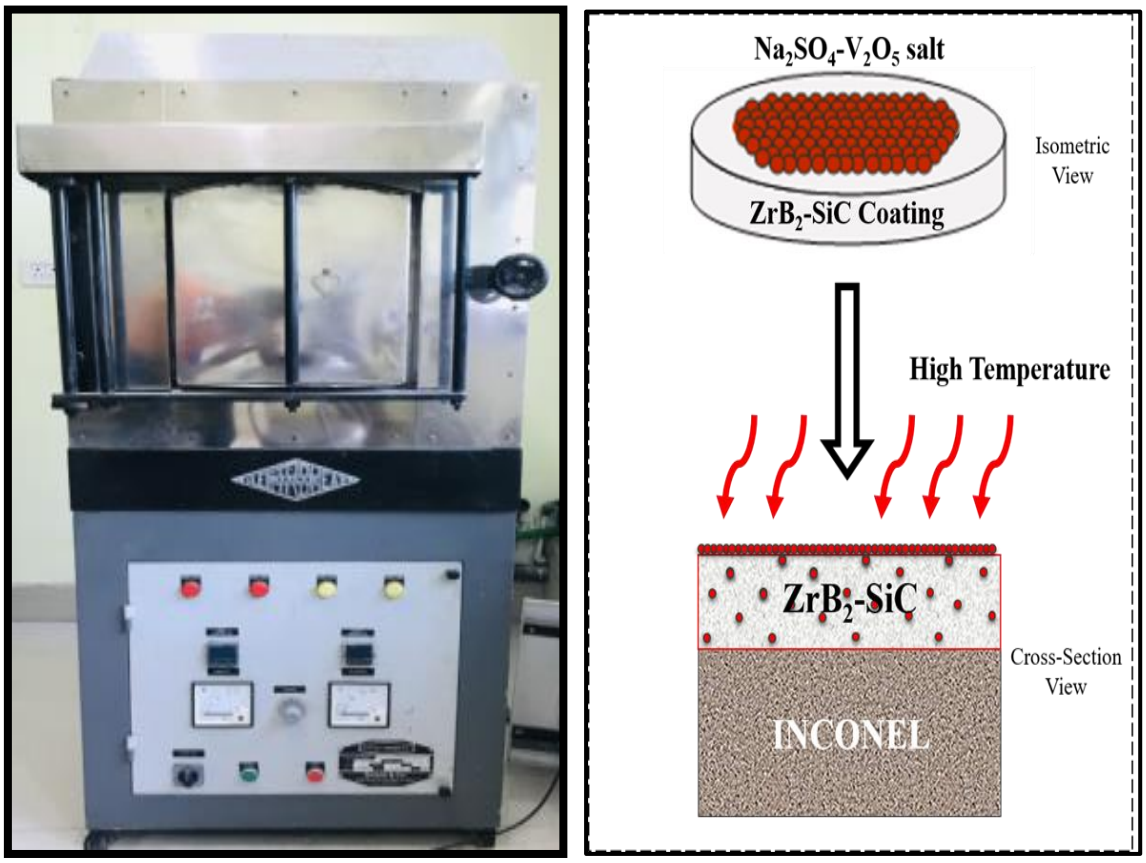

(a) (b)

Figure 3.11: High Temperature Furnace for Hot Corrosion Test (b) Penetration apparatus of molten Corrosive salts through ZrB_2-SiC coating under elevated temperature environment.

3.4.4 Residual Stress Measurement

Residual stress pertains to the inner tensions present within a coated material subsequent to the completion of the plasma spray deposition process. These tensions emerge due to the temperature differentials and mechanical interactions that take place during the swift cooling and solidification of the molten particles as they affix to the substrate. These stresses can be measured using experimental methods or a combination of experiments and mathematical analysis. Process variables like deposition speed, spray gun velocity, coating temperature, and thickness influence residual stress generation. The coating procedure affects the quality of particle drive, its impact, distortion, coating development, splat interfaces, pore development, and ultimate layer formation. Compressive residual stresses are preferred, while tensile stresses can lead to coating issues like fatigue failure, crack initiation, and delamination. Drilling is a common method to assess residual stresses, involving micro-level drilling until reaching the substrate with controlled parameters to minimize induced stresses. The assessment of internal stresses present within the composite coatings was conducted using a Pulstec residual stress analyser (model: -X360, XRD). The evaluation of residual stress employed the cos (α) method, which is rooted in Bragg's law. The analyser had an LED marker, CCD camera sustenance, and a power and sensor unit, that is accessible at DTU. This approach is illustrated in fig. 3.13 (a, b) and is supported by a 45^0 X-ray indentation and a sensor unit. The diverse orientations of grain crystals that fulfil Bragg's law prompt X-ray diffraction. Due to these crystal orientation differences; the diffracted X-rays create a cone pattern around the axis of the incident X-ray. The relationship utilized is $n\lambda = 2d \sin\theta$, where "n" (an integer) signifies the reflection order, "λ"; wavelength (incident X-rays), "d"; interplanar spacing of the crystal, and "θ"; angle of incidence, equal to the angle of scattering.

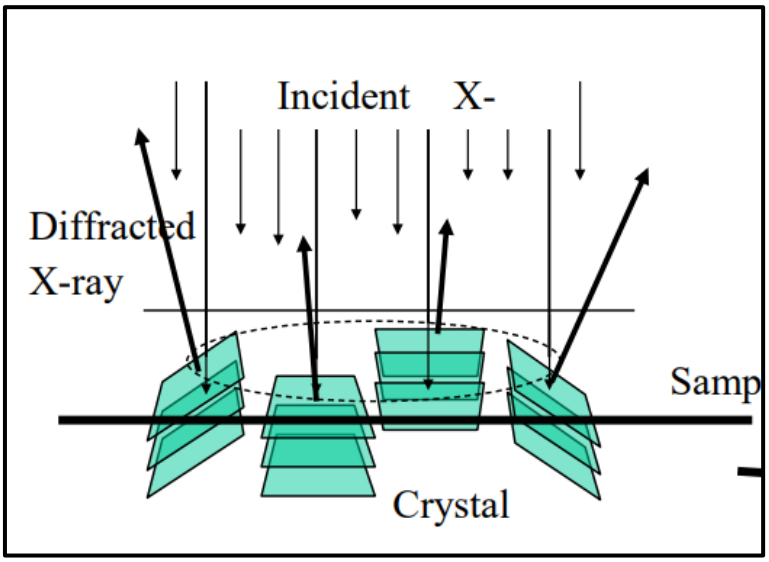

Figure 3.12 (a) Mechanism of cosine-a method for measuring residual stress

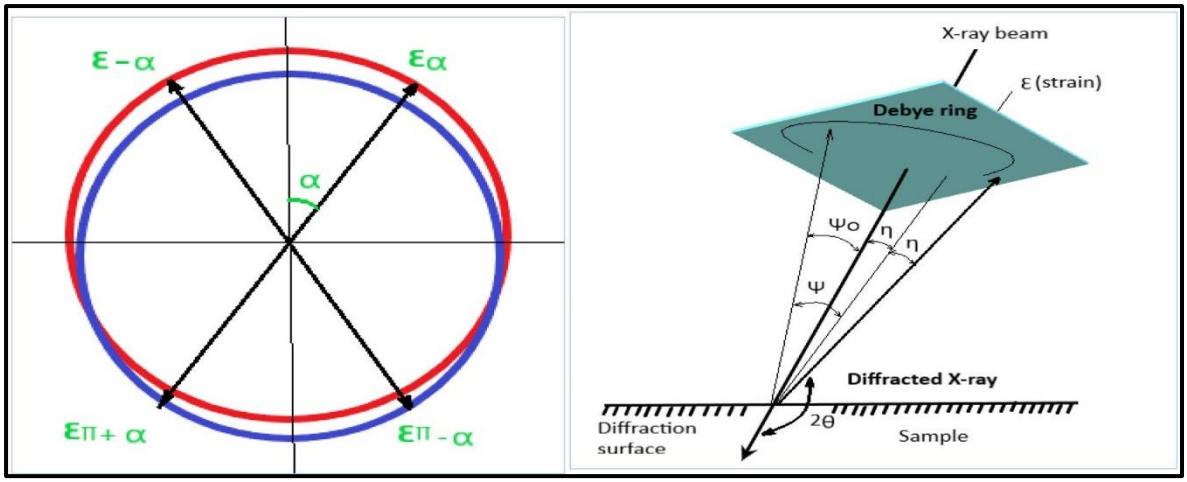

Figure 3.12 (b): Graphical representation of cosine-a method

3.4.5 Wear Study

The Wear study employed in the present investigation to analyse the friction coefficient, material removal rate, and the force of friction experienced between two materials engaged in relative motion.

For measuring the tribological properties of W–WC–NiCr–Mo, pin-on –disk Tribometer is used with configuration of (TR-20L-PHM800-DHM850). Figure. 3.14 depicts image of Pin on disk tribo-meter. The load of 20 N-200 N was considered with sliding velocity of 300 rpm (up to) at varying temperatures range of 850 °C and 800 °C. LVDT instrument was used for measuring the wear. In the current research work, the temperature of disc has increased not the pin and disc temperature.

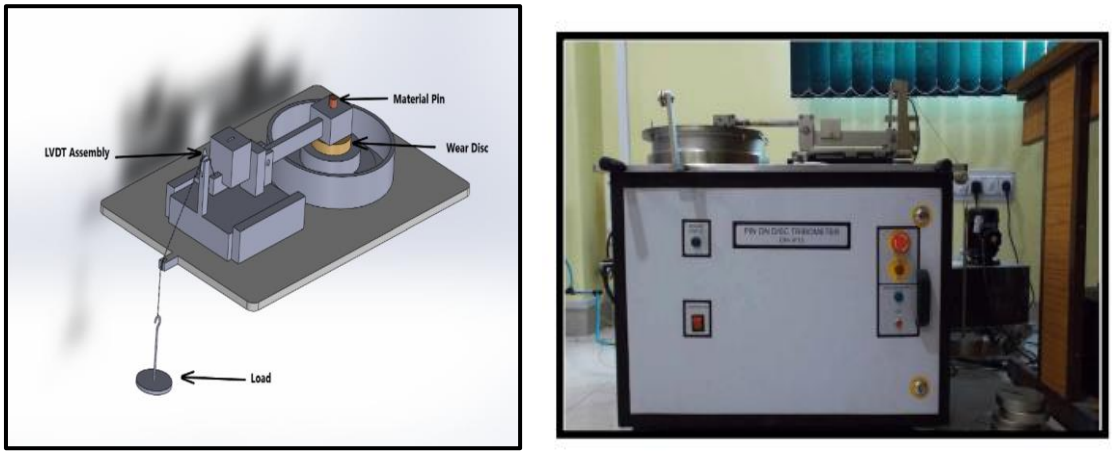

(a) (b)

Fig: 3.13 (a) Graphic representations of pin-on-disc Tribometer, and (b) High Temperature pin on disc tribometer used for testing

The four set was considered for performing wear test with pin diameter of 8 mm (EN-31) and disc dia of 60 mm with 2mm of thickness. The pin has worked as a counterpart and it shape was circular flat with 8 mm dia. At last the tribological properties was examined for developed coatings with considering fixed parameters such as such as load (N), temperature (°C), sliding velocity (m/s) and sliding distance (m). Table 3.4, 3.5 and 3.6 shows the variable tribo test conditions for performing the experiments.

Table 3.4: Tribo-test condition

Sr. No	Considered Parameters	Taken Values
1	Temperature (°C)	100, 200, 300, 400
2	Load (N)	55, 65, 75, 85
3	Speed (m/s)	1.0,1.5, 2.0, 2.5

Table 3.5: Considered Experimental condition

Test No	Temperature # (°C)	Load # (N)	Speed # (m/s)
Testing # 01	100	55	1.0
Testing # 02	200	65	1.5
Testing # 03	300	75	2.0
Testing # 04	400	85	2.5

Table 3.6: Constant parameters

S. No.	Parameter	Condition
1	Counter body	Pin of Ø8mm EN-31 was similar for all the test
2	Disc	Disc of Ø60mm and thickness 2 mm of mild steel with composite coating W-WC-Mo-NiCr
3	Lubrication	Dry

The tribological wear test of ZrB_2-SiC composite coating conducted with the help of ball on disk tribometer by means of tungsten carbide ball, for 3600s, 250 rpm of speed, 5 N of normal load with diameter of wear track diameter is 6 mm. Additionally, ZrB_2-SiC in the modification of in dry non lubricated conditions at sliding against counter body of WC ball and corrosive molten salt (55 wt. % V_2O_5 + 45 wt. % Na_2SO_4) intrusion will also be explored. According to Archard's equation is applied for resolve of specific wear rate.

The formula for calculating wear rate using the volume loss method is as follows:

$$W = \frac{V}{A\,N} \qquad \text{---------} \qquad \text{Equation: 3.5}$$

Wear Rate (mm^3/m) = (Volume Loss) / (Sliding Distance x Applied Load)

Where V; volume loss (mm^3) A; normal load (N) and N; sliding distance

W; wear rate (mm^3/Nm)

Here, A shows the area among the coating and the ball, N shows the speed V shows the wear loss. COF graph with respect to time is plotted for each developed coating (Mo-NiCr-WC-W) at all the three applied loads. These plotted graphs showed the variation of COF values entire test duration of fifty minutes. The tribometer is connected to computer which is WINDUCOM^{TM} software enabled were used to records the value of COF after every seconds. Then this graph is transferred into excel sheet and graph was plotted for load and three testing temperature for comparison purpose.

Furthermore, the wear behaviour and wear morphology of worn surface of both the developed coatings via plasma spray and HVOF thermal Spray were evaluated through FESEM and SEM equipped EDS.

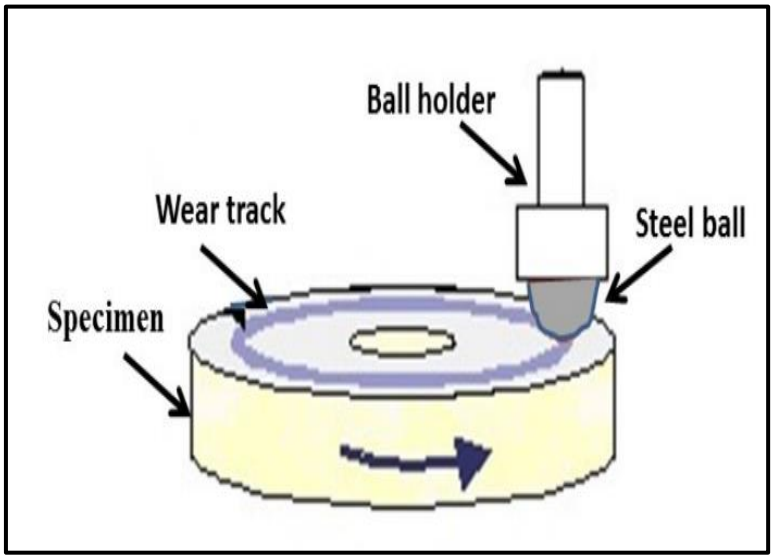

Figure: 3.14 Schematic diagram representing Ball on Disc wear Tester

CHAPTER – 4: RESULTS AND DISCUSSIONS

Development of Composite coating (Mo–NiCr–WC–W) on Mild Steel Substrate and understanding its Tribological behavior under different Temperatures.

In current research work, HVOF sprayed *Mo–NiCr–WC–W blend* composite coating tribological properties are studied under distinguish temperature ranges. In first phase, powders are prepared for coating by employing ball milling procedure. In second phase, the prepared powders are sprayed on the surface of substrate (4 specimen) by employing HVOF technique. In next stage, tribological properties of developed coating were studied by using high temperature pin on disk Tribometer at varying load, varying temperature and fixed sliding speed. XRD, FESEM and micro hardness tester was used characterize the developed coatings and hardness measuring purpose in developed wear tracks. The COF and wear rate were calculated by employing weight loss and m/c outcomes method. At last, the results are analyzed and discussed in detail.

4.1 Powder Characterization of Coating Material

4.1.1 Microstructural Characterizations of Mo, NiCr, W coating powders.

Figure 4.1 depicts the SEM micrographs of commercially obtained feed powders feed (a) Mo (b) NiCr, (c) Tungsten and (d) Tungsten carbide powders which were used for developing the coating onto the surface of the substrate by using HVOF spray technology. It has been observed from the obtained SEM image that the shape of particles is in spherical in structure. The average size of Mo, NiCr, W and WC obtained by spray dried process are from 40 to 65 ± 5 μm[157], [158].

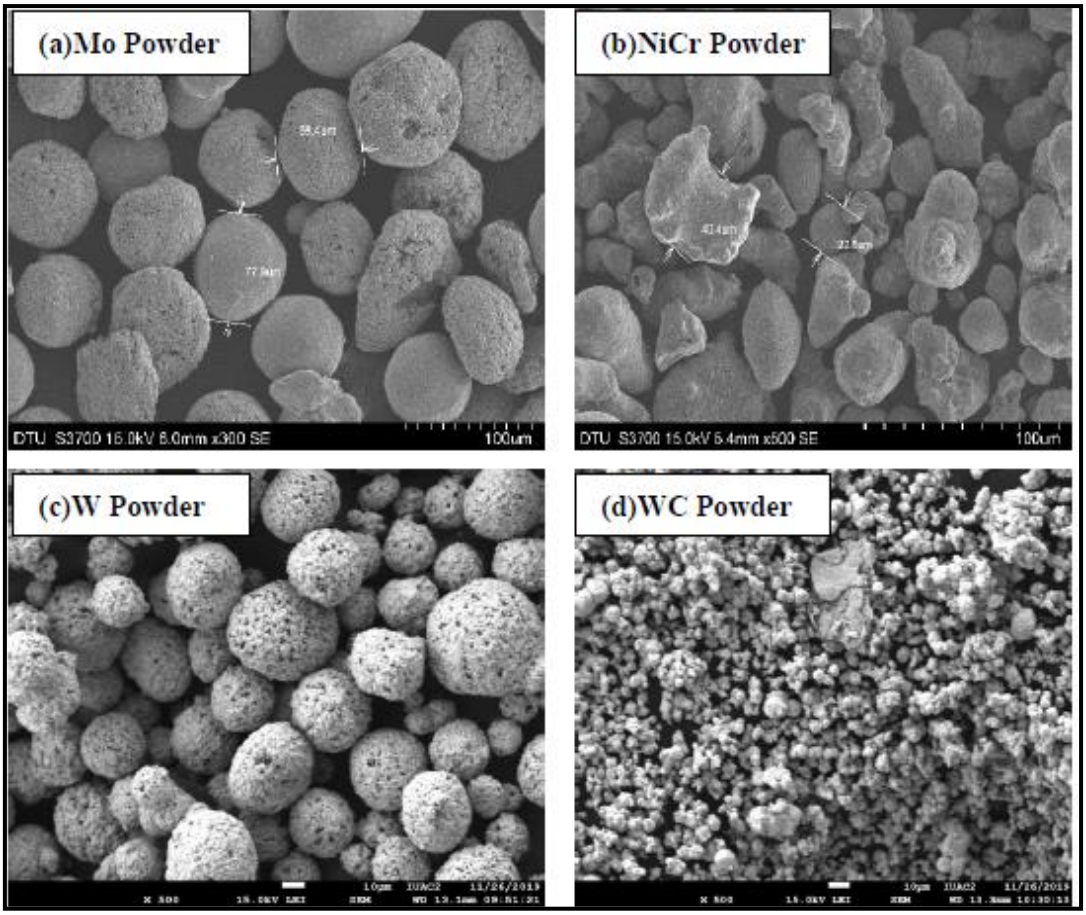

Figure 4.1: SEM micrographs of commercially obtained feed powders for HVOF coating.

4.1.2 XRD Analysis Mo, Ni-Cr, W and WC powder

The phase and purity of commercially obtained coating material were examined with the help of XRD Analysis. In order to ensure uniform mixing of the powder particles, the obtained coating materials were first milled in a laboratory ball mill for 2h. Figure 4.2 depicts the XRD pattern of sprayed dried Mo, NiCr, W and WC showing sharp crystalline peaks of cubic structure. No foreign peaks other than Mo, NiCr, W and WC, it shows the powder are contamination free. This analysis confirmed that tungsten carbide was a strong intensity peak as compared to others.

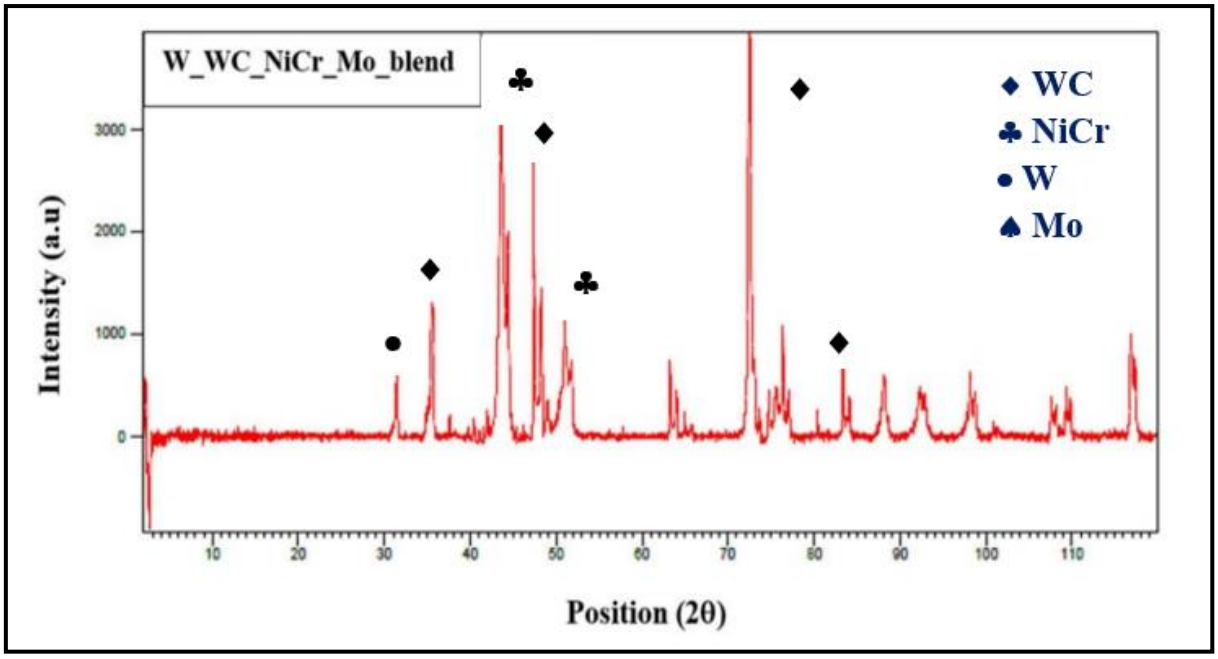

Figure 4.2: XRD spectra of the sprayed Mo, NiCr, W and WC powder

4.2 Characterisation of Mo-NiCr-W Developed Composite Coating

4.2.1 Morphology and Coating Thickness

The surface morphology of HVOF-deposited coatings was analysed using FESEM. Figure 4.3 (a) depicts as-sprayed coating Surface Morphology. The micrograph reveals that the coating in its molten state, depicting a flawless deposition process. The as-sprayed coating reveals the existence of pancake-shaped and disc splats. Partially melted regions are also evident. The outstanding quality of the deposition becomes evident when observing the coating cross-sectional area. The deposited coating on steel substrate is excellent & can be seen in the obtained FESEM image. The highly magnified cross-sectional images give the clear appearance of perfectly bonded matrixes, leading to improved hardness and wear resistance properties in fabricated coatings. Figure 4.4 shows the coating cross-section thickness. The thickness obtained from the developed coating was 370–380 μm.

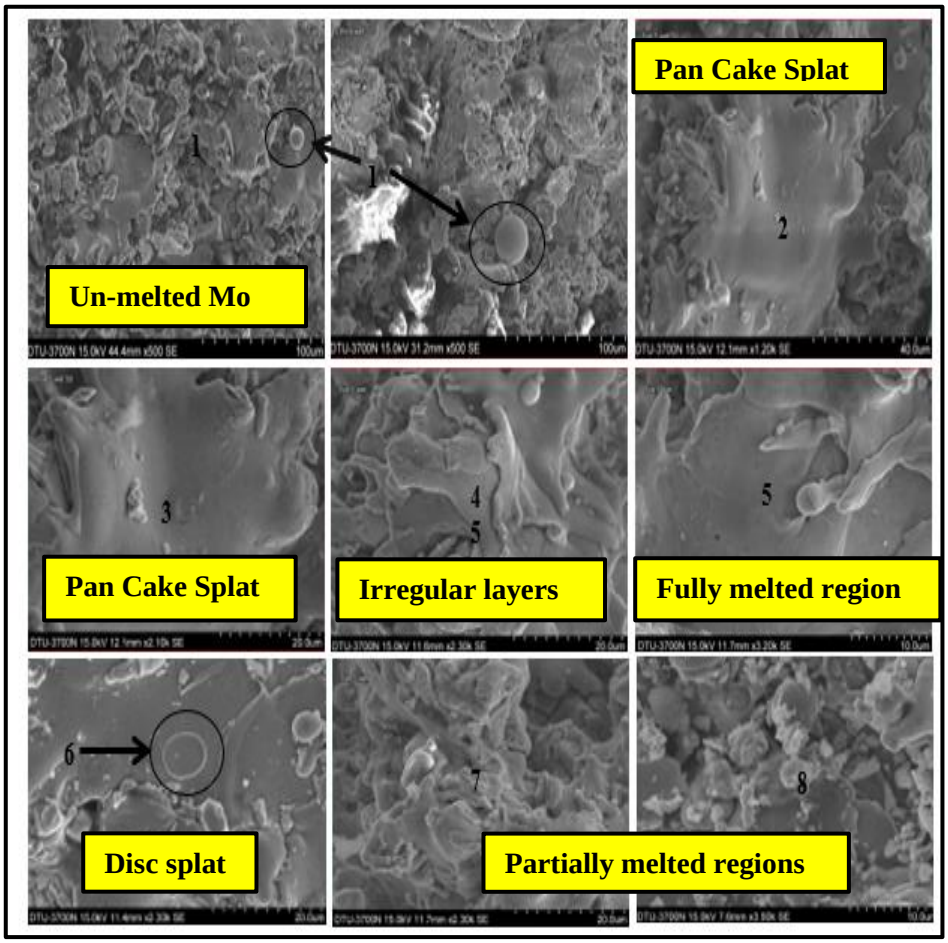

Figure 4.3: FSEM Micrographs of deposited coating

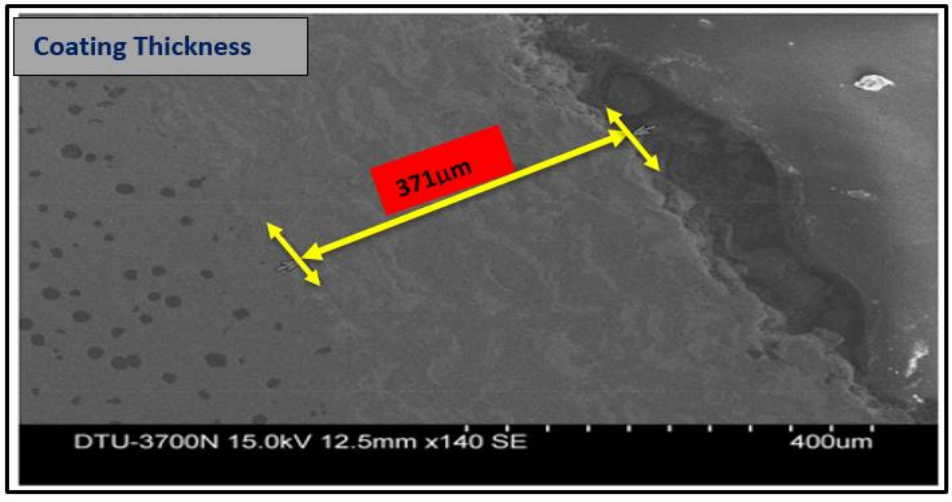

Figure 4.4: Cross-Sectional View depicting Coating thickness

4.2.2 EDS Analysis of Mo-NiCr-W Composite Coating

Figure 4.5 shows the elemental compositions of powders Mo, NiCr, W, and WC, where elemental mapping analysis was performed. In the EDX diagram peaks of Ni, Cr, and C are given off as the X-ray returns to the K electron shell. The peak of W is given off by M electron shell and the peak of Mo is given by the L electron shell. Elemental mapping involves analysing the spatial distribution of elements using techniques like EDS in conjunction with SEM. This elemental mapping technique was performed to study the distribution of elements present in powders such as Mo, Ni, Cr, W, and WC within the sample. From this study, it has been perceived that Mo. Ni, Cr, and W were extant with their oxides on substrate surface .Figure 4.6 illustrates the distribution of carbon elements in the magenta regions; purple, yellow, orange, green, and grey are the corresponding figures for Molybdenum, nickel, tungsten, oxygen, and chromium. The manifestation of elements is also assured through peaks of EDS images depicts in Figure 4.5.

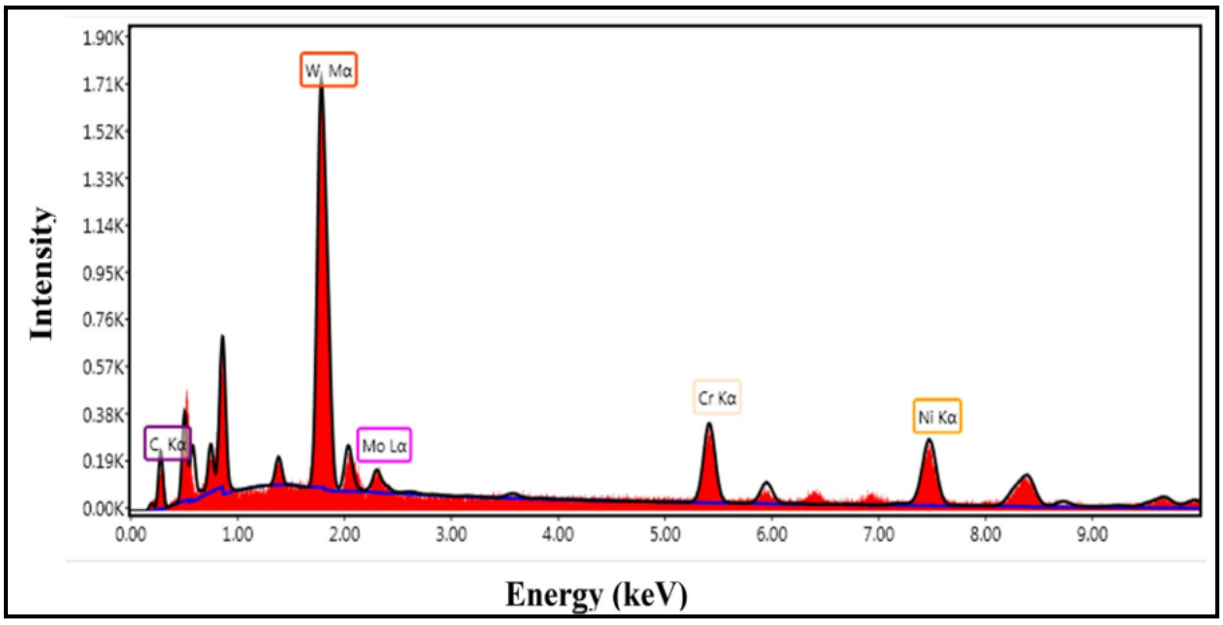

Figure 4.5: EDS analysis of HVOF deposited surface

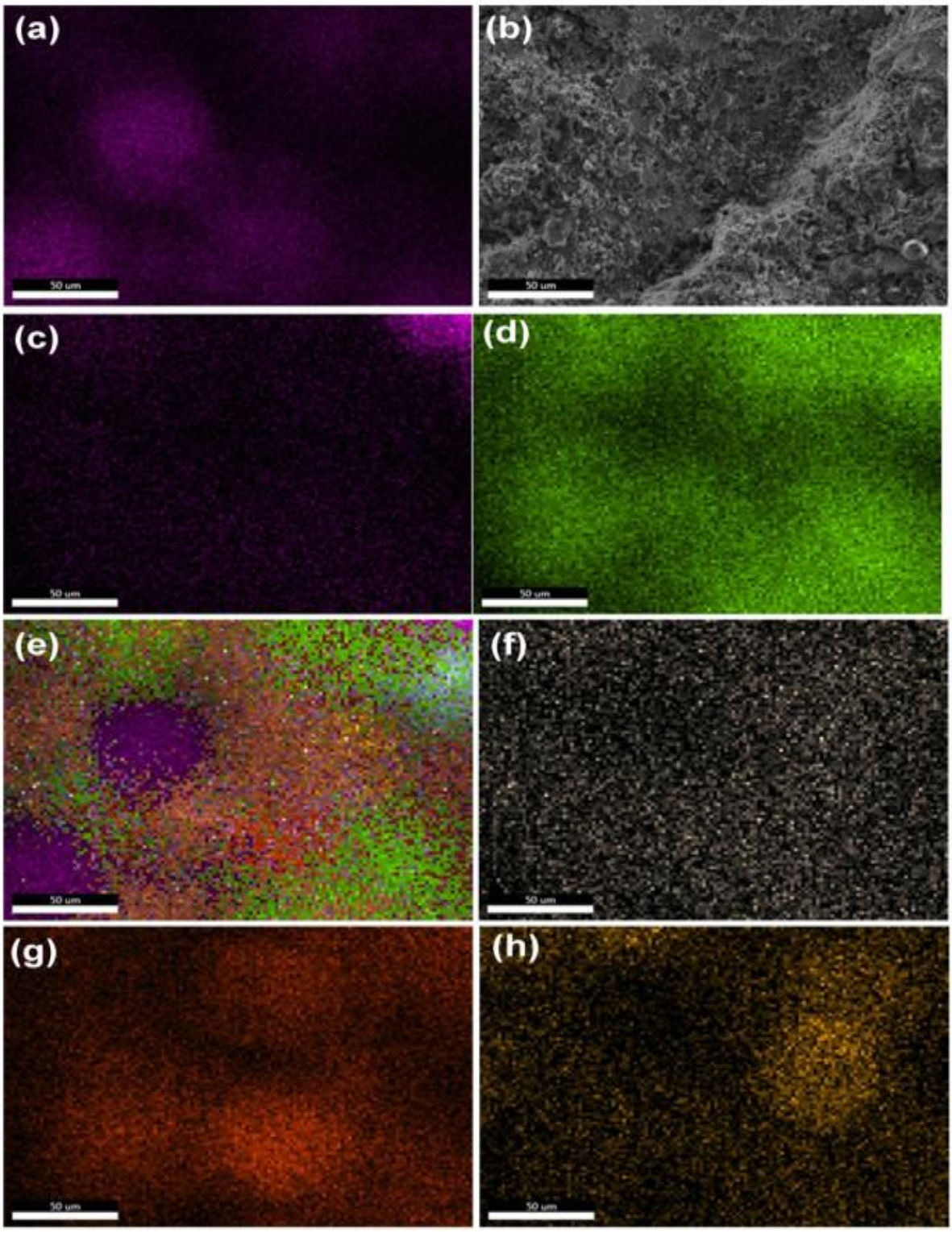

Figure 4.6: Distribution of elements through elemental mapping showing (a) Carbon (b) Morphology coating powder (c) Molybdenum (d) Oxygen (e) Complete mapping (f) Chromium (g) Tungsten (h) Nickel and

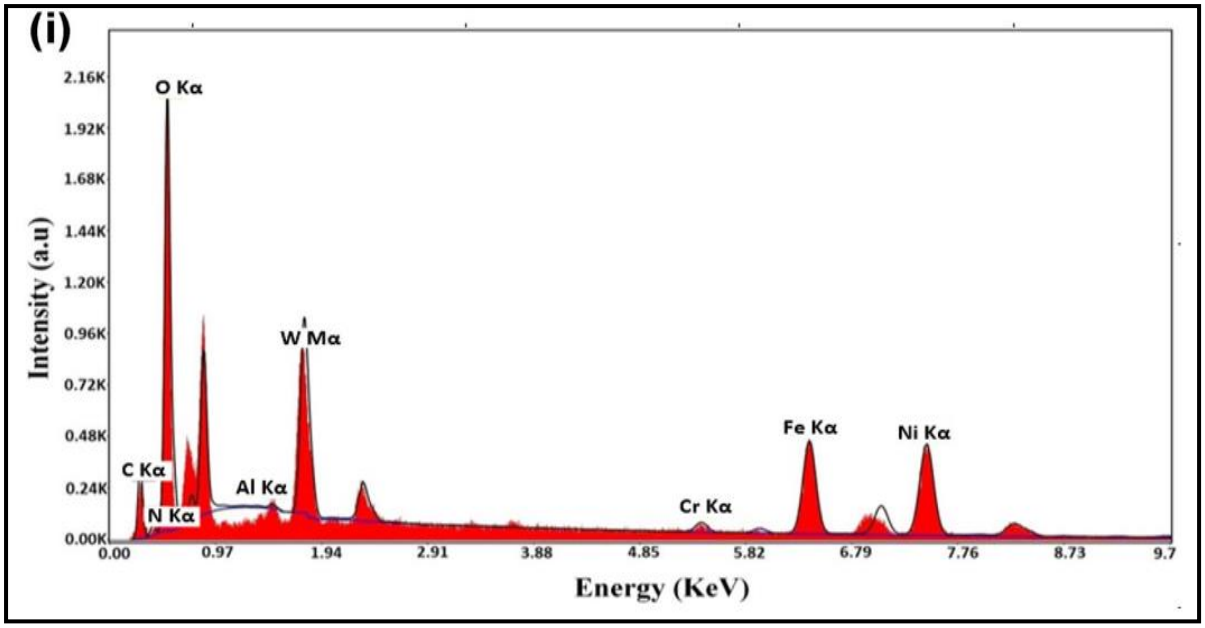

Figure 4.6: (i) Morphology and EDS analysis of coating powder

4.3 Tribological Study of Mo-NiCr-W Composite Coating

4.3.1 Wear and Frictional Behaviour of HVOF Coating

The tribological tests were performed at various normal loads such as 55, 65, 75, and 85 N at high temperatures (100, 200, 300, and 400^{o}C) for 60 minutes using EN-31 steel disc. The sliding distance was taken at 1500 mm constantly for all the test conditions. The counter body has a pin diameter of 8 mm made of EN-31 materials, and the disc diameter is 60 mm with a thickness of 2 mm of mild steel. This test was carried out in dry conditions.

Figure 4.7 (a) depicts the value of COF of developed coating (tungsten-based composite coating) at various temperatures, at sliding velocities of 1 m/s ,1.5 m/s, 2 m/s, and 2.5 m/s at an applied load of 55 N, 65 N, 75 N and 85 N in dry condition with 1500 m sliding distance. The value of COF at 55 N is 0.622 at 65 N is 0.317 at 75 N is 0.436 and 85 N is 0.314.

The trend in COF values suggests that the friction behaviour of the composite coating is sensitive to the applied normal force. Generally, higher normal forces lead to increased contact pressure between the pin and the disc, which can influence the frictional behaviour. This behaviour might arise due to changes in material deformation, adhesion, wear mechanisms, and contact area under different loads[159].

The mean value of COF from T # 01, T # 02, T # 03, and T # 04 are 0.622, 0.317,0. 463 and 0.314 at distinguishing temperatures i.e. 100, 200, 300, and 400^{0}C respectively.

The decreasing trend in COF from T#01 to Test#2 suggests that the friction behaviour improves with increasing temperature. This may be because of creation of a defensive oxide film on the substrate surface at higher temperatures, reducing direct contact between the composite coating and the counter body, thus lowering friction[160].

The slight increase in COF from Test 02 to Test 03 might indicate a change in wear mechanisms or the development of a different type of surface interaction at this temperature range.

The decrease in COF from Test 03 to Test 04 suggests that at 400°C, the composite coating might exhibit a more favourable friction behaviour, potentially because of variations in the material's properties or the surface characteristics.

Figure 4.7 (b) depicts the wear versus temperature curve of the composite coatings. It shows that wear keeps on decreasing with the increase of the temperature. The decreasing wear trend with increasing temperature suggests that higher temperatures are generally beneficial for wear resistance in this specific composite coating[161], [162]. This could be attributed to multiple factors including formation of oxide Layers, lubrication effects, changes in wear mechanisms and others. In general, elevated temperatures promote the formation of oxide layers on the coating's surface. These oxide layers can act as barriers against wear by reducing direct contact between the surfaces.

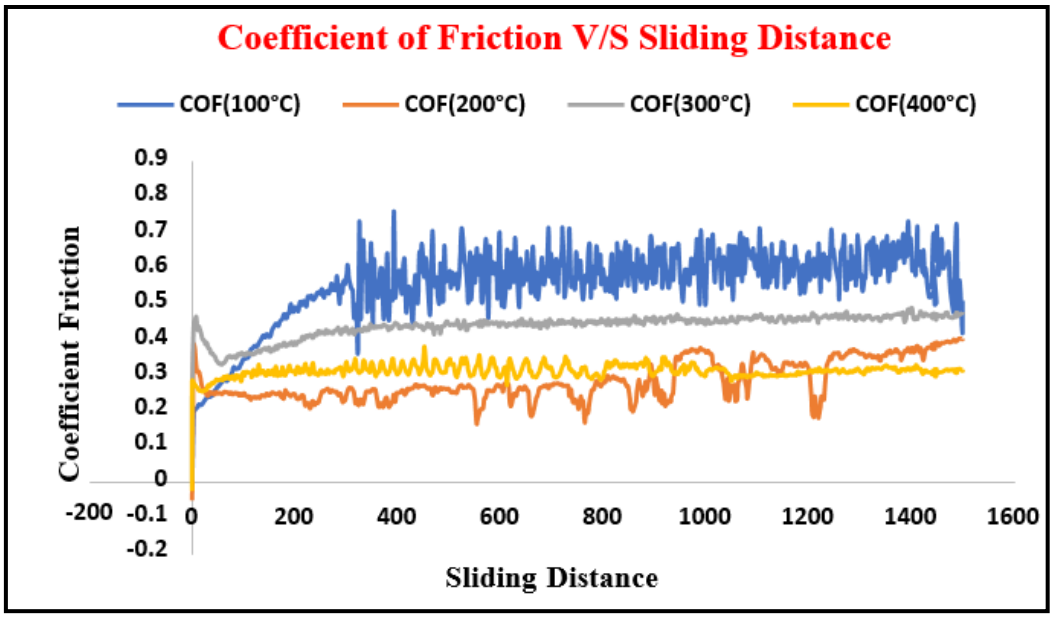

(a)

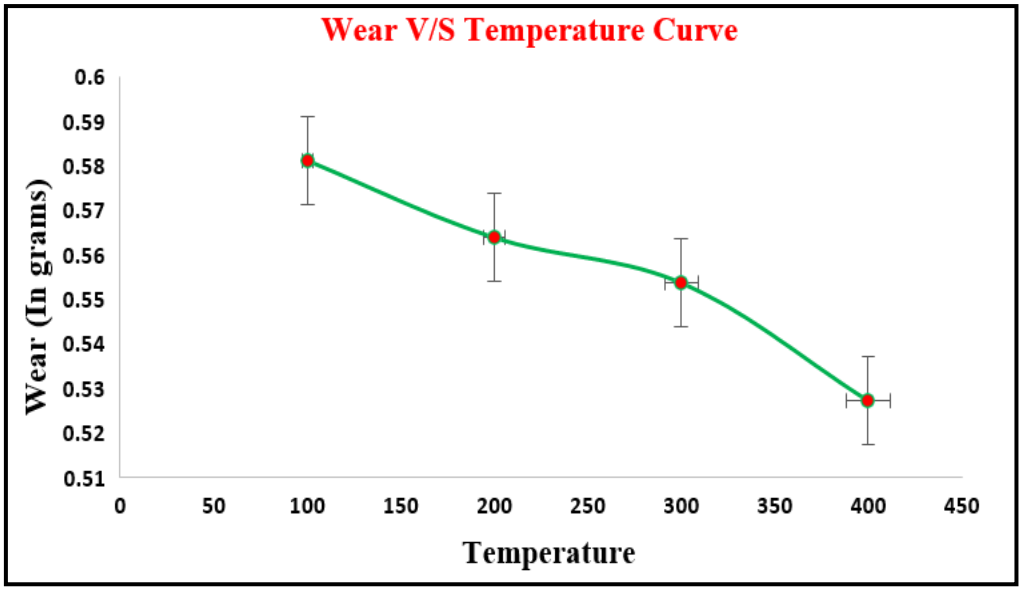

(b)

Figure 4.7: (a) Variation in Coefficient of Friction with Sliding Distance for Mo-NiCr-WC-W Coating, (b) Wear trend in Mo-NiCr-WC-W coating with respect to temperature.

Higher temperatures can alter the wear mechanisms that are dominant at lower temperatures, leading to a shift towards mechanisms that are less detrimental to the material. Effect of temperature on the micro hardness value is also the evidence of reduced wear mechanism.

4.4 Mechanical Properties of Mo-NiCr-W composite coatings

In this section we have demonstrated the mechanical properties including micro hardness & residual stress of HVOF sprayed Mo–NiCr–WC–W composite coating and understanding its behavior with respect to temperature.

4.4.1 Effect of Temperature on Micro hardness property of Mo–NiCr–WC–W HVOF Coating

At an increasing temperature 100 to 400 °C in the interval of 100 °C, micro-hardness of the Mo–NiCr–WC–W HVOF Coating was calculated. The values are observed; 240.75 ± 5, 240.8 ± 5, 284.29 ± 5 and 290.8 ± 5 HV respectively shown in Figure. 4.8. For developed composite coating, the micro-hardness value at 400 °C was higher than 100, 200 and 300 °C due to interfacial strength amongst the micro particles used in coating and due to modification of grain positioning at elevated temperature[163]. The coated micro-carbon particles help as a resistance to plastic deformation and chiefly raise the hardness.

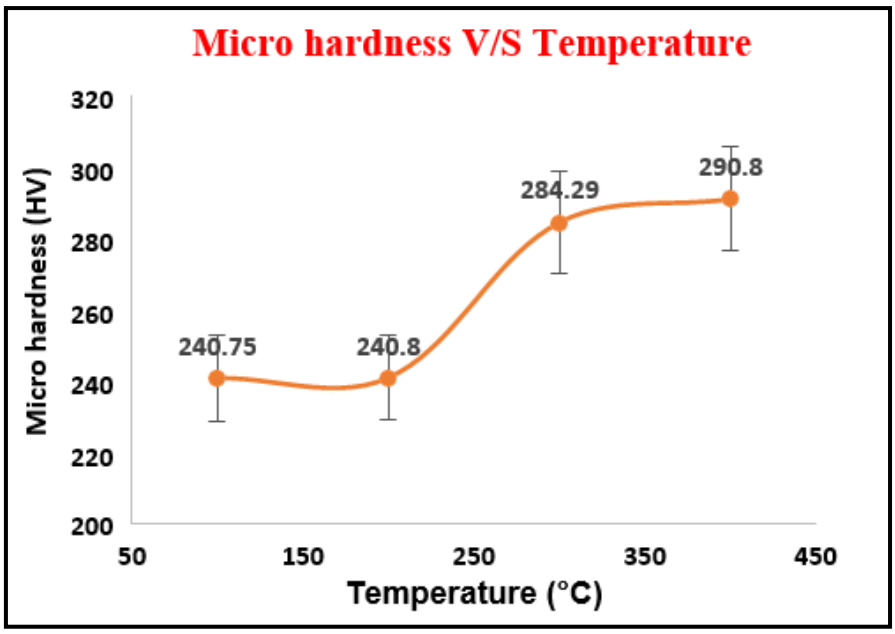

Figure 4.8: Micro hardness value of Mo–NiCr–WC–W HVOF Coating w.r.t temperature.

4.4.2 Effect of Temperature on Residual stress of property of Mo–NiCr–WC–W composite Coating

The residual stress (Fig. 4.9) of the Mo–NiCr–WC–W composite Coating was perceived as 354 ±5, 124 ±5, 114 ±5 and 80 ±5 MPa at an growing temperature from 100 to 400 °C in the break of 100°C, respectively. This decline in residual stress can be attributed to stress relief mechanisms or alterations in the grain direction of the coated material, resulting in reduced residual stress levels[164].

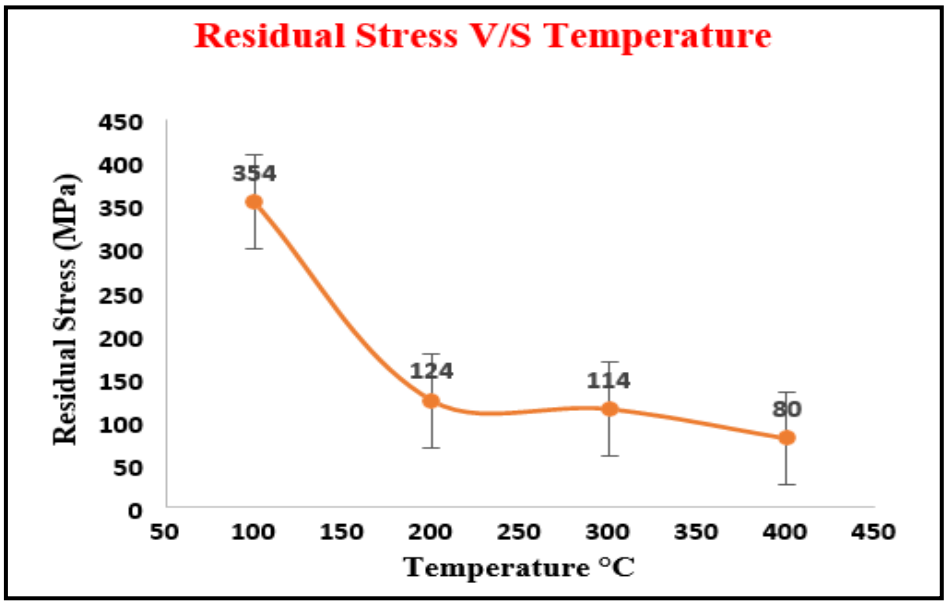

Figure 4.9: Variation in residual stress of Mo–NiCr–WC–W HVOF Coating w.r.t temperature.

Laboratory setups employing X-ray micro diffraction, along with advanced 2D detectors, enable the assessment of materials with exceptional spatial precision. This study introduces an innovative approach for residual stress evaluation, centred around the analysis of a solitary Debye ring with varied temperature range. This technique proves especially adept for stress analysis in coatings and samples featuring intricate geometries. Figure 4.10 depicts the Debye rings 2D, 3D and distortion ring at numerous temperatures from 100 to 400°C in the gap of 100°C. Collectively, Figure 4.10 furnishes valuable insights into the thermal conduct of the material and the integrity of its crystal structure.

At 100°C, the Debye rings present a well-defined pattern, characterized by distinct spacing between them. Upon raising the temperature to 200°C, the clarity of the rings slightly diminishes, revealing some blurring at the edges. Progressing to 300°C, the distortion ring gains prominence, indicating significant structural modifications within the material. Subsequently, at 400°C, the Debye rings undergo substantial distortion, implying a transformative alteration in the crystal lattice.

The 2D and 3D rings are no longer distinguishable at this temperature. The distortion ring exhibits a complex pattern featuring irregular spacing and shapes. These observed shifts in the Debye rings strongly suggest that the material experiences a phase transition as the temperature ascends. These findings carry significant implications for comprehending the material's characteristics and its potential applications.

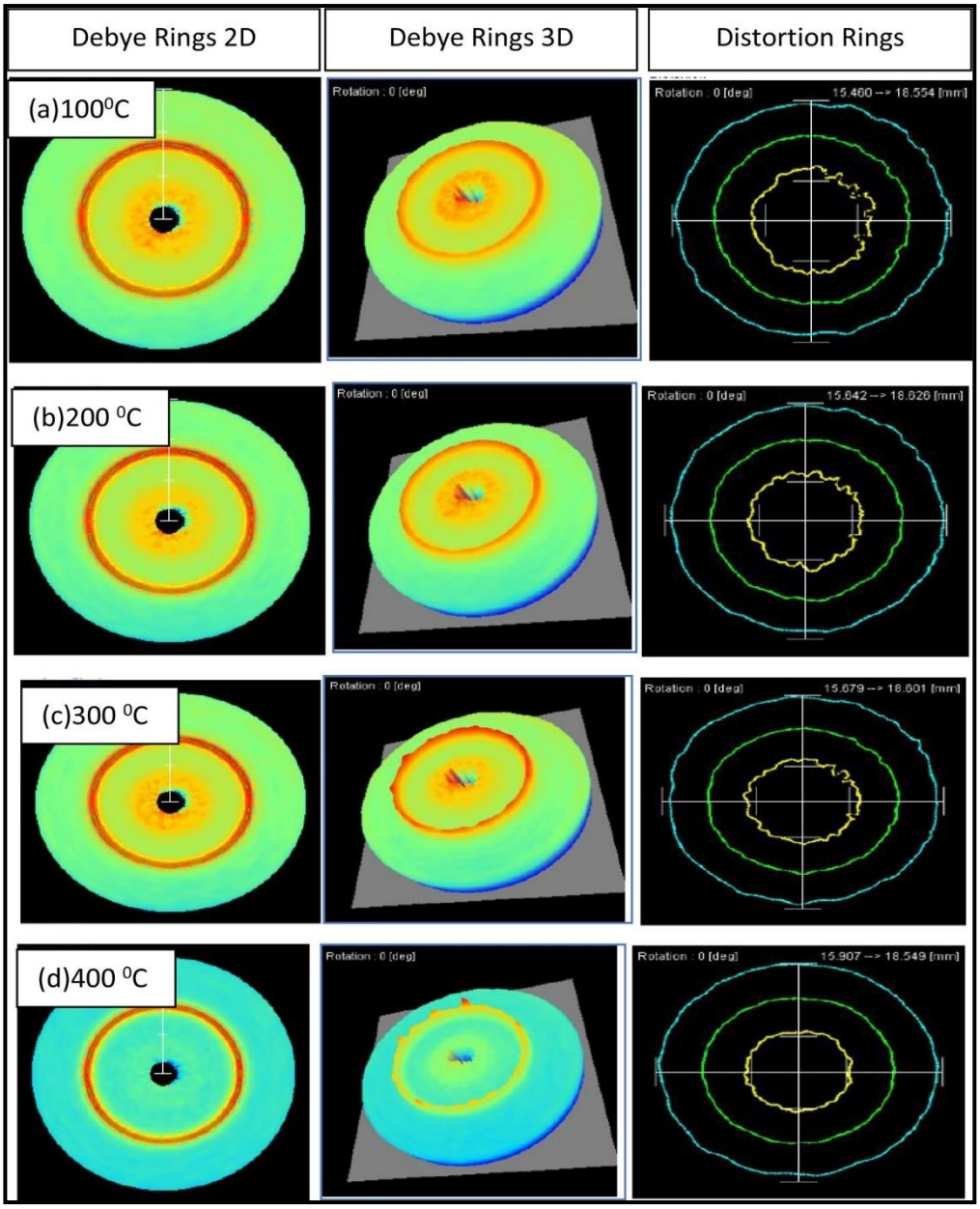

Figure 4.10: Debye rings at different temperatures ranging from 100 to 400°C, with intervals of 100°C, showcasing the 2D, 3D, and distortion rings.

4.5 Microstructural investigation of Worn-out surfaces.

To examine the wear-out nature of the composite coating, the FESEM images worn surfaces of Mo–NiCr–WC–W composite coating are displayed in figure 4.11 (a–d).

The figure declares the actuality of abrasive wear. In abrasive wear, hard particles or surfaces encounter the material's surface, leading to material removal through mechanical forces[165]. The presence of micron-size carbon particles figure 4.11(a, b) on the worn surfaces indicates that abrasion is a significant contributor to the overall developed coating wear behaviour. Furthermore, cracks presence on worn surface, draws attention to a potential mode of wear

propagation. Cracks are generated due to various factors such as stress concentrations induced at the periphery of pits and cavities, thermal cycles due to rapid quenching during operating condition, or material properties. The fact that these cracks are observed on the worn surfaces suggests that they could serve as initiation points for the abrasive wear process. Oxidation is a chemical process that can lead to the degradation of material properties. The development and formation of oxides on the worn surfaces[166]. The presence of oxides could indicate that chemical reactions takes place on the surface due to wear interactions, further contributing to the overall wear process. Another critical aspect of wear failure mechanism observed in the present study is the layer debonding figure 4.11 (d), which refers to the separation of different layers within the coating. Layer debonding might be influenced by factors such as adhesion strength, thermal stresses, or microstructural inconsistencies[167].

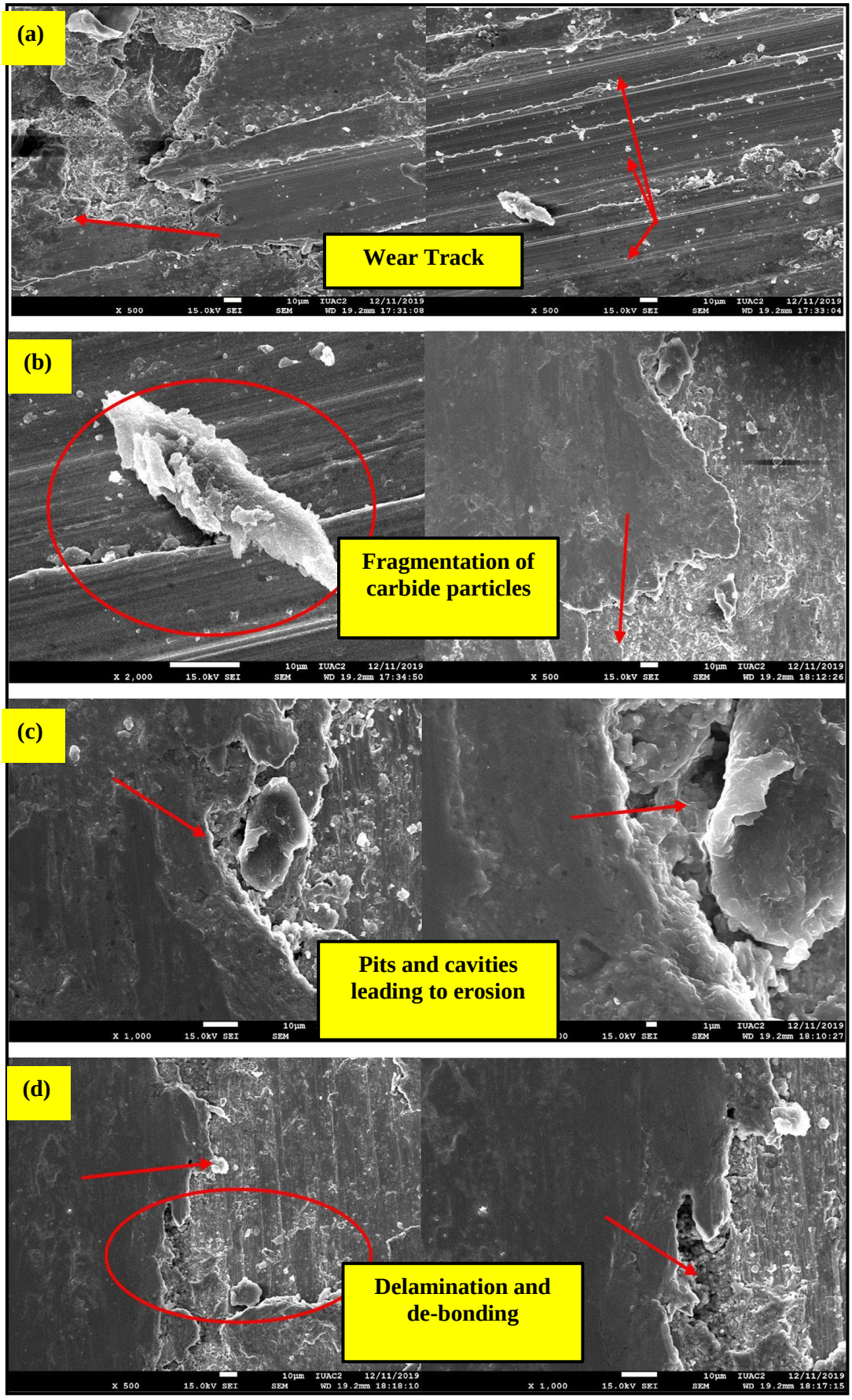

Figure 4.11: Micrographs of wear out surfaces- FESEM.

4.6 Summary

In short, HVOF technique was employed for developing the blend composite coating (Mo–NiCr WC–W) on steel substrate. The tribological properties were studied at increasing temperature by using pin on disk Tribometer. The excellent improvement in micro-hardness with increasing temperature is obtained i.e. at 400 °obtained micro hardness was about 290.8Hv.In residual test, at increasing temperature, value of residual stress tends to seem decreased i.e. at 100 ℃ (354 MPa) and minimum at 400 ℃ (80 MPa).At temperature range from 100 °C to 400 ℃ Debye rings appears. At 100℃ the value of COF is maximum and it minimum at 400 ℃ when considered sliding distance was 1500 meter while at 200℃ and 300℃ were deceits amid above temperature. At 100℃, wear rate of developed coating was observed maximum and minimum at 400℃. FESEM images were taken to analyse the Microstructural of developed coating and it's worn out surface. These worn out surface carried of several oxides films, delamination layers and cracks.

CHAPTER – 5

Development of Composite coating (ZrB_2-SiC) using Plasma Spray and understanding its thermo-chemical behavior

The objective of the present work is to sightsee the potential of ZrB_2-SiC- based ceramic coatings as a shielding layer for Inconel 718 substrates. The work targets on the use of shrouded plasma spraying technology to deposit the coating and investigates the effect of exposure to molten sulfate-vanadate salts (45% Na_2SO_4 and 55% V_2O_5) on its properties. By conducting a comprehensive examination of oxidation and corrosion resistance, tribological behavior, and interactions with molten salts, the study contributes essential insights to the field of advanced ceramic coatings and their performance under demanding conditions.

This chapter contains five major sections. The first and second section examines the Microstructural and XRD analysis of Powder and coatings respectively, while the third section is intended to understand the Tribological wear property of ZrB_2-SiC composite coating. The fourth section inspects the Hot corrosion behavior of composite coating after subjected to corrosive salts. The fifth section contains the XRD analysis of ZrB_2-SiC Composite coating before and after Hot corrosion.

5.1 Microstructural investigation of Powder and Plasma sprayed ZrB_2-SiC Coatings

5.1.1 Powder Characterizations through FESEM study

Figure 5.1 shows the high and low magnification FESEM images of ZrB_2-SiC powders which were used for developing the coating onto the surface of the substrate by using plasma spray technology. Figure (a) and (b) shows the spherical shape powder particles with an average size of 40-70-micron meter. The coarse structure can be seen in the obtained FESEM image due to non-uniformity in morphology and sharp corners of base materials responsible for complete agglomeration.

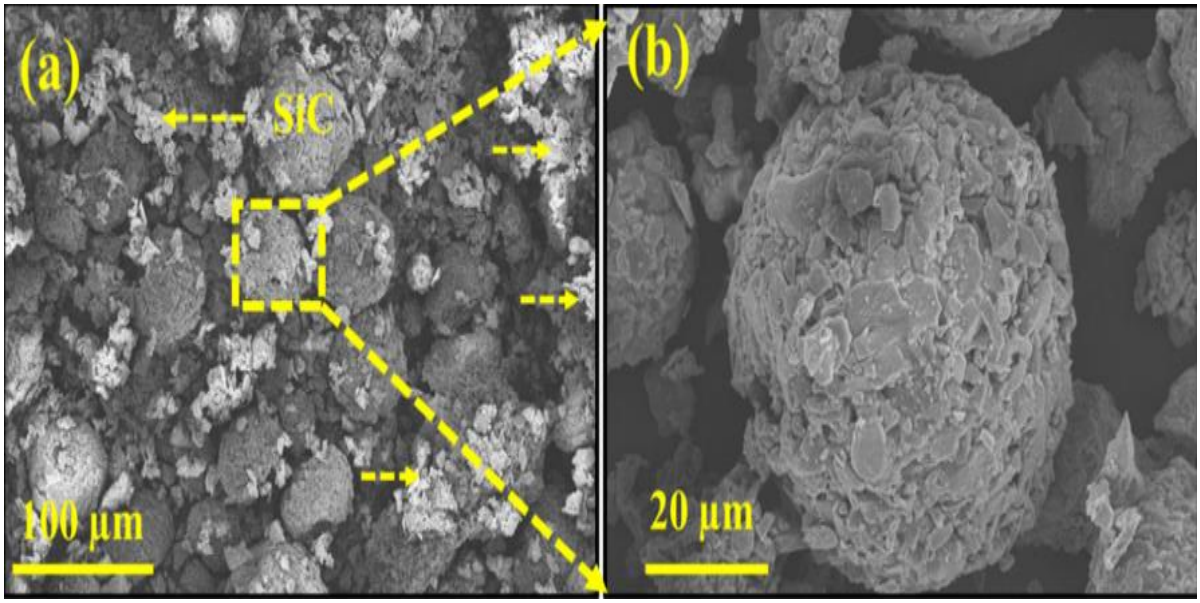

Figure 5.1 :(a-b) FESEM images of the ZrB_2-SiC powder at lower and higher magnification, demonstrating spherical shape.

5.1.2 EDS Analysis of Coating Powder

Figure 5.2 shows the elemental compositions of powders (ZrB_2-SiC) where elemental mapping analysis was performed. This elemental mapping technique was performed to study the distribution of elements present in the sample's powders, such as Zr, B, Si, and C. Figure 5.2 (a) gives the full knowledge of the ZrB_2-SiC powder microstructure. Figure 5.2 (e) shows the elemental mapping techniques that help us investigate the scattering of elements such as Zr, B Si, and Carbon within the sample. This analysis is essential because it proves the presence of the elemental ratio of ZrB_2-SiC with the required composition. Figure 5.2 (f) shows the plot against the elemental ratio versus desired specifications. Through this processing, the properties of materials and processing conditions can be optimized.

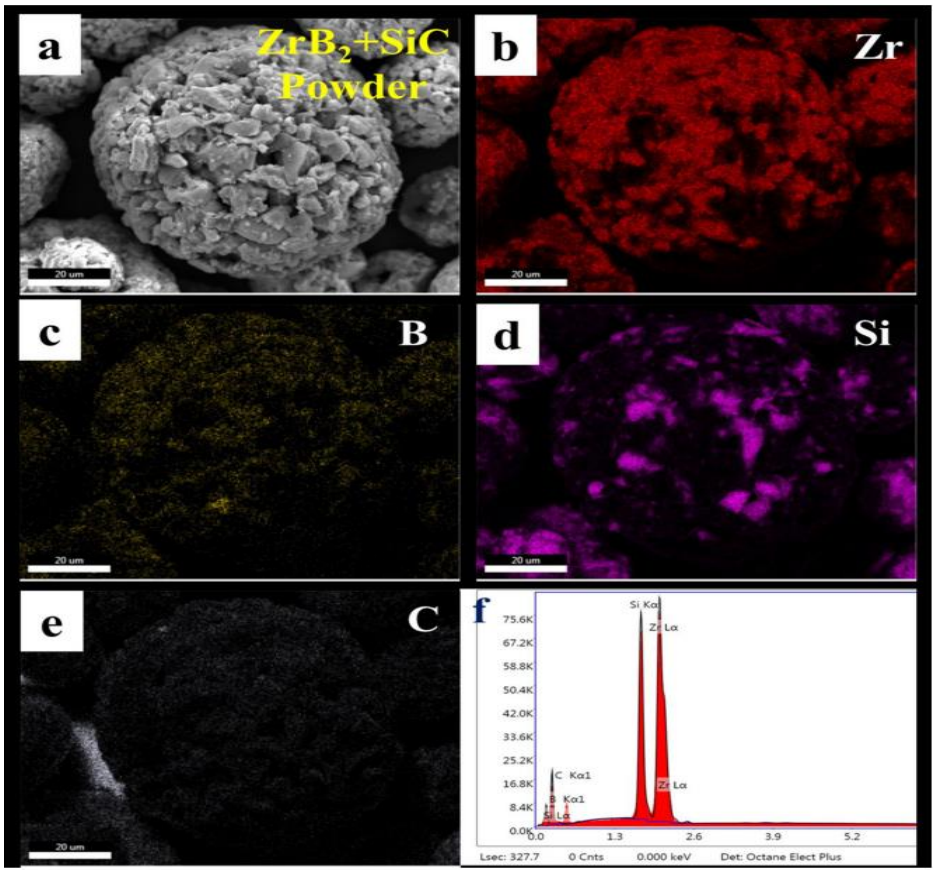

Figure 5.2: (a) FESEM image of ZrB_2-SiC feedstock powder, (b-e) EDS mapping is showing the EDAX spectrum quantifying presence of Zr, B, Si, and C elements.

5.1.3 Coating Thickness and Morphology of ZrB_2-SiC Composite Coating

Figure 5.3 (a) shows the thickness cross-sectional view of the developed coating. The thickness of plasma developed coating was achieved between 300 to 400-micron-m and showed the bereft of defects with greater integrity with the substrate. Figure 5.3 (b) shows the developed coatings' theoretical and measured densities. The density obtained from composite coatings is 86.4 ± 1.3% of the theoretical density. As we know, the indirect relation between porosity and density, that why we calculated the porosity of developed coatings, i.e., approximately 13%. Figure 5.3 (c) shows the image of plasma sprayed ZrB_2-SiC coating in the environment of shroud gasses on the Inconel-718 substrate. Figure 5.3 (d) shows a bimodal-like sponge of ZrB_2-SiC coating with an averagely melted zone. The dense structure seems to be seen due to a completely melted zone in high magnified FESEM image.

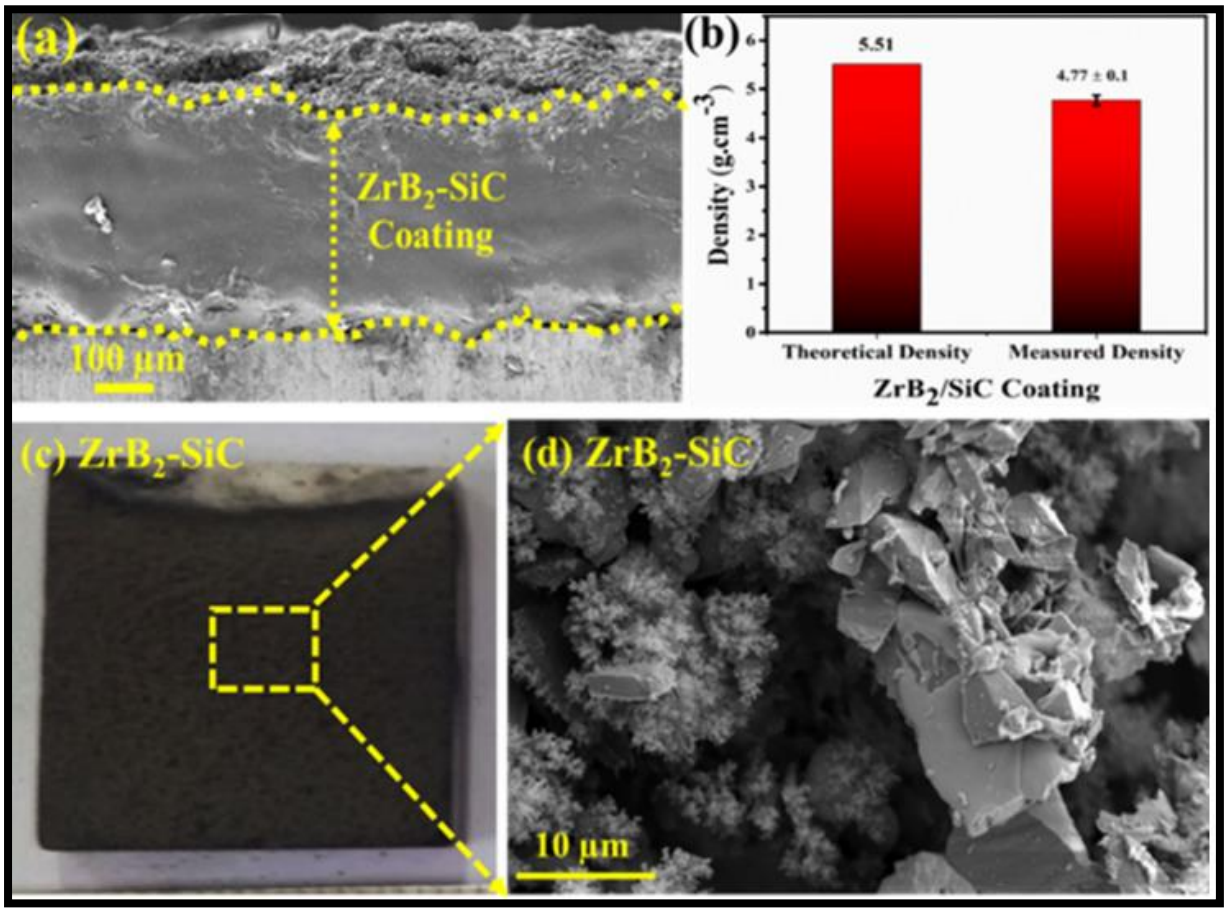

Figure 5.3: (a) FESEM image (Cross-sectional area) of ZrB_2-SiC plasma sprayed coatings and (b) depicts the graph between the theoretical density versus measured density (c) Plasma spray coating on Inconel-718 substrate (d) High magnified image of ZrB_2-SiC plasma sprayed coatings.

Figure 5.4 (a) and (b) shows FESEM images of the fragmented surface of as-sprayed ZrB_2-SiC coating, which showed a specific splat-like microstructure chiefly made up of superimposing lamellae demarcated from splat borders and fenced from a connection of micro cracks. Thermal conductivity and heat transmission are commonly affected by splat boundaries. Tension relaxation during fast cooling causes horizontal micro-cracks to emerge at splat edges. Splat boundaries form due to the weak connection between deposited splats caused by the collision of fast solidification and their molten droplets.

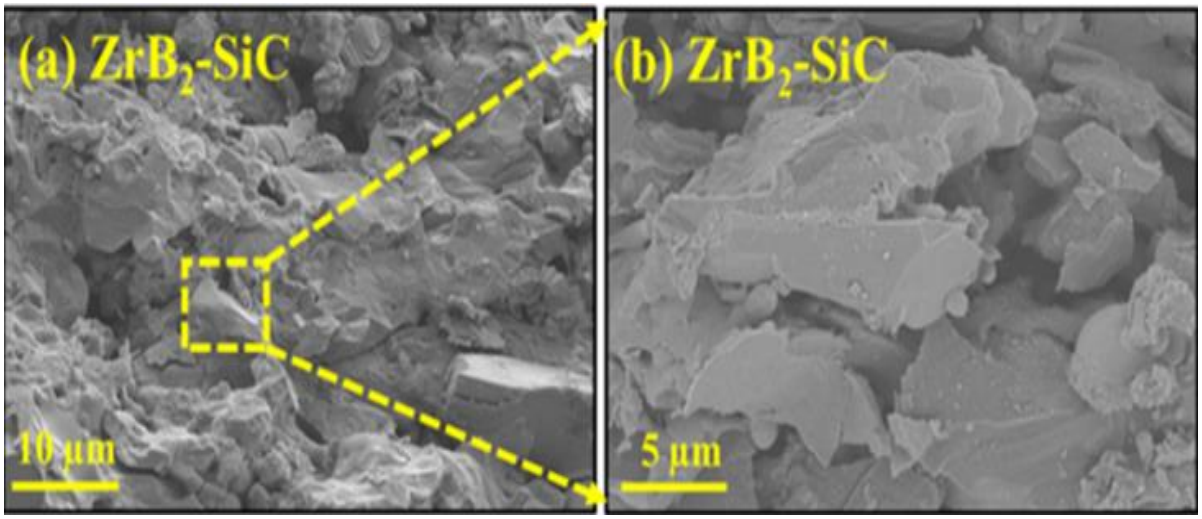

Figure 5.4: (a-b) Ahigh magnification image (FESEM) of a fragmented cross-section of plasma sprayed ZrB_2-SiC coating in an atmosphere of shroud gases.

5.2 XRD Analysis of ZrB_2-SiC Composite Coating and Powders

Figure 5.5 shows the X-ray diffraction pattern of sprayed dried ZrB_2-SiC powder and developed coatings. In the XRD graph, the right shifting of peaks can be seen in the case of developed coating because of the contraction of the lattice inside the crystal at the time of solidification of melted particles on the substrate surface. As per the JCPDS data, the highest peak in the ZrB_2-SiC coatings obtained is Alpha in ZrB_2 and gamma in SiC with Beta in ZrO_2. For ZrB_2, which is hexagonal in nature. For hexagonal SiC, (00-036-0420) for monoclinic ZrO_2 (m-ZrO_2), and (00-024-1164) for tetragonal ZrO_2 (t-ZrO_2). t-ZrO2 was recognized in the sprayed coating since some of the t-ZrO_2 may not be changed to m-ZrO_2 during the quick cooling from high to ambient temperature. The XRD test could not recognize the SiO_2 because of its slow concentration and amorphous nature. Apart from this, the low intensity of silicon carbide might be the reason for the breakdown of silicon carbide with oxidation at high temperatures That's why according to this, the biggest phase of developed coating is ZrB_2 (Reference code: 01-089-3930). Though, silicon carbide peaks, as per the reference code 00-022-1317, can be seen in the XRD pattern. In difference, (00-036- 0420) for monoclinic ZrO_2 (m-ZrO_2) and (00-024-1164) for tetragonal ZrO_2 (t-ZrO_2). However, XRD patterns indicate that the coatings retained ZrB_2 and SiC phases.

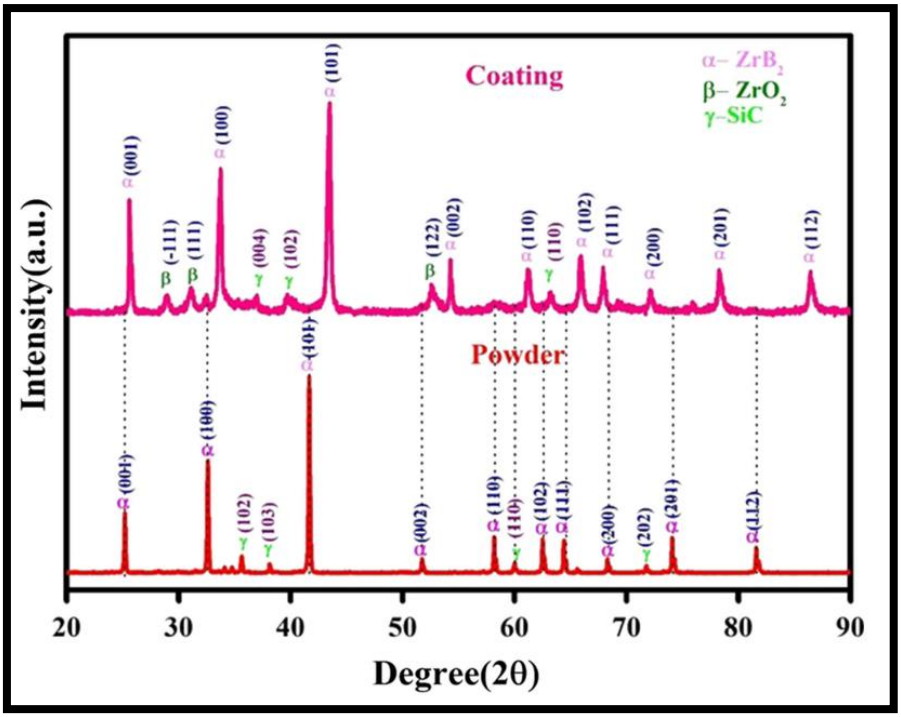

Figure 5.5: X-ray diffraction (XRD) spectra of the ZrB_2-SiC powder and Composite coating

5.3 Tribological investigation of Plasma Sprayed ZrB_2-SiC Coatings

Figure 5.6 (a) shows the value of COF, wear rate, and wear volume loss data of uncoated and coated substrates. It has been observed from obtained results that the value of COF and wear volume loss has reduced significantly. The decrement in the average value of COF has been observed, i.e., 0.57 for the uncoated substrate and 0.3 for the ZrB_2-SiC substrate. The wear volume loss of bare Inconel-718 and ZrB_2-SiC was calculated to correspondingly 2.63 ± 0.5 and 1.90 ± 0.8 mm^3. Figure 5.6 (b) shows the graph of decreasing wear rate values for the coating substrate to the uncoated substrate. The wear rate for ZrB_2-SiC coated samples was noted ($2.02 \pm 0.03\ 10^{-3}$ /N-m), and for uncoated samples, is ($2.8 \pm 0.04\ 10^{-3}$ /N-m). The tribological properties influenced the hardness and toughness of materials. These findings of results are dependable on the Archard equation for abrasive wear. This equation helps assume that the harder materials will be lower for abrasive wear and wear rate. Therefore, the wear debris will be less formed in harder materials (ZrB_2-SiC) whose hardness is which leads to good wear resistance and low value of COF as compared to bare (Uncoated) substrate. The tribological properties of ZrB_2 have also improved by adding SiC to the composite powder. In the current study, the hydrated silica layers are formed after reacting with moisture present in the air. The half-wear track was covered by this produced lubricate film, which saved the surface of the substrate through wear.

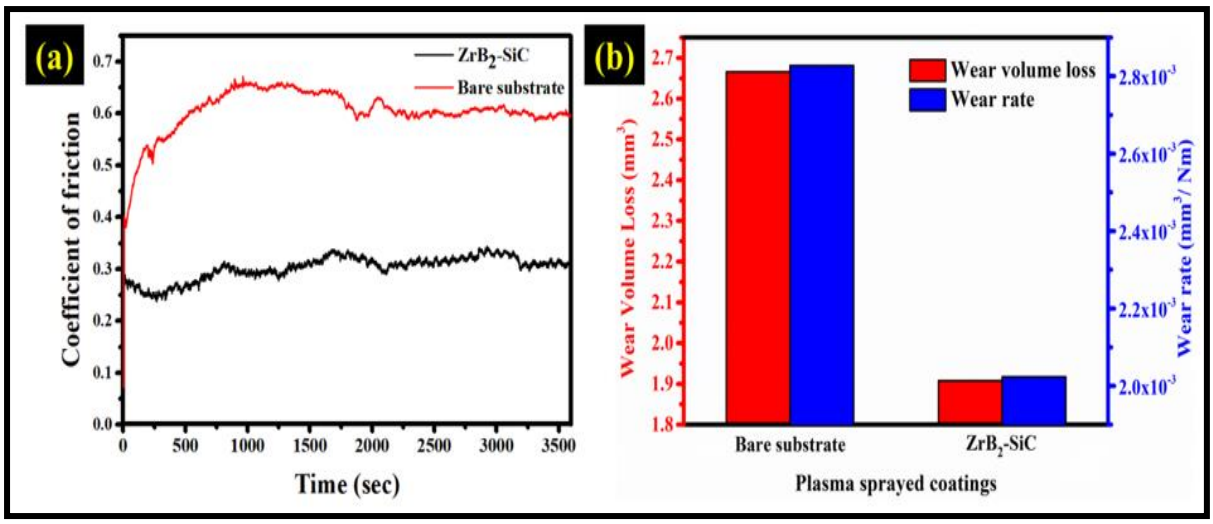

Figure 5.6: (a) COF of bare substrate and ZrB_2-SiC coating (b) Graph depicting wear volume loss along with wear rate.

5.4 Hot Corrosion behaviour of Plasma sprayed ZrB_2-SiC Composite coating

Hot corrosion behaviour of Plasma sprayed ZrB_2-SiC Composite coating under vanadate and sulphate salts with different compositions has been presented in this section. Before the introduction of corrosive salts, the composite coating was preheated at 250^0C using high temperature chamber furnace for 1 h to achieve better adhesion on the coating surface. A quantity of 5 gm/cm^2 Na_2SO_4-V_2O5 salt was evenly distributed on the coatings surface using a glass fibre brush and then placed inside a furnace set to 1600^0C.

The digital picture of ZrB_2-SiC has been seen in Figure 5.7 (a) before conducting the hot corrosion testing. Whereas figures 5.7 (a) and 5.7 (c) show the plasma sprayed ZrB_2-SiC coating morphology after thirty hours of exposure to corrosive salts (V_2O_5 + Na_2SO_4) at 1600^0C. It has been seen in the present study after conducting the hot corrosion at 1600^0C with V_2O_5 + Na_2SO_4, ZrB_2-SiC is turned into monoclinic ZrO_2, and Sio_2 is produced from silicon carbide, and little amount of silicon replication is noted. Figure 5.7 (c) shows the coated surface covered by corrosion products. The clear topography of the ZrB_2-SiC coating (Plasma Sprayed) surface can be seen in Figure 5.7 (d-e) on the surface of the substrate after exposure of 30 hours in the pool of corrosive salts V_2O_5 + Na_2SO_4 at a temperature of 1600^0C. It was observed that several cylindrical-shaped and crystal dendritic was formed over the surface of the ZrB_2-SiC coating. The porous surface with fewer cracks (cylindrical and dendritic shape) has been shown in ZrB_2-SiC surface morphology.

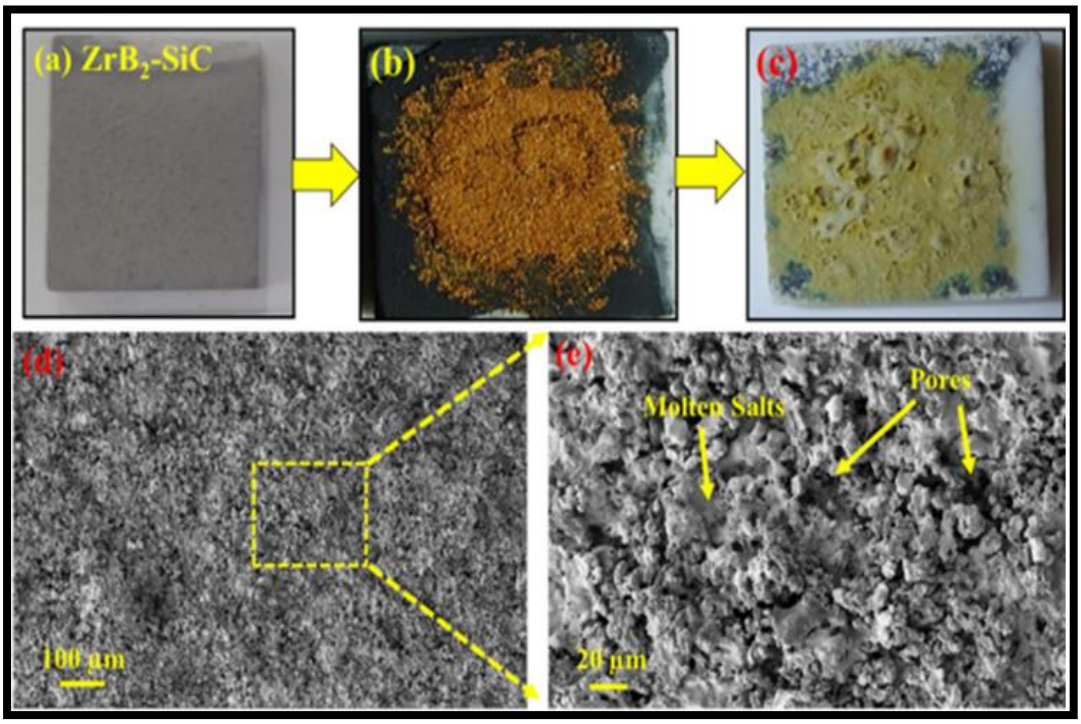

Figure 5.7: (a) ZrB_2-SiC coating before the hot corrosion test. (b) V_2O_5 +Na_2SO_4 salt onto the ZrB_2-SiC coating and (c) Post-hot corrosion on coatings (d) FESEM picture shows the surface of ZrB_2-SiC coating after the hot corrosion test, and (e) high magnification picture of marked area (Fig 5.7 d), arrow shows pores and molten salts of $NaSO_4$ and V_2O_5 deposited and corroded over the surface.

The topmost surface of the developed coating before the hot corrosion can be seen in Figure 5.7 (a). Here 3 different regions are found. The EDAX spectrum was employed to verify elements such as Zr, B, Carbon, and Si. The top surface of the developed coating after hot corrosion has been seen in Figure 5.7 (c). In the present case, the three different areas were considered to authenticate that how much area has suffered from corrosion with the corrosive materials. Figure 5.8: (a, c) shows the FESEM images of ZrB_2–SiC composite coating before and after hot corrosion. Figure 5.8: (b, d) shows the EDAX spectrum of ZrB_2–SiC composite coating before and after corrosion.

The EDAX scanning image of the developed coating surface can be seen in Figure 5.8 (d) after performing the hot corrosion test at three different stages. These experiments confirmed the presence of Zr, O, B, Si, Na, C, V and S after reacting with dissolved corrosive salts. In this experiment, it has been observed that these corrosive salts (Na_2SO_4-V_2O_5) melts at high temperature and start reacting with ZrB_2/SiC, forming oxides, i.e., ZrO_2 and SiO_2. The results of

oxides formations help to protect the coating layer and stop the auxiliary reactions of salts with the developed coatings.

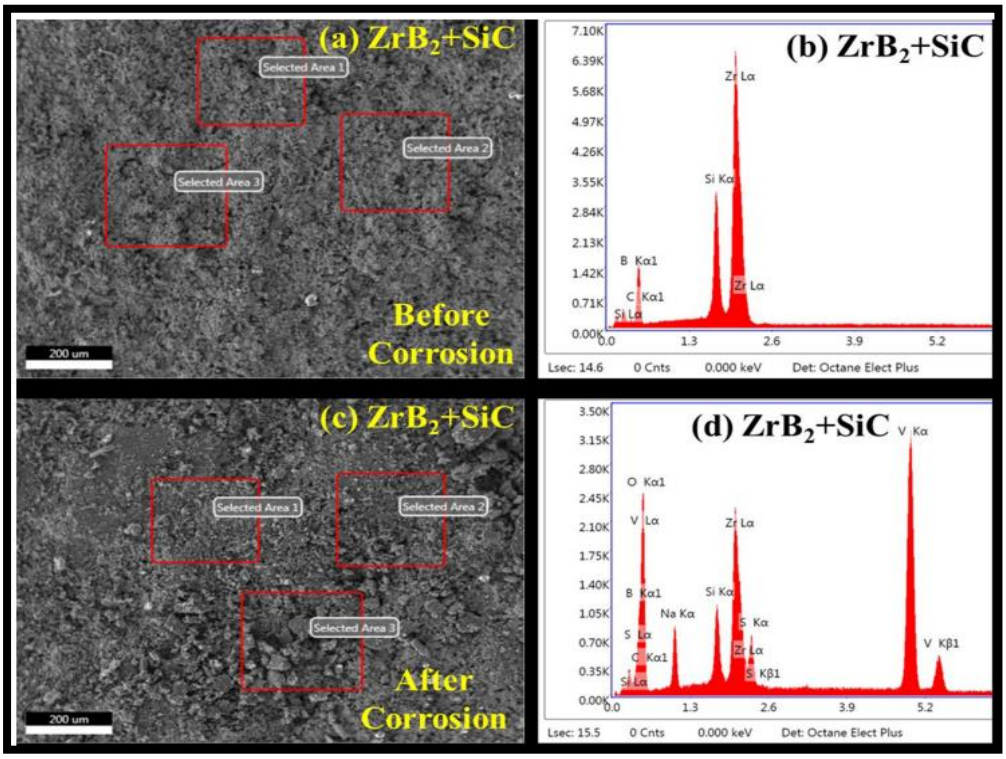

Figure 5.8: (a, c) FESEM images of ZrB_2 – SiC composite coating before and after hot corrosion. (b, d) EDAX spectrum of ZrB_2 – SiC composite coating before and after corrosion

For a better understanding, due to the comparatively low melting point, i.e., 690^o C, the chances of melting V_2O_5 first in the mixed sulphate-vanadate salt. The reactions are summarised in equation (3).

$V_2O_5 + Na_2SO_4 = SO_3 + NaVO_3$ ……. Equation -1

$V_2O_5 + Na_2O = 2NaVO_3$…… Equation -2

$V_2O_5 + 3Na_2O = 2Na_3VO_4$…… Equation -3

When the ZrB_2-SiC coating was in direct contact to V_2O_5- Na_2SO_4 molten corrosive salts, a molten mixture of Na_2O-$NaVO_3$-Na_2SO_4-V_2O_5 -Na_3VO_4 likely to cover the coating's surface because these reactions might not be completed entirely and their reversibility should be addressed. This combination might have entered the coating through the built-up pores, resulting in micro-cracks over the coated surface from the plasma spraying process. According to a study

conducted by Hakon Flood and Hermann Lux, when acid and base start to react with inorganic salts, it is showcased as acidic through the acceptor of oxide ion (O^{-2}) and behaves as basic after donating the oxide ion. This acid and basic concept can be taken as a kinetic revival of the oxygen theory for both acid and base shown in the equation below:[168].

O^{-2} +Acid =Base…… Equation -4

Or

SO_3 (acid) + Na_2O (Base) = Na_3SO_4(Salt)…… Equation-5

In the present work, Meta vanadate and sodium ortho are the majorly salt used. The sodium vanadate. The sodium vanadate is shown below equation [7-8]:

Na_2O (Base) + V_2O_5(acid)= $2NaVO_3$(Salt)…… Equation -6

Result of this, the thermodynamic reactions that occur due to plasma spraying are given as follows:

$ZrB_2 + SiC + NaVO_3 \rightarrow ZrO_2 + Na2CO_3 + SiO_2 + V_2O_5 + B_2O_3$ Equation -7

$4B_2O_3 + 4ZrO_2 + 5SiC + 10NaVO_3 = 4ZrB_2 + 2NaO + 5SiO_2 + V_2O_5 + 5V_2O_5 + 3CO_2$

Equation -8

As discussed earlier, the loss of ZrO_2 and SiO_2 took place when the interaction of melted corrosive salts which leads to the production of a ZrO_2 crystalline phase which caused the formation of ZrO_2 to become unstable and change for the aforementioned stable monoclinic (m) crystalline stricture of ZrO_2. The volume expansion of approximately 2-6% occurs due to the transition of tetragonal t' to monoclinic m ZrO_2 which results in cracking and spallation of ZrO_2- SiC-based plasma sprayed coating. It has been seen that as the volumetric pressure releases, it may cause fractures in the coatings, which fail coatings.

$(ZrO_2)_{tetragonal} = (ZrO_2)_{monoclinic}$ …… Equation -9

Therefore, the Lux flood-based reactions are used to evaluate the interactions among the ceramics with vanadium salts as the primary test, which is explainable for oxides if compared with acid and basic nature. The low-affected stabilizer oxides must be acidic to interact with V_2O_5 and $NaVO_3$.

5.5 XRD analysis of ZrB_2-SiC Composite coating before and after Hot corrosion

Figure 5.9 shows the XRD pattern of the plasma sprayed SiC-ZrB_2 coating before and after the hot corrosion test. After the hot corrosion experiment was completed, zirconia was found in the monoclinic and tetragonal phases, even though plasma sprayed coating merely possessed the tetragonal phase. Apart from this, some SiO_2 and V_2O_5 peaks were also visible in corroded ZrB_2-SiC coating. Through XRD, it has validated the presence of SiO_2 on the top surface of corroded ZrB_2-SiC substrate coating. Though, the corroded ZrB2-SiC coating's XRD spectra exposed sizable ZrB_2 peaking. Furthermore, the binary phases, such as SiO_2, SiC, and ZrO_2 products after the reaction, can be found in the ZrB2-SiC plasma sprayed coating. The developed B_2O_3 has expected to evaporate at 1400 ^{0}C. The ZrB_2Si bonds weaken and produce a disilicide phase, generating a less thermodynamically stable Zr_2BSi phase. According to a study conducted by Kumar et al.at 1400 ^{0}C or above, the SiO_2 reacts with ZrO_2 to produce $ZrSiO_4$ and ZrO_2, which also reacts to TiO_2 and forms titanium full zirconium titanate phase, i.e., $Zr_5Ti_7O_2$[169]. But in the present study, ZrO_2 and SiO_2 do not react with other oxides elements, which results in oxygen ions starting to react with ZrB_2-SiC on the exposure of components to produce their respective oxides. V_2O_5 and Na_2SO_5 diffraction patterns can be seen in the ceramic exposed salted surface because of the remaining salts on the coating surface.

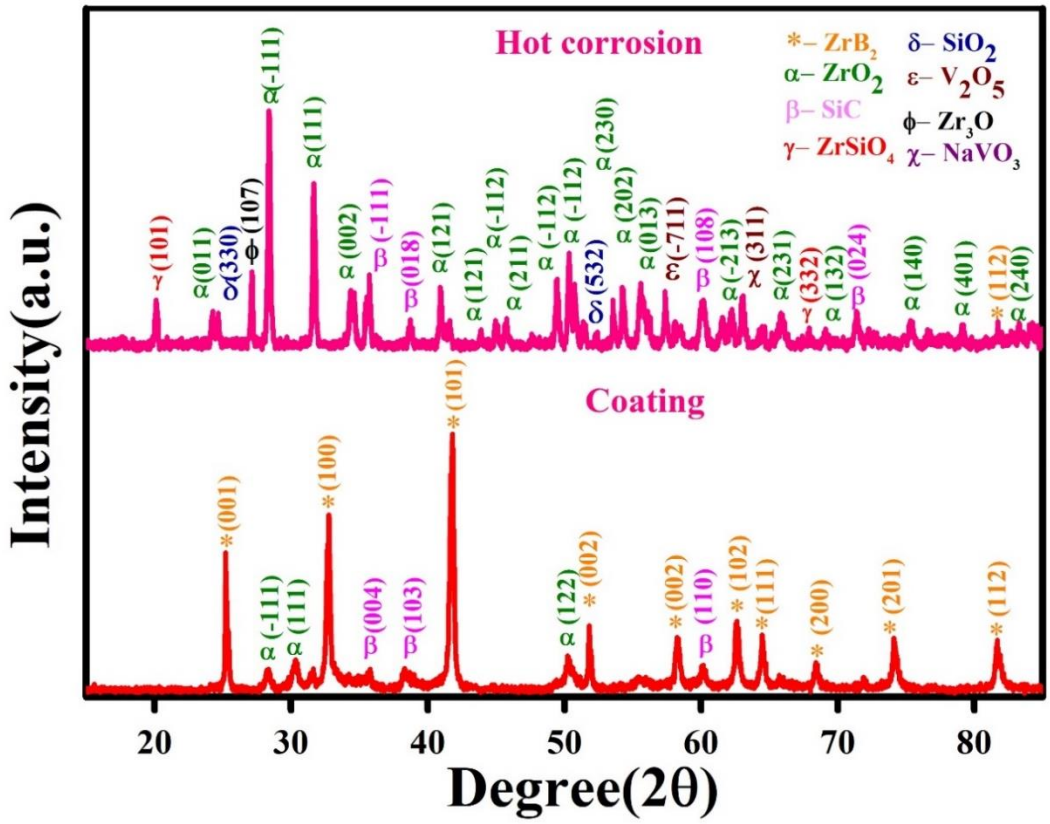

Figure 5.9: XRD spectra of the ZrB_2 – SiC plasma sprayed coating before and after hot corrosion test.

The XRD pattern shows that when the ceramic is exposed to molten salt, the diffracted peaks related to $ZrSiO_4$ binary compounds become more evident; this might be because the molten salt creates an oxidizing atmosphere. Previous research on the electrochemical behaviour of ZrB_2 has revealed that metal behaves passively in acidic chloride or neutral solutions. During chemical deterioration, the presence of the SiC phase generates a thin protective layer of Si-O, demonstrating passive metal behaviour[170], [171].

5.6 Summary

In this study, a coating was produced with the aim of providing resistance against corrosive environments at 1600°C for 30 h and having a relatively low coefficient of friction (COF) on its surface. The coating was made using plasma spray technology and consisted of a mixture of ZrB_2 and SiC with a thickness of 300-400µm, on Inconel-718 substrate. The COF values for the coated substrates ranged from 0.57 to 0.3. The wear rate of the ZrB_2-SiC coating was found to be $2.02 \pm 0.03 \times 10^{-3}$ (mm^3/Nm), which was lower than that of the bare Inconel-718 substrate ($2.8 \pm 0.04 \times 10^{-3}$ (mm^3/Nm)). The coated surfaces were then subjected to hot corrosion tests using molten sulphate/vanadate salt mixtures, and it was found that the ZrO_2 component of the coating formed a protective layer that prevented further penetration of the salts. The study suggests that nanostructured ZrB_2-SiC coatings can be a potential candidate for further development as hypersonic features with improved resistance to hot corrosion via sulphate/vanadate melts.

CHAPTER – 6

Conclusions

The end note of the present research work is discussed in this section. Climaxes important conclusions are given here as follows.

- A composite coating (ZrB_2 and SiC) was developed using the thermal spray plasma spraying technique with a 300-400µm coating thickness on Inconel-718 substrate to provide resistance beside corrosive surroundings at 1600 ^{0}C for 30 h with low COF on its surface.
- The COF values for the coated substrates ranged from 0.57 to 0.7. The wear rate of the ZrB_2-SiC coating was found to be 2.02 ± 0.03 X10^{-3} (mm^3 /Nm), which was lower than that of the bare Inconel-718 substrate (2.8 ± 0.04 X10^{-3}) (mm^3 / Nm)). The coefficient of friction were almost constant with the variation of loads because of this peculiar properties this can also be used in the disk break of automobile.
- The hot corrosion tests were performed on coated samples employing molten sulphate/vanadate salt mixtures and observed that ZrO_2 component of the coating formed a protective layer that prevented further penetration of the salts.
- The study shows that nanostructured ZrB_2-SiC coatings can be a potential candidate for further development as hypersonic features with improved resistance to hot corrosion via sulphate/vanadate melt.
- Developed Mo-NiCr-WC-W blend composite coating on the mild steel substrate by taking constant HVOF process parameters such as carrier gas flow used, air pressure, etc. We used a simple, scalable, single-step HVOF spray technique to prepare these surfaces.
- The wear and friction behaviour of developed coating were investigated at increasing temperatures using a pin-on-disc tribometer.
- The remarkable improvement in hardness has been obtained in temperature increasing trend. The highest hardness was obtained at 400˚C, which is about 290.8V.
- The decreasing behaviour of residual stress has been obtained with increasing temperature. The maximum value of residual stress was obtained at 100 ˚C, i.e., 354 MPa, and the minimum value at 400^{0}C, i.e., 80MPa. Debye's rings also show the same results.

- The maximum value of COF has been obtained at 100˚C and the minimum at 400˚C at a sliding distance of 1500m, whereas at 200˚C and 300˚C the values were come between above the temperature, and the wear rate was obtained at a maximum on 100˚C and lowest on 400˚C.
- The cracks, oxide layers, abrasion, erosion, worn surface, and delamination of layers are obtained through FESEM.

Scope for future work

Drawing from the findings of this thesis, several suggestions for forthcoming research can be put forward. Subsequent investigations will enable:

- To understand the Wear and Hot Corrosion behaviour of different. Further investigating how different materials perform under various conditions can provide insights into their durability, performance, and potential failure mechanisms. The findings from such studies could lead to the identification of novel materials and coatings that exhibit improved resistance to wear and corrosion, with applications across industries ranging from aerospace to manufacturing.
- To conduct tribological studies at different testing parameters like load, temperature, and sliding speed, one can gain a deeper understanding of how these factors affect the performance of materials and coatings.
- To understand the cost-effectiveness analyses for the developed coatings, one can provide valuable insights to industries regarding the economic viability of adopting these coatings. This analysis considers factors such as manufacturing costs, application methods, maintenance requirements, and potential savings due to improved durability.
- Mathematical modelling and analysis have not been addressed in the present thesis. Therefore, it is essential to examine the wear characteristics and coefficient of friction performance of these compositions.

References

[1] K. Holmberg and A. Erdemir, “Influence of tribology on global energy consumption, costs and emissions,” Friction, vol. 5, no. 3. Tsinghua University Press, pp. 263–284, Sep. 01, 2017. doi: 10.1007/s40544-017-0183-5.

[2] C. Vergne, C. Boher, C. Levaillant, and R. Gras, “Analysis of the friction and wear behavior of hot work tool scale: application to the hot rolling process,” Wear, Vol.250 no.1-12, pp322-333, 2001. doi.org/10.1016/S0043-1648(01)00598-1

[3] J. Hardell and B. Prakash, “Tribological performance of surface engineered tool steel at elevated temperatures,” Int. J. Refract. Met. Hard Mater., vol. 28, no. 1, pp. 106–114, Jan. 2010, doi: 10.1016/j.ijrmhm.2009.07.009.

[4] A. K. Noor, S. L. Venneri, D. B. Paul, and M. A. Hopkins, “Structures technology for future aerospace systems,” Comput. Struct., vol. 74, no. 5, pp. 507–519, 2000, doi: 10.1016/S0045-7949(99)00067-X.

[5] M. M. Opeka, I. G. Talmy, and J. A. Zaykoski, “Oxidation-based materials selection for 2000°C+ hypersonic aerosurfaces: Theoretical considerations and historical experience,” in Journal of Materials Science, Oct. 2004, vol. 39, no. 19, pp. 5887–5904. doi: 10.1023/B:JMSC.0000041686.21788.77.

[6] S. D. Kasen, “Thermal Management at Hypersonic Leading Edges,” University of Virginia 2013. doi.org/10.18130/V3DF75.

[7] S. D. Kasen and H. N. G. Wadley, “Heat Pipe Thermal Management at Hypersonic Vehicle Leading Edges: A Low-Temperature Model Study,” J. Therm. Sci. Eng. Appl., vol. 11, no. 6, 2019, doi: 10.1115/1.4042988.

[8] G. Bolelli et al., “Tribology of HVOF- and HVAF-sprayed WC-10Co4Cr hardmetal coatings: A comparative assessment,” Surf. Coatings Technol., vol. 265, pp. 125–144, Mar. 2015, doi: 10.1016/j.surfcoat.2015.01.048.

[9] C. W. Lee, J. H. Han, J. Yoon, M. C. Shin, and S. I. Kwun, “A study on powder mixing for high fracture toughness and wear resistance of WC-Co-Cr coatings sprayed by HVOF,” Surf. Coatings Technol., vol. 204, no. 14, pp. 2223–2229, Apr. 2010, doi: 10.1016/j.surfcoat.2009.12.014.

[10] R. Keshavamurthy, M. Sudhan, A. Kumar, V. Ranjan, P. Singh, and A. Singh, “Wear Behaviour of Hard Chrome and Tungsten Carbide-HVOF Coatings,” Materials Today:

Proceedings,Volume 5, Issue 11, Part 3,2018, doi.org/10.1016/j.matpr.2018.10.256.

[11] P. Drobný, D. Mercier, V. Koula, S. I. Škrobáková, L. Čaplovič, and M. Sahul, "Evaluation of adhesion properties of hard coatings by means of indentation and acoustic emission," Coatings, vol. 11, no. 8, Aug. 2021, doi: 10.3390/coatings11080919.

[12] I. Vance F. Dippold and N. G. R. Center, "Design and Analyses of High Aspect Ratio Nozzles for Distributed Propulsion Acoustic Measurements," In 34th AIAA Applied Aerodynamics Conference, pp.3876, 2016. doi.org/10.2514/6.2016-3876.

[13] L. H. Townend, "Some design aspects of space shuttle orbiters," Prog. Aerosp. Sci., vol. 13, no. C, pp. 81–135, 1972, doi: 10.1016/0376-0421(72)90015-2.

[14] E. Wuchina, E. Opila, M. Opeka, W. Fahrenholtz, and I. Talmy, "UHTCs: Ultra-High Temperature Ceramic materials for extreme environment applications," Electrochem. Soc. Interface, vol. 16, no. 4, pp. 30–36, 2007, doi: 10.1149/2.f04074if.

[15] T. A. Parthasarathy, M. D. Petry, G. Jefferson, M. K. Cinibulk, T. Mathur, and M. R. Gruber, "Development of a test to evaluate aerothermal response of materials to hypersonic flow using a scramjet wind tunnel," Int. J. Appl. Ceram. Technol., vol. 8, no. 4, pp. 832–847, Jul. 2011, doi: 10.1111/j.1744-7402.2010.02515.x.

[16] Gasch, Matthew J., Donald T. Ellerby, and Sylvia M. Johnson. "Ultra high temperature ceramic composites." Handbook of ceramic composites. Boston, vol.165, MA: Springer Us, 2005. 197-224.

[17] J. D. Anderson, Hypersonic and High Temperature Gas Dynamics. 2006.

[18] J. F. Justin and A. Jankowiak, "Ultra High Temperature Ceramics: Densification, Properties and Thermal Stability," AerospaceLab J., vol. 3, no. October, pp. AL3-08, 2011.

[19] M. M. Opeka, I. G. Talmy, E. J. Wuchina, J. A. Zaykoski, and S. J. Causey, "Mechanical, Thermal, and Oxidation Properties of Refractory Hafnium and zirconium Compounds," J. Eur. Ceram. Soc., vol. 19, no. 13–14, pp. 2405–2414, 1999, doi: 10.1016/s0955-2219(99)00129-6.

[20] W. G. Fahrenholtz, G. E. Hilmas, I. G. Talmy, and J. A. Zaykoski, "Refractory diborides of zirconium and hafnium," J. Am. Ceram. Soc., vol. 90, no. 5, pp. 1347–1364, May 2007, doi: 10.1111/j.1551-2916.2007.01583.x.

[21] R. J. R. W. J. Clougherty E.V. Hill and E. T. Peters, "Research and development of refractory oxidation-resistant diborides, Part II, Volume II: processing and characterization," Tech. Rep. AFML-TR-68-190, vol. II, pp. 1–2, 1970.

[22] S. Chakraborty et al., "Microscopic, mechanical and thermal properties of spark plasma

sintered ZrB2 based composite containing polycarbosilane derived SiC," Int. J. Refract. Met. Hard Mater., vol. 52, pp. 176–182, Jun. 2015, doi: 10.1016/j.ijrmhm.2015.06.010.

[23] T. Kowalski, "A Thermostructural Analysis of a Diboride Composite Leading Edge," Nasa Tech. Memo., no. July, 1996.

[24] T. H. Squire and J. Marschall, "Material property requirements for analysis and design of UHTC components in hypersonic applications," J. Eur. Ceram. Soc., vol. 30, no. 11, pp. 2239–2251, Aug. 2010, doi: 10.1016/j.jeurceramsoc.2010.01.026.

[25] Z. Wu, Y. Xu, W. Wang, and R. Hu, "Review of shock wave detection method in CFD post-processing," Chinese J. Aeronaut., vol. 26, no. 3, pp. 501–513, 2013, doi: 10.1016/j.cja.2013.05.001.

[26] S. C. Tung and H. Gao, "Tribological characteristics and surface interaction between piston ring coatings and a blend of energy-conserving oils and ethanol fuels," Wear, vol. 255, no. 7–12, pp. 1276–1285, 2003, doi: 10.1016/S0043-1648(03)00240-0.

[27] J. Ilavsky et al., "Microstructure-Wear and Corrosion Relationships for Thermally Sprayed Metallic Deposits," in Proceedings of the International Thermal Spray Conference, 2000, pp. 449–454. doi: 10.31399/asm.cp.itsc2000p0449.

[28] H. Kashani, A. Amadeh, and H. M. Ghasemi, "Room and high temperature wear behaviors of nickel and cobalt base weld overlay coatings on hot forging dies," Wear, vol. 262, no. 7–8, pp. 800–806, Mar. 2007, doi: 10.1016/j.wear.2006.08.028.

[29] T. Altan, G. Ngaile, and G. Shen, "Cold and Hot Forging: Fundamentals and Applications,"AMSInt.,p.341,2005,doi:https://doi.org/10.31399/asm.tb.chffa.9781627083003.

[30] P. Dabreo, S. Pashte, L. Dmonte, and L. Dabre, "Estimation of Tool Life by Industrial Method and Taylors Method Using Coated Carbide Insert in Turning of Work-Material Ss316l," IOP Conf. Ser. Mater. Sci. Eng., vol. 1070, no. 1, p. 012101, Feb. 2021, doi: 10.1088/1757-899x/1070/1/012101.

[31] Metalworking: Bulk Forming. ASM International, 2005. doi: 10.31399/asm.hb.vol.14a.9781627081856.

[32] M. Salmanzade, M. J. Azizpour, and H. M. Majd, "Evaluation of the Effect of Spray Distance on Fracture Toughness of Thermally Sprayed Coatings," J. Appl. Sci., vol. 15, no. 4, pp. 709–714, 2015, doi: 10.3923/jas.2015.709.714.

[33] W. Kaiming, L. Yulong, F. Hanguang, L. Yongping, S. Zhenqing, and M. Pengfei, "A study of laser cladding NiCrBSi/Mo composite coatings," Surf. Eng., vol. 34, no. 4, pp. 267–275, Apr. 2018, doi: 10.1080/02670844.2016.1259096.

[34] Š. Houdková, E. Smazalová, M. Vostřák, and J. Schubert, “Properties of NiCrBSi coating, as sprayed and remelted by different technologies,” Surf. Coatings Technol., vol. 253, pp. 14–26, Aug. 2014, doi: 10.1016/j.surfcoat.2014.05.009.

[35] R. Chattopadhyay, Surface wear : analysis, treatment, and prevention. ASM International, 2001.

[36] X. H. Cui, S. Q. Wang, M. X. Wei, and Z. R. Yang, “Wear characteristics and mechanisms of h13 steel with various tempered structures,” J. Mater. Eng. Perform., vol. 20, no. 6, pp. 1055–1062, Aug. 2011, doi: 10.1007/s11665-010-9723-0.

[37] I. C. Grigorescu, C. Di Rauso, R. Drira-Halouani, B. Lavelle, R. Di Giampaolo, and J. Lira, “Phase characterization in Ni alloy-hard carbide composites for fused coatings,” Surf. Coatings Technol., vol. 76–77, no. PART 2, pp. 494–498, 1995, doi: 10.1016/0257-8972(95)02511-1.

[38] A. Zikin, M. Antonov, I. Hussainova, L. Katona, and A. Gavrilović, “High temperature wear of cermet particle reinforced NiCrBSi hardfacings,” Tribol. Int., vol. 68, pp. 45–55, 2013, doi: 10.1016/j.triboint.2012.08.013.

[39] A. García, M. R. Fernández, J. M. Cuetos, R. González, A. Ortiz, and M. Cadenas, “Study of the Sliding Wear and Friction Behavior of WC + NiCrBSi Laser Cladding Coatings as a Function of Actual Concentration of WC Reinforcement Particles in Ball-on-Disk Test,” Tribol. Lett., vol. 63, no. 3, Sep. 2016, doi: 10.1007/s11249-016-0734-3.

[40] O. P. Umanskyi et al., “Structure and Wear Resistance of Plasma-Sprayed NiCrBSiC–TiCrC Composite Powder Coatings,” Powder Metall. Met. Ceram., vol. 59, no. 7–8, pp. 434–444, Nov. 2020, doi: 10.1007/s11106-020-00177-y.

[41] R. N. Gupta, A. K. Das, Nagahanumaiah, and S. Henal, “Pulse Electrocodeposited Ni-WC Composite Coating,” Mater. Manuf. Process., vol. 31, no. 1, pp. 42–47, Jan. 2016, doi: 10.1080/10426914.2015.1019087.

[42] J. R. Davis, “Thermal Spray Technology,” Technology, pp. 1–11, 2004, doi: https://doi.org/10.31399/asm.hb.v05a.9781627081719.

[43] N. L. Parthasarathi and M. Duraiselvam, “High temperature tribological properties of NiCrBSiCFe plasma-sprayed coating on austenitic stainless steel substrate,” J. Alloys Compd., vol. 505, no. 2, pp. 824–831, Sep. 2010, doi: 10.1016/j.jallcom.2010.06.149.

[44] K. Komvopoulos, “Surface engineering and microtribology for microelectromechanical systems,” Wear, vol. 200, no. 1–2, pp. 305–327, 1996, doi: 10.1016/S0043-1648(96)07328-0.

[45] J. Gu, X. Wu, H. Cuypers, and J. Wastiels, “Transactions on Engineering Sciences vol 21,

© 1998 WIT Press, www.witpress.com, ISSN 1743-3533," vol. 17, pp. 589–598, 1998.

[46] J. Ilavsky and J. K. Stalick, "Phase composition and its changes during annealing of plasma-sprayed YSZ," Surf. Coatings Technol., vol. 127, no. 2–3, pp. 120–129, 2000, doi: 10.1016/S0257-8972(00)00562-4.

[47] P. Chattopadhyay, W. H. Glick, and G. P. Huber, "Organizational actions in response to threats and opportunities," Acad. Manag. J., vol. 44, no. 5, pp. 937–955, 2001, doi: 10.2307/3069439.

[48] B. Fotovvati, N. Namdari, and A. Dehghanghadikolaei, "On coating techniques for surface protection: A review," J. Manuf. Mater. Process., vol. 3, no. 1, 2019, doi: 10.3390/jmmp3010028.

[49] T. Schneller, R. Waser, M. Kosec, and D. Payne, Theodor Schneller · Rainer Waser Marija Kosec · David Payne. 2013.

[50] Shim, E. "Bonding requirements in coating and laminating of textiles." In Joining textiles, pp. 309-351. Woodhead Publishing, 2013. doi: 10.1533/9780857093967.2.309.

[51] P. Panjan, A. Drnovšek, P. Gselman, M. Čekada, and M. Panjan, Review of growth defects in thin films prepared by PVD techniques, vol. 10, no. 5. 2020. doi: 10.3390/COATINGS10050447.

[52] D. P. MacWan, P. N. Dave, and S. Chaturvedi, "A review on nano-TiO2 sol-gel type syntheses and its applications," J. Mater. Sci., vol. 46, no. 11, pp. 3669–3686, 2011, doi: 10.1007/s10853-011-5378-y.

[53] L. Sexton, S. Lavin, G. Byrne, and A. Kennedy, "Laser cladding of aerospace materials," J. Mater. Process. Technol., vol. 122, no. 1, pp. 63–68, 2002, doi: 10.1016/S0924-0136(01)01121-9.

[54] T. Shinoda, J. Q. Li, Y. Katoh, and T. Yashiro, "Effect of process parameters during friction coating on properties of non-dilution coating layers," Surf. Eng., vol. 14, no. 3, pp. 211–216, 1998, doi: 10.1179/sur.1998.14.3.211.

[55] Vander Voort, George F., Steven R. Lampman, Bonnie R. Sanders, Gayle J. Anton, Carol Polakowski, Jill Kinson, Kathryn Muldoon, Scott D. Henry, and William W. Scott Jr. "ASM handbook." Metallography and microstructures 9 (2004): 44073-0002.

[56] McMinn, Beth W., C. R. Newman, Robert C. McCrillis, and Michael Kosusko "VOC prevention options for surface coating" EPA/600/A-92/146, 1992.

[57] Pourhashem, Sepideh, Farhad Saba, Jizhou Duan, Alimorad Rashidi, Fang Guan, Elham Garmroudi Nezhad, and Baorong Hou. "Polymer/Inorganic nanocomposite coatings with superior corrosion protection performance: A review." Journal of Industrial and

Engineering Chemistry 88 (2020): 29-57.

[58] C. Donnet and A. Erdemir, “Historical developments and new trends in tribological and solid lubricant coatings,” Surf. Coatings Technol., vol. 180–181, pp. 76–84, 2004, doi: 10.1016/j.surfcoat.2003.10.022.

[59] J. A. Hooker and P. J. Doorbar, “Metal matrix composites for aeroengines,” Mater. Sci. Technol., vol. 16, no. 7–8, pp. 725–731, 2000, doi: 10.1179/026708300101508414.

[60] J. M. Guilemany, J. M. Miguel, S. Armada, S. Vizcaino, and F. Climent, “Use of scanning white light interferometry in the characterization of wear mechanisms in thermal-sprayed coatings,” Mater. Charact., vol. 47, no. 3–4, pp. 307–314, 2001, doi: 10.1016/S1044-5803(02)00180-8.

[61] S. Amin, H. Panchal, and A. Professor, “A Review on Thermal Spray Coating Processes,” Int. J. Curr. Trends Eng. Res. Sci. J. Impact Factor, vol. 2, no. 4, pp. 556–563, 2016, [Online]. Available: http://www.ijcter.com

[62] H. Liao, B. Normand, and C. Coddet, “Influence of coating microstructure on the abrasive wear resistance of WC/Co cermet coatings,” Surf. Coatings Technol., vol. 124, no. 2–3, pp. 235–242, 2000, doi: 10.1016/S0257-8972(99)00653-2.

[63] P. Vuoristo, Thermal Spray Coating Processes, vol. 4. Elsevier, 2014. doi: 10.1016/B978-0-08-096532-1.00407-6.

[64] A. Kumar, S. K. Nayak, P. Bijalwan, M. Dutta, A. Banerjee, and T. Laha, “Optimization of mechanical and corrosion properties of plasma sprayed low-chromium containing Fe-based amorphous/nanocrystalline composite coating,” Surf. Coatings Technol., vol. 370, no. June 2021, pp. 255–268, 2019, doi: 10.1016/j.surfcoat.2019.05.010.

[65] Szeri, A. Z. "Some extensions of the lubrication theory of Osborne Reynolds." ASME, Transactions, Journal of Tribology 109 (1987): 21-36.

[66] J. K. Katiyar, J. Al Hammad, and A. S. Mohammed, Tribological Properties of Light Metal Matrix Composites, vol. 1, no. 1. Elsevier Ltd., 2021. doi: 10.1016/B978-0-12-819724-0.00104-X.

[67] R. A. Al-Samarai, A. S. Mahmood, and Y. Al-Douri, Surface modification, including polymerization, nanocoating, and microencapsulation, vol. 2. INC, 2020. doi: 10.1016/B978-0-12-817505-7.00005-1.

[68] P. Dašić, F. Franek, E. Assenova, and M. Radovanović, “International standardization and organizations in the field of tribology,” Ind. Lubr. Tribol., vol. 55, no. 6, pp. 287–291, 2003, doi: 10.1108/00368790310496437.

[69] I. Hutchings and P. Shipway, Friction and Wear of Engineering Materials. 2017. doi:

10.1016/B978-0-08-100910-9.00003-9.

[70] S. A. Musmar, A. Alrousan, and I. Tlili, “Effect of cylinder-liner rotation on wear rate: An experimental study,” Heliyon, vol.5, no.7, p.e02065, 2019, doi: 10.1016/j.heliyon.2019.e02065.

[71] L. Zhang et al., “Research on wear detection mechanism of cylinder liner-piston ring based on energy dissipation and AE,” Wear, vol. 508–509, no. March, p. 204472, 2022, doi: 10.1016/j.wear.2022.204472.

[72] F. Lyu et al., “Research on wear prediction of piston/cylinder pair in axial piston pumps,” Wear, vol. 456–457, no. March, p. 203338, 2020, doi: 10.1016/j.wear.2020.203338.

[73] J. R. Laguna-Camacho et al., “A study of the wear damage on gas turbine blades,” Eng. Fail. Anal., vol. 61, pp. 88–99, 2016, doi: 10.1016/j.engfailanal.2015.10.002.

[74] B. Page, “Rigid metal packaging,” Packag. Technol., pp. 122–162, 2012, doi: 10.1533/9780857095701.2.122.

[75] G. H. Paulino, Z.-H. Jin, R. H. Dodds, S. . Sahu, N. D. Badgayan, and P. S. Rama Sreekanth, Failure of Functionally Graded Materials, no. August 2015. 2017. doi: 10.1016/b978-0-12-803581-8.00875-4.

[76] P. Fauchais, A. Vardelle, and M. Vardelle, Thermally Sprayed Nanoceramic and Nanocomposite Coatings. Elsevier Ltd., 2015. doi: 10.1016/B978-0-12-799947-0.00010-9.

[77] E. Sloman, “BP Oil UK Ltd,” 2002, doi: 10.1016/B978-0-7506-4452-5.50095-X.

[78] S. N. Karlsdóttir, 7.08 - Corrosion, Scaling and Material Selection in Geothermal Power Production, vol. 7. Elsevier Ltd., 2012. doi: 10.1016/B978-0-08-087872-0.00706-X.

[79] Https://www.google.co.in/,

[80] J. R. Deardorff, “Non-destructive testing for protective coatings: Implementing a lifetime corrosion prevention program,” Met. Finish., vol. 107, no. 10, pp. 31–39, 2009, doi: 10.1016/S0026-0576(09)80254-7.

[81] Uhlig, Herbert H. "Stress-corrosion cracking." In Engineering Fundamentals and Environmental Effects, pp. 645-677. Academic Press, 1971. doi: 10.1016/B978-0-12-449703-0.50016-3.

[82] S. Zhang et al., “Research progress on active thermal protection for hypersonic vehicles,” Prog. Aerosp. Sci., vol. 119, no. June, p. 100646, 2020, doi: 10.1016/j.paerosci.2020.100646.

[83] G. Gao, J. J. Gou, C. L. Gong, J. X. Hu, and R. C. Gao, “A novel mechanical-thermal-electrical thermal protection system concept and its multi-scale performance evaluation

for hypersonic launch vehicles," Compos. Struct., vol. 268, no. March, p. 113962, 2021, doi: 10.1016/j.compstruct.2021.113962.

[84] V. T. Le, N. S. Ha, and N. S. Goo, "Advanced sandwich structures for thermal protection systems in hypersonic vehicles: A review," Compos. Part B Eng., vol. 226, no. September, p. 109301, 2021, doi: 10.1016/j.compositesb.2021.109301.

[85] R. J. Tobe and R. V. Grandhi, "Hypersonic vehicle thermal protection system model optimization and validation with vibration tests," Aerosp. Sci. Technol., vol. 28, no. 1, pp. 208–213, 2013, doi: 10.1016/j.ast.2012.11.001.

[86] Misra, A. "Composite materials for aerospace propulsion related to air and space transportation." In Lightweight Composite Structures in Transport, pp. 305-327. Woodhead Publishing, 2016. Elsevier Ltd, 2016. doi: 10.1016/B978-1-78242-325-6.00012-8.

[87] O. Uyanna and H. Najafi, "Thermal protection systems for space vehicles: A review on technology development, current challenges and future prospects," Acta Astronaut., vol. 176, no. June, pp. 341–356, 2020, doi: 10.1016/j.actaastro.2020.06.047.

[88] L. Mercatelli et al., "Ultra-refractory diboride ceramics for solar plant receivers," Energy Procedia, vol. 49, pp. 468–477, 2014, doi: 10.1016/j.egypro.2014.03.050.

[89] X. Liu, G. Wang, L. Liu, Z. Wang, Z. Wu, and M. Liu, "Hot corrosion behavior of ZrB2-SiC-graphite composite in NaCl and Na2SO4molten salts," J. Ceram. Sci. Technol., vol. 9, no. 3, pp. 309–318, 2018, doi: 10.4416/JCST2018-00020.

[90] M. Shojaie-Bahaabad and A. Hasani-Arefi, "Ablation properties of ZrC-SiC-HfB2 ceramic with different amount of carbon fiber under an oxyacetylene flame," Mater. Res. Express, vol. 7, no. 2, 2020, doi: 10.1088/2053-1591/ab70db.

[91] Graham, H. C., H. H. Davis, I. A. Kvernes, and W. C. Tripp. "Microstructural features of oxide scales formed on zirconium diboride materials." In Ceramics in Severe Environments: Proceedings of the Sixth University Conference on Ceramic Science North Carolina State University at Raleigh December 7–9, 1970, pp. 35-48. Boston, MA: Springer US, 1971.

[92] R. S. Colbert and G. W. Sawyer, "Thermal dependence of the wear of molybdenum disulphide coatings," Wear, vol. 269, no. 11–12, pp. 719–723, 2010, doi: 10.1016/j.wear.2010.07.008.

[93] M. Gasch, D. Ellerby, E. Irby, S. Beckman, M. Gusman, and S. Johnson, "Processing, properties and arc jet oxidation of hafnium diboride/silicon carbide ultra high temperature ceramics," J. Mater. Sci., vol. 39, no. 19, pp. 5925–5937, 2004, doi:

10.1023/B:JMSC.0000041689.90456.af.

[94] X. Yang, C. Zhao-Hui, and C. Feng, “High-temperature protective coatings for C/SiC composites,” J. Asian Ceram. Soc., vol. 2, pp. 305–309, 2014, doi: 10.1016/j.jascer.2014.07.004.

[95] S. H. Lee, Y. Sakka, and Y. Kagawa, “Corrosion of ZrB2 powder during wet processing - Analysis and control,” J. Am. Ceram. Soc., vol. 91, no. 5, pp. 1715–1717, 2008, doi: 10.1111/j.1551-2916.2008.02343.x.

[96] X. Zhang, L. Xu, S. Du, J. Han, P. Hu, and W. Han, “Fabrication and mechanical properties of ZrB2-SiCw ceramic matrix composite,” Mater. Lett., vol. 62, no. 6–7, pp. 1058–1060, 2008, doi: 10.1016/j.matlet.2007.07.044.

[97] D. Huang et al., “Fabrication and ablation property of carbon/carbon composites with novel SiC-ZrB2 coating,” Trans. Nonferrous Met. Soc. China (English Ed., vol. 25, no. 11, pp. 3708–3715, 2015, doi: 10.1016/S1003-6326(15)64012-2.

[98] F. Yang, X. Zhang, J. Han, and S. Du, “Processing and mechanical properties of short carbon fibers toughened zirconium diboride-based ceramics,” Mater. Des., vol. 29, no. 9, pp. 1817–1820, 2008, doi: 10.1016/j.matdes.2008.03.011.

[99] C. Tian, D. Gao, Y. Zhang, C. Xu, Y. Song, and X. Shi, “Oxidation behaviour of zirconium diboride-silicon carbide ceramic composites under low oxygen partial pressure,” Corros. Sci., vol. 53, no. 11, pp. 3742–3746, 2011, doi: 10.1016/j.corsci.2011.07.020.

[100] F. Yang, X. Zhang, J. Han, and S. Du, “Characterization of hot-pressed short carbon fiber reinforced ZrB2-SiC ultra-high temperature ceramic composites,” J. Alloys Compd., vol. 472, no. 1–2, pp. 395–399, 2009, doi: 10.1016/j.jallcom.2008.04.092.

[101] X. Zhang, Z. Wang, X. Sun, W. Han, and C. Hong, “Effect of graphite flake on the mechanical properties of hot pressed ZrB2-SiC ceramics,” Mater. Lett., vol. 62, no. 28, pp. 4360–4362, 2008, doi: 10.1016/j.matlet.2008.07.027.

[102] T. Huang, G. E. Hilmas, W. G. Fahrenholtz, and M. C. Leu, “Dispersion of zirconium diboride in an aqueous, high-solids paste,” Int. J. Appl. Ceram. Technol., vol. 4, no. 5, pp. 470–479, 2007, doi: 10.1111/j.1744-7402.2007.02157.x.

[103] C. Monticelli, A. Bellosi, and M. Dal Colle, “Electrochemical Behavior of ZrB[sub 2] in Aqueous Solutions,” J. Electrochem. Soc., vol. 151, no. 6, p. B331, 2004, doi: 10.1149/1.1739219.

[104] V. O. Lavrenko, V. A. Shvets, V. M. Talash, V. A. Kotenko, and T. V. Khomko, “Electrochemical oxidation of ZrB_2-$MoSi_2$ ceramics in a 3% NaCl solution,” Powder

Metall. Met. Ceram., vol. 50, no. 11–12, pp. 749–753, 2012, doi: 10.1007/s11106-012-9385-6.

[105] K. O. Hao Lin , Yangyang Liu , Wenping Liang , Qiang Miao , Shaoyun Zhou, Jiayu Sun, Yan Qi, Xiguang Gao, Yingdong Song, "Ultra-high temperature ceramics Oxidation-based materials selection for 2000^0C + hypersonic aerosurfaces: Theoretical considerations and historical experience," J. Eur. Ceram. Soc., vol. 42, no. 12, pp. 4770–4782, 2022, [Online]. Available: https://doi.org/10.1016/j.jeurceramsoc.2022.05.006

[106] W. Xie, Q. Fu, C. Cheng, P. Wang, J. Li, and N. Yan, "Effect of Lu_2O_3 addition on the oxidation behavior of SiC-ZrB_2 composite coating at 1500℃: Experimental and theoretical study," Corros. Sci., vol. 192, no. May, p. 109803, 2021, doi: 10.1016/j.corsci.2021.109803.

[107] J. Liu et al., "Microstructure and properties of ZrB_2-SiC continuous gradient coating prepared by high speed laser cladding," Tribol. Int., vol. 173, no. May, p. 107645, 2022, doi: 10.1016/j.triboint.2022.107645.

[108] A. V. Matteo Mor,Matthias Meiser, Nico Langhof, "Tribological behavior of carbon fiber reinforced ZrB_2 based ultra high temperature ceramics," J. Eur. Ceram. Soc., vol. 43, no. 13, pp. 5413–5424, 2023.

[109] N. Savchenko et al., "Subsurface multilayer evolution of ZrB_2–SiC ceramics in high-speed sliding and adhesion transfer conditions," Wear, vol. 482–483, no. February, p. 203956, 2021, doi: 10.1016/j.wear.2021.203956.

[110] H. Chen, Z. Wu, W. Hai, L. Liu, and W. Sun, "Tribo-oxidation and tribological behaviour of ZrB_2-20%volSiC composites coupled with WC and Al_2O_3 at high temperatures," Wear, vol. 464–465, no. October 2020, p. 203534, 2021, doi: 10.1016/j.wear.2020.203534.

[111] B. V. M. K. Yashpal Gupta, "ZrB2–SiC composites for sliding wear contacts: Influence of SiC content and counter body.," Ceram. Int., vol. 48, no. 10, pp. 14560–14567, 2022, [Online]. Available: https://doi.org/10.1016/j.ceramint.2022.01.349

[112] Mallik, M., P. Mitra, N. Srivastava, A. Narain, S. G. Dastidar, A. Singh, and T. R. Paul. "Abrasive wear performance of zirconium diboride based ceramic composite." International Journal of Refractory Metals and Hard Materials 79 (2019): 224-232.

[113] Sonber, J. K., K. Raju, TSR Ch Murthy, K. Sairam, A. Nagaraj, Sanjib Majumdar, and Vivekanand Kain. "Friction and wear properties of zirconium diboride in sliding against WC ball." International Journal of Refractory Metals and Hard Materials 76 (2018): 41-48.

[114] S. Chakraborty, D. Debnath, A. R. Mallick, and P. K. Das, "Mechanical and thermal

properties of hot pressed ZrB_2 system with TiB2," Int. J. Refract. Met. Hard Mater., vol. 46, pp. 35–42, 2014, doi: 10.1016/j.ijrmhm.2014.05.004.

[115] S. Zhu, W. G. Fahrenholtz, G. E. Hilmas, and S. C. Zhang, "Pressureless sintering of zirconium diboride using boron carbide and carbon additions," J. Am. Ceram. Soc., vol. 90, no. 11, pp. 3660–3663, 2007, doi: 10.1111/j.1551-2916.2007.01936.x.

[116] M. Shahedi Asl et al., "Toughening of ZrB_2-based composites with in-situ synthesized ZrC from ZrO_2 and graphite precursors," J. Sci. Adv. Mater. Devices, vol. 6, no. 1, pp. 42–48, 2021, doi: 10.1016/j.jsamd.2020.09.014.

[117] H. Assadi, F. Gärtner, T. Stoltenhoff, and H. Kreye, "Bonding mechanism in cold gas spraying," Acta Mater., vol. 51, no. 15, pp. 4379–4394, 2003, doi: 10.1016/S1359-6454(03)00274-X.

[118] G. Bae et al., "Bonding features and associated mechanisms in kinetic sprayed titanium coatings,"ActaMater., vol.57, no.19, pp.5654-5666, 2009, doi:10.1016/j.actamat.2009.07.061.

[119] X. Lian, H. Cui, Q. Wang, X. Song, X. Yang, and Z. Cui, "Corrosion and mechanical behavior of amorphous-nanocrystalline NiCrMo coatings," J. Alloys Compd., vol. 927, p. 167010, 2022, doi: 10.1016/j.jallcom.2022.167010.

[120] C. Dai, H. Luo, J. Li, C. Du, Z. Liu, and J. Yao, "X-ray photoelectron spectroscopy and electrochemical investigation of the passive behavior of high-entropy FeCoCrNiMox alloys in sulfuric acid," Appl. Surf. Sci., vol. 499, no. May 2019, p. 143903, 2020, doi: 10.1016/j.apsusc.2019.143903.

[121] W. Wu, X. Cheng, J. Zhao, and X. Li, "Benefit of the corrosion product film formed on a new weathering steel containing 3% nickel under marine atmosphere in Maldives," Corros. Sci., vol. 165, no. September, p. 108416, 2020, doi: 10.1016/j.corsci.2019.108416.

[122] C. A. C. Souza, D. V. Ribeiro, and C. S. Kiminami, "Corrosion resistance of Fe-Cr-based amorphous alloys: An overview," J. Non. Cryst. Solids, vol. 442, pp. 56–66, 2016, doi: 10.1016/j.jnoncrysol.2016.04.009.

[123] R. Hu, G. M. Cheng, J. Q. Zhang, J. S. Li, T. B. Zhang, and H. Z. Fu, "First principles investigation on the stability and elastic properties of Ni_2Cr1-xMx (M = Nb, Mo, Ta, and W) superlattices," Intermetallics, vol. 33, pp. 60–66, 2013, doi: 10.1016/j.intermet.2012.09.017.

[124] K. H. Lo, C. H. Shek, and J. K. L. Lai, "Recent developments in stainless steels," Mater. Sci. Eng. R Reports, vol. 65, no. 4–6, pp. 39–104, 2009, doi: 10.1016/j.mser.2009.03.001.

[125] Q. Y. Wang, X. Z. Wang, H. Luo, and J. L. Luo, “A study on corrosion behaviors of Ni-Cr-Mo laser coating, 316 stainless steel and X70 steel in simulated solutions with H_2S and CO_2,” Surf. Coatings Technol., vol. 291, pp. 250–257, 2016, doi: 10.1016/j.surfcoat.2016.02.017.

[126] Q. Y. Wang, S. L. Bai, Y. F. Zhang, and Z. De Liu, “Improvement of Ni-Cr-Mo coating performance by laser cladding combined re-melting,” Appl. Surf. Sci., vol. 308, pp. 285–292, 2014, doi: 10.1016/j.apsusc.2014.04.156.

[127] M. Sun, Y. Pang, C. Du, X. Li, and Y. Wu, “Optimization of Mo on the corrosion resistance of Cr-advanced weathering steel designed for tropical marine atmosphere,” Constr. Build. Mater., vol. 302, no. July, p. 124346, 2021, doi: 10.1016/j.conbuildmat.2021.124346.

[128] X. zhi Li, Z. de Liu, H. chuan Li, Y. tian Wang, and B. Li, “Investigations on the behavior of laser cladding Ni-Cr-Mo alloy coating on TP347H stainless steel tube in HCl rich environment,” Surf. Coatings Technol., vol. 232, pp. 627–639, 2013, doi: 10.1016/j.surfcoat.2013.06.048.

[129] D. Kesavan and M. Kamaraj, “The microstructure and high temperature wear performance of a nickel base hardfaced coating,” Surf. Coatings Technol., vol. 204, no. 24, pp. 4034–4043, Sep. 2010, doi: 10.1016/j.surfcoat.2010.05.022.

[130] N. Y. Sari and M. Yilmaz, “Investigation of abrasive + erosive wear behaviour of surface hardening methods applied to AISI 1050 steel,” Mater. Des., vol. 27, no. 6, pp. 470–478, 2006, doi: 10.1016/j.matdes.2004.11.020.

[131] H. Winkelmann, E. Badisch, M. Varga, and H. Danninger, “Wear mechanisms at high temperatures. part 3: Changes of the wear mechanism in the continuous impact abrasion test with increasing testing temperature,” Tribol. Lett., vol. 37, no. 2, pp. 419–429, Feb. 2010, doi: 10.1007/s11249-009-9534-3.

[132] D. Z. Guo, F. L. Li, J. Y. Wang, and J. S. Sun, “Effects of post-coating processing on structure and erosive wear characteristics of flame and plasma spray coatings,” Surf. Coatings Technol., vol. 73, no. 1–2, pp. 73–76, 1995, doi: 10.1016/0257-8972(94)02364-6.

[133] T. B. Torgerson, S. A. Mantri, R. Banerjee, and T. W. Scharf, “Room and elevated temperature sliding wear behavior and mechanisms of additively manufactured novel precipitation strengthened metallic composites,” Wear, vol. 426–427, pp. 942–951, Apr. 2019, doi: 10.1016/j.wear.2018.12.046.

[134] Z. Weng, A. Wang, X. Wu, Y. Wang, and Z. Yang, “Wear resistance of diode laser-clad

Ni/WC composite coatings at different temperatures," Surf. Coatings Technol., vol. 304, pp. 283–292, Oct. 2016, doi: 10.1016/j.surfcoat.2016.06.081.

[135] M. Chen, H. Li, X. Yao, G. Kou, Y. Jia, and C. Zhang, "High temperature oxidation resistance of La_2O_3-modified ZrB_2-SiC coating for SiC-coated carbon/carbon composites," J. Alloys Compd., vol. 765, pp. 37–45, Oct. 2018, doi: 10.1016/j.jallcom.2018.06.230.

[136] P. Sarin et al., "In situ studies of oxidation of ZrB_2 and ZrB_2-SiC composites at high temperatures," J. Eur. Ceram. Soc., vol. 30, no. 11, pp. 2375–2386, Aug. 2010, doi: 10.1016/j.jeurceramsoc.2010.03.009.

[137] V. Guérineau, A. Julian-Jankowiak, G. Vilmart, and N. Dorval, "In situ study of the oxidation of ZrB_2 and ZrB_2-SiC materials by monitoring the LIF signal of BO_2 radicals," Corros. Sci., vol. 148, pp. 31–38, Mar. 2019, doi: 10.1016/j.corsci.2018.11.032.

[138] Y. Gupta and B. V. Manoj Kumar, "ZrB_2–SiC composites for sliding wear contacts: Influence of SiC content and counterbody," Ceram. Int., vol. 48, no. 10, pp. 14560–14567, 2022, doi: 10.1016/j.ceramint.2022.01.349.

[139] M. J. Tobar, C. Álvarez, J. M. Amado, G. Rodríguez, and A. Yáñez, "Morphology and characterization of laser clad composite NiCrBSi-WC coatings on stainless steel," Surf. Coatings Technol., vol. 200, no. 22-23 SPEC. ISS., pp. 6313–6317, 2006, doi: 10.1016/j.surfcoat.2005.11.093.

[140] C. Katsich and E. Badisch, "Effect of carbide degradation in a Ni-based hardfacing under abrasive and combined impact/abrasive conditions," Surf. Coatings Technol., vol. 206, no. 6, pp. 1062–1068, 2011, doi: 10.1016/j.surfcoat.2011.07.064.

[141] C. Guo, J. Zhou, J. Chen, J. Zhao, Y. Yu, and H. Zhou, "High temperature wear resistance of laser cladding NiCrBSi and NiCrBSi/WC-Ni composite coatings," Wear, vol. 270, no. 7–8, pp. 492–498, 2011, doi: 10.1016/j.wear.2011.01.003.

[142] S. Kumar and S. M. Pandey, "Effect of Y_2O_3 and TiO_2 addition of dispersed powder on phase evolution and microstructural analysis of (Al, Cu)3Ti intermetallic synthesised via mechanical alloying and powder metallurgy route," Adv. Mater. Process. Technol., vol. 00, no. 00, pp. 1–16, 2022, doi: 10.1080/2374068X.2022.2123418.

[143] S. cong Gu, S. zhen Zhu, Z. Ma, S. peng Han, and Y. bo Liu, "Preparation and properties of ZrB_2 -$MoSi_2$-glass composite powders for plasma sprayed high temperature oxidation resistance coating on C/SiC composites," Powder Technol., vol. 345, pp. 544–552, 2019, doi: 10.1016/j.powtec.2019.01.044.

[144] Li, Yongkun, Shuaiying Xi, Guodong Ma, Ying Xiao, Lu Li, Zhentao Yuan, Yuanhuai

He, Rongfeng Zhou, and Yehua Jiang. "Understanding the influencing mechanism of sub-micron sized TiB2p on the microstructures and properties of rheological squeeze casting hypereutectic Al–Si alloys." J. Mater. Res. Technol., vol. 14, pp. 57–68, 2021, doi: 10.1016/j.jmrt.2021.06.048.

[145] S. M. Tavana, M. Hojjati, A. C. Liberati, and C. Moreau, “Erosion resistance enhancement of polymeric composites with air plasma sprayed coatings,” Surf. Coatings Technol., vol. 455, no. November 2022, p. 129211, 2023, doi: 10.1016/j.surfcoat.2022.129211.

[146] A. Bruera et al., “Adhesion of cold sprayed soft coatings: Effect of substrate roughness and hardness,” Surf. Coatings Technol., vol. 466, no. April, 2023, doi: 10.1016/j.surfcoat.2023.129651.

[147] P. Tawade, S. Shembale, S. Hussain, and K. Sabiruddin, “Effects of Different Grit Blasting Environments on the Prepared Steel Surface,” J. Therm. Spray Technol., vol. 32, no. 5, pp. 1535–1553, 2023, doi: 10.1007/s11666-023-01585-3.

[148] N. Singh, A. Mehta, H. Vasudev, and P. S. Samra, “A review on the design and analysis for the application of Wear and corrosion resistance coatings,” Int. J. Interact. Des. Manuf., 2023, doi: 10.1007/s12008-023-01411-8.

[149] X. Lu et al., “Prolonged thermal durability of plasma-sprayed lanthanum hexaluminate thermal barrier coating by optimizing crystallinity,” Ceram. Int., vol. 49, no. 19, pp. 32205–32217, 2023, doi: 10.1016/j.ceramint.2023.07.195.

[150] Y. Ozgurluk, A. Gulec, D. Ozkan, G. Binal, and A. Cahit Karaoglanli, “Structural characteristics, oxidation performance and failure mechanism of thermal barrier coatings fabricated by atmospheric plasma spraying and detonation gun spraying,” Eng. Fail. Anal., vol. 152, no. July, p. 107499, 2023, doi: 10.1016/j.engfailanal.2023.107499.

[151] A. Ali, Y. W. Chiang, and R. M. Santos, “X-Ray Diffraction Techniques for Mineral Characterization: A Review for Engineers of the Fundamentals, Applications, and Research Directions,” Minerals, vol. 12, no. 2, 2022, doi: 10.3390/min12020205.

[152] F. Rubino, D. Merino, A. T. Silvestri, C. Munez, and P. Poza, “Mechanical properties optimization of Cr_3C_2-NiCr coatings produced by compact plasma spray process,” Surf. Coatings Technol., vol. 465, no. April, p. 129570, 2023, doi: 10.1016/j.surfcoat.2023.129570.

[153] M. Ramezani, Z. Mohd Ripin, T. Pasang, and C. P. Jiang, “Surface Engineering of Metals: Techniques, Characterizations and Applications,” Metals (Basel)., vol. 13, no. 7, 2023, doi: 10.3390/met13071299.

[154] Mohanty, Sutanuka, Soumyabrata Basak, Debasis Saran, Kajari Chatterjee, Turin Datta,

Atul Kumar, Chandra Prakash, Doo-Man Chun, Sung-Tae Hong, and Kisor Kumar Sahu. "Advanced Surface Engineering Approaches for Exotic Applications." International Journal of Precision Engineering and Manufacturing (2023): 1-33, 2023. doi: 10.1007/s12541-023-00870-z.

[155] Long, Xu, Ruipeng Dong, Yutai Su, and Chao Chang. "Critical Review of Nanoindentation-Based Numerical Methods for Evaluating Elastoplastic Material Properties." Coatings 13, no. 8 (2023): 1334.,

[156] A. Iqbal and G. Moskal "Recent Development in Advance Ceramic Materials and Understanding the Mechanisms of Thermal Barrier Coatings Degradation",pp1-42, Archives of Computational Methods in Engineering 2023. doi: 10.1007/s11831-023-09960-7.

[157] S. Singh, C. C. Berndt, R. K. Singh Raman, H. Singh, and A. S. M. Ang, "Applications and Developments of Thermal Spray Coatings for the Iron and Steel Industry," Materials (Basel)., vol. 16, no. 2, pp. 1–27, 2023, doi: 10.3390/ma16020516.

[158] D. Klenam et al., "Cold Spray Coatings of Complex Concentrated Alloys: Critical Assessment of Milestones, Challenges, and Opportunities," Coatings, vol. 13, no. 3, 2023, doi: 10.3390/coatings13030538.

[159] A. R. Govande, A. Chandak, B. R. Sunil, and R. Dumpala, "Carbide-based thermal spray coatings: A review on performance characteristics and post-treatment," Int. J. Refract. Met. Hard Mater., vol. 103, no. November 2021, p. 105772, 2022, doi: 10.1016/j.ijrmhm.2021.105772.

[160] M. M. Al-Asadi and H. A. Al-Tameemi, "A review of tribological properties and deposition methods for selected hard protective coatings," Tribol. Int., vol. 176, no. September, p. 107919, 2022, doi: 10.1016/j.triboint.2022.107919.

[161] Y. Liu, K. Wang, and H. Fu, "Improvement of the High Temperature Wear Resistance of Laser Cladding Nickel-Based Coating: A Review," Metals (Basel)., vol. 13, no. 5, pp. 1–16, 2023, doi: 10.3390/met13050840.

[162] S. Du, Z. Li, Z. He, H. Ding, X. Wang, and Y. Zhang, "Effect of temperature on the friction and wear behavior of electroless Ni–P–MoS_2–CaF_2 self-lubricating composite coatings," Tribol. Int., vol. 128, no. July, pp. 197–203, 2018, doi: 10.1016/j.triboint.2018.07.026.

[163] X. Ren et al., "Surface modification technologies for enhancing the tribological properties of cemented carbides: A review," Tribol. Int., vol. 180, no. November 2022, p. 108257, 2023, doi: 10.1016/j.triboint.2023.108257.

[164] W. Dai et al., “A review on the fatigue performance of micro-arc oxidation coated Al alloys with micro-defects and residual stress,” J. Mater. Res. Technol., vol. 25, pp. 4554–4581, 2023, doi: 10.1016/j.jmrt.2023.06.244.

[165] C. V. V. & H. S. N. D. G. Pradeep, “Review on Tribological and Mechanical Behavior in HVOF Thermal-sprayed Composite Coatings,” J. Bio- Tribo-Corrosion, vol. 30, pp30. 8, 2022,doi.org/10.1007/s40735-022-00631-x

[166] D. K. Devarajan, B. Rangasamy, and K. K. Amirtharaj Mosas, “State-of-the-Art Developments in Advanced Hard Ceramic Coatings Using PVD Techniques for High-Temperature Tribological Applications,” Ceramics, vol. 6, no. 1, pp. 301–329, 2023, doi: 10.3390/ceramics6010019.

[167] Y. Wang and T. Monetta, “Systematic study of preparation technology, microstructure characteristics and mechanical behaviors for SiC particle-reinforced metal matrix composites,” J. Mater. Res. Technol., vol. 25, pp. 7470–7497, 2023, doi: 10.1016/j.jmrt.2023.07.145.

[168] Scholz, Fritz, Heike Kahlert, Fritz Scholz, and Heike Kahlert. "Complex Formation Equilibria." Chemical Equilibria in Analytical Chemistry: The Theory of Acid–Base, Complex, Precipitation and Redox Equilibria", pp. 93-105. 2019. doi: 10.1007/978-3-030-17180-3_4.

[169] K. P. Ranjith, M. A. Hasan, A. Dey, and B. Basu, “Development of ZrB_2-based single layer absorber coating and molten salt corrosion of bulk ZrB_2-SiC ceramic for concentrated solar power application,” vol.125, pp.13581-13589, J. Phys. Chem. C, 2021, doi: 10.1021/acs.jpcc.1c01984.

[170] C. Monticelli, F. Zucchi, A. Pagnoni, and M. Dal Colle, “Corrosion of a zirconium diboride/silicon carbide composite in aqueous solutions,” Electrochim. Acta, vol. 50, no. 16–17, pp. 3461–3469, 2005, doi: 10.1016/j.electacta.2004.12.023.

[171] K. O. Hao Lin , Yangyang Liu , Wenping Liang , Qiang Miao , Shaoyun Zhou, Jiayu Sun, Yan Qi, Xiguang Gao, Yingdong Song, “Electrochemical Behavior of ZrB[sub 2] in Aqueous Solutions,” J. Eur. Ceram. Soc., vol. 42, no. 12, pp. 4770–4782, 2022, doi: 10.1149/1.1739219.

LIST OF PUBLICATION

List of papers published in SCI/SCIE indexed journals:

1. Gupta, Kalpana, Qasim Murtaza, and N. Yuvraj. "Measurement of Tribological Characteristics of Composite Coating under Different Temperatures." MAPAN 37.4 (2022): 811-822.
2. Gupta, Kalpana, Qasim Murtaza, and N. Yuvraj. "Development of ZrB2-SiC Plasma-Sprayed Ceramic Coating for Thermo-chemical Protection in Hypersonic Vehicles." Journal of Materials Engineering and Performance (2023): 1-10.
3. Tyagi, A., Pandey, S. M., Gupta, K., Walia, R. S., Murtaza, Q., & Krishen, K. Tribological behavior of sustainable carbon-based composite coating for wear resistance applications. Materials Research Express, (2019): 6(12), 125601.

List of papers published in ESCI & SCOPUS indexed journals:

1. Gupta, Kalpana, et al. "Tribological behaviour of (CrC) X+ (Mo+ Fe) + (NiCr) X alloy coating by atmospheric plasma spraying on piston ring with liner contact." Advances in Materials and Processing Technologies 8.2 (2022): 1292-1303.

LIST OF CONFERENCES

1. Kem, L., Tyagi, L., Gupta, K., & Pandey, S. M. (2023). Effect of Forging on Mechanical and Tribological Properties of Aluminum Alloy Composites: A Review. Recent Trends in Mechanical Engineering: Select Proceedings of PRIME 2021, 819-829.
2. Tyagi, A., Pandey, S. M., Murtaza, Q., & Gupta, K. (2023). A Critical Review on Design and Examination of High-Temperature Thermal Spray Carbon-Based Composite Coatings at High Temperature. Recent Trends in Mechanical Engineering: Select Proceedings of PRIME 2021, 853-860.